Optimizing a Hammer Forging Progression for a Large Hand Tool

Edgar Espinoza
Marquette University

OPTIMIZING A HAMMER FORGING PROGRESSION FOR A LARGE HAND TOOL

by

Edgar Espinoza, B.A.

A Thesis submitted to the Faculty of the Graduate School,
Marquette University,
in Partial Fulfillment of the Requirements for
the Degree of Masters of Science

Milwaukee, Wisconsin

December 2015

ABSTRACT
OPTIMIZING A HAMMER FORGING PROGRESSION FOR
A LARGE HAND TOOL

Edgar Espinoza, B.A.

Marquette University, 2015

In the forging industry of today the need for United States based companies to reduce cost and maintain or improve the quality of a product has become essential in order to remain competitive. A company such as Green Bay Drop Forge (GBDF), a manufacturer of standard and custom steel forgings, was tasked with improving the forging process of one of their large hand tool products. A large wrench, forged at GBDF was noticed to contain a large amount of flash and excessive amount of hammer blows required to forge the part. The large amounts of flash and excessive hammer blows increased forging time and money spent on scrap material.

Rather than spending significant time and money in trial and error on the shop floor, the use of Computer Aided Design (CAD) and Finite Element (FE) based softwares such as Unigraphics NX 8.5 and DEFORM were used to propose an optimized forging process. Validation of the process model was conducted through simulations of the existing forging process and comparisons with forged platters obtained from GBDF. Once validated, changes to the billet and impression geometries were proposed and simulated in DEFORM to predict forging results. Forging trials were performed on the shop floor and the results were compared to the DEFORM model predictions. The proposed changes helped to reduce the total number of blows in the forging process by 22% and the flash by 4% while improving metal flow in the preform operation and die fill in the forging dies.

Mamá y Papá
Gracias por el apoyo incondicional que siempre me han brindado

ACKNOWLDEGMENTS

Edgar Espinoza, B.S.

I would like to take the time to offer my gratitude to those who assisted me throughout the course of the project. These include my advisor Dr. Joseph P. Domblesky, for all his support and guidance during my time in Graduate School and the development of the project. The Forging Industry Educational and Research Foundation (FIERF) members Carola Sekreter and Suzanne Tkach for their support, knowledge, and advice during the simulation process. The Green Bay Drop Forge personnel including Mike LaFier, Dan Heesacker, Dave Gilliam, and Ben Selner for their support and feedback regarding forging tips and experimental trials. And the staff at DEFORM including Chris Fischer and James Miller for their guidance in setting – up simulation models and debugging simulation errors.

I would also like to thank my parents, Edgar and Amada, as well as my siblings Henry and Vilma for their unconditional support in this journey. Their words of encouragement and faith in me, have led me down the right path.

Finally I would like to offer a sincere Thank You, to all my relatives and friends who in one way or another have supported me throughout my years in school.

TABLE OF CONTENTS

List of Tables

List of Figures

CHAPTER 1

INTRODUCTION

1.1 Overview of the Forging Process

In the modern world of manufacturing, forging continues to be a widely used industrial process for a variety of products. Some common applications of forged products include aerospace, automotive, hand tools, and industrial equipment [5]. Forging is a manufacturing process involving the plastic deformation of a metal part through the use of two dies and compressive pressure. The compressive pressures can be either impact or gradual pressure, which are used to produce a desired geometry. The modern forging process is capable of producing parts in a wide range of sizes, from items that weigh only a few grams to large items on the order of several tons [5].

Apart from its flexibility in part size, the achievable mechanical properties and material utilization sets forging apart from other manufacturing processes. Forging is capable of refining the grain structure which, in turn, affects the grain flow, positively affecting the tensile strength, ductility, impact toughness, fracture toughness and fatigue strength of the forged part [5]. Excellent structural integrity is also obtained from forging. This means that the forged part will not contain internal voids or porosities, allowing it to have uniform mechanical properties as well as a uniform response to heat treatments [5]. Forging has flexibility with variable cross sections and thicknesses that can achieved, which allows for better material usage.

Forging processes can be divided into two main categories which include open – die forging and impression – die forging. Preference as to which process is used is

dictated by material flow. For example, if material is allowed to flow freely, the use of open – die forging is preferred. Although the final desired shape may not be obtained after open – die forging, the tools used and the required set – up for such processes is much simpler. An example of a simple open – die forging operation is the upset forging of a part with a cylindrical cross section. In the upset forging operation, two flat dies are used to compress the cylinder such that the height of the part is reduced while its diameter is increased. A schematic representation of this process is shown in Figure 1.1.1.

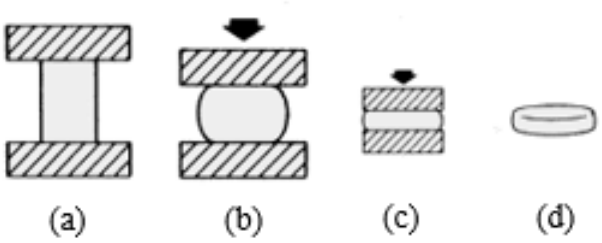

Figure 1.1.1 Simple upset operation of a cylinder. (a) Start of plastic deformation, (b) Workpiece under partial compression, (c) Final compression, and (e) Workpiece at the end of the operation [11]

Other examples of open die forging operations include fullering, edging, and cogging. Fullering and edging operations are similar in the sense that the cross section of the part is reduced while the material is redistributed for further shaping. The difference is that fullering dies have convex surfaces whereas edging dies have concave surfaces. Cogging on the other hand involves compression along the length of the workpiece, meaning that the length increases as the cross section decreases.

Impression – die forging is more restricting of the metal flow, but it is capable of producing parts closer to the desired shape. Unlike open – die forging, impression – die forging processes require the use of more complex dies for forged products. Typically

multiple operations are required to obtain the desired geometry. Simple upset and/or roll forming, are common preform operations used in conjunction with impression – die forging processes. A schematic of an impression – die forging process is presented shown Figure 1.1.2.

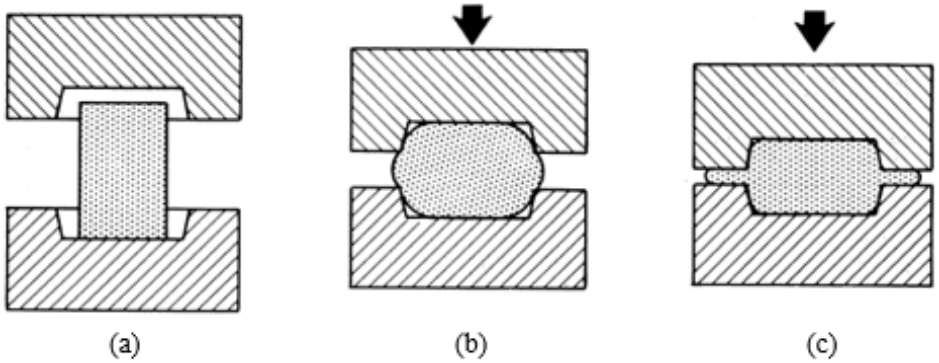

Figure 1.1.2 Impression – die forging operation for a simple geometry.
(a) Step prior to plastic deformation, (b) Intermediate step with partial compression, and (c) Final step with full compression [9]

When dealing with impression – die forging or closed – die forging, it is important to consider the function of the flash and how it affects the process. The use of flash is necessary in impression – die forging due to the complex geometries and large tolerances encountered during the operations. As the flash begins to form on the perimeter of the die impression, as seen in Figure 1.1.2 (c), the friction tends to limit the material flow outward in the direction of the flash. As a result, more material is constrained within the die cavity. However, control of the flash thickness is important, if the flash is too thin, it will cool down much faster, which in turn will increase the resistance to deformation as well as the compression pressure. This will affect the load encountered by the dies, too large of a load can be problematic since it could increase the stress beyond the yield point of the die material. Normally a trimming operation is used

to remove the flash at the end of the forging process and machining can be used for further detailing.

When dealing with flashless forging or true closed – die forging, all material is used in the part and the workpiece is completely contained within the die cavity. This prevents any flash from ever forming. However, flashless forging requires careful process control and very tight tolerances. Too much material can increase the pressures, potentially causing damage to the dies or forging equipment, while too little can prevent proper die fill. Due to the complexity of the process, flashless forging is restricted to simple part geometries and materials such as aluminum and magnesium [18].

The forging process can be further divided into three main subcategories on the basis of temperature use. These subcategories are cold, warm, and hot forging, each with its own set of advantages and disadvantages. Cold forging is commonly performed at room temperature without any prior heat up. Advantages of cold forging include close dimensional tolerances, good surface finish, good mechanical properties and the prevention of scale buildup [18]. The use of cold forging however can affect the plastic flow of the material as well as the forming pressures, which will require the use of more powerful, heavier equipment [22]. Warm forging on the other hand tends to decrease the forming pressure and improve material flow seen in cold forging. Warm forging is typically performed at temperatures ranging between 800 ˚F to 1800 ˚F for steels. This combines the advantages of cold and hot forging such as being able to forge parts with more complex shapes like those for hot forging, but with tolerances closer to those seen in cold forging [18]. Disadvantages of warm forging include high tooling cost and the need for such tools to withstand higher temperatures [22]. Hot forging is perhaps the

most widely used amongst the three subcategories mentioned. The temperature range for hot forging of steels is approximately between 2100 ˚F and 2300 ˚F. The increase in temperature improves the ease of plastic deformation and the ductility of the part being forged. The higher temperatures used for hot forging help to reduce the loads exerted on the dies and forging equipment, meaning lower tool cost. The disadvantage of hot forging however, is that with increasing temperature there is an increase in scale build – up, and larger dimensional tolerances are also required.

The characteristics of the forging equipment used is an important factor that needs to be considered before optimizing a process. The forging equipment selected can have a major influence in the forging process because it affects the deformation rate, forging temperature, and rate of production [13]. There are a variety of machines associated with individual forming processes, the forging equipment mentioned here includes load – restricted, stroke – restricted, and energy – restricted machines. Load – restricted machines, such as hydraulic presses are limited by the maximum load (force) capacity that can be exerted on the workpiece. Hydraulic presses can be used for both open – die and closed – die forging. Their operation is simple since motion and force is defined by a hydraulic piston guided in a cylinder [13]. Hydraulic presses have the capability of applying large loads at slower speeds once the top die comes into contact with the surface of the workpiece. This helps when forging materials such as aluminum, which are likely to rupture at high deformation rates. However, due to its slow speeds and high loads, there is an increase in die wear and chilling.

Stroke – restricted machines such as mechanical presses are limited to a constant length – stroke due to its full eccentric type of drive shaft. The mechanical press

functions as a slider – crank mechanism which converts rotary motion and energy from a flywheel to linear motion. The converted linear motion drives the ram up and down during operation [12]. Mechanical presses are capable of providing close – tolerance parts and have high production rates. Their design also permits the use of automatic feed and transfer mechanisms between dies, which contributes to better productivity in the forging process. However due to the contact time and squeezing force encountered by the dies, harder die materials are required which can be expensive.

Finally, energy – restricted machines such as screw – type presses and hammers are limited by the amount of energy that is available prior to contact between the top die and workpiece. Screw – type presses work in a similar way as mechanical and hydraulic presses. However, friction, gear, electric, or hydraulic drives are used to accelerate a flywheel, which in turn converts the angular kinetic energy in the flywheel to linear energy of the ram [13]. Similar to hammers, the top and bottom dies will "kiss" during blows when using a screw – type press. Contact times between dies however are longer when compared to hammers. Hammers are the most flexible in terms of forging operations it can perform and the least expensive of forging equipment which make them somewhat unique. Hammers are capable of applying large forces while having shorter contact times. Unlike mechanical presses, hammers, require multiple blows to forge a part and there are also larger tolerances since process control is mainly operator based. There are a variety of different hammer equipment than can be selected, and a more in depth description is provided in Chapter 2.

When discussing forging it is crucial to review the importance of preforms and how they affect the overall forging process. Having a good preform in which volume has

been properly distributed can help reduce material usage, forging time, loads and energy. Preforms are commonly used with impression – die or closed – die forging and there are a variety of different preforming operations that can be performed. Simple upsets with two flat dies as well as edging, fullering, drawing, cogging and even roll forging operations are very common in the preforming stages of forging. When selecting the tools for a preform it is important to keep in mind the type of part geometry that is desired in order to select the proper equipment. One type of preform operation that provides good metal distribution in a simple and quick manner is roll forging. Roll forging utilizes two sets of rolling dies that contain a series of segments which are used to decrease or increase the cross – sectional area of the billet as it passes between the rollers. A more in depth description of the roll forging process will be provided in Chapter 2.

1.2 Improving Forging Process Efficiency

Due to cost pressures from customers and overseas competitors, it is necessary for United States based forging companies to reduce cost and maintain or improve product quality in order to remain competitive. Forging companies in developing countries have the advantages of lower wages and a highly motivated labor force. Some of those companies even have the privilege of obtaining support from their governments through tax breaks, free training, and an artificially maintained, yet favorable currency foreign exchange rate [31]. Since companies in the United States function differently, the demand for an improvement in process efficiency and product quality is greatly increasing. In order to obtain a more efficient process and remain competitive, United States based forging companies need to do the following; maintain quality of a product by reducing

scrap rates as well as flash losses, reduce die wear and improve die life, introduce die making methods to reduce lead time in die manufacturing and reduce die cost, implement process modeling techniques using 3D Finite Element (FE) based simulation software, and work closely with customers in developing future applications [31]. It is important to point out that in the past couple of years the use of computer softwares such as Computer Aided Design (CAD) based or Finite Element (FE) based softwares have played an important role in the improvement of quality and productivity in many forging companies.

1.3 Problem Statement

Green Bay Drop Forge Co. (GBDF), a privately owned Wisconsin – based manufacturer of custom and standard steel forgings, uses gravity drop hammers as part of the manufacturing process for its products. Some of the custom steel forgings produced at GBDF include hand tools, custom tee – bolts, and rigging hardware. Standard steel forging products include small – to – medium sized linkage and fastening components such as clevises, yokes, turnbuckles, lever handles, lever nuts, and chain hooks used in lifting or hoisting applications.

Upon inspection of one of the hand tools manufactured at GBDF, a large wrench, to be specific, it was observed that the existing forging process yields platters that contain excess flash in areas where it is not needed. It was also identified that a large number of hammer blows are needed to forge the part as seen by the forged platters shown in Figure 1.3.1. Note that the words “hammer blow” will be used to represent the occurrence of the top and bottom die blocks coming into contact with one another. An excessive number of

hammer blows and too much flash increase production time and cost, while reducing process efficiency.

Figure 1.3.1 GBDF forged platters of the existing wrench forging process

In order to have a better understanding of the existing forging process, Figure 1.3.2, depicting the flow schematic of the process for a typical large wrench forging produced at GBDF, has been provided.

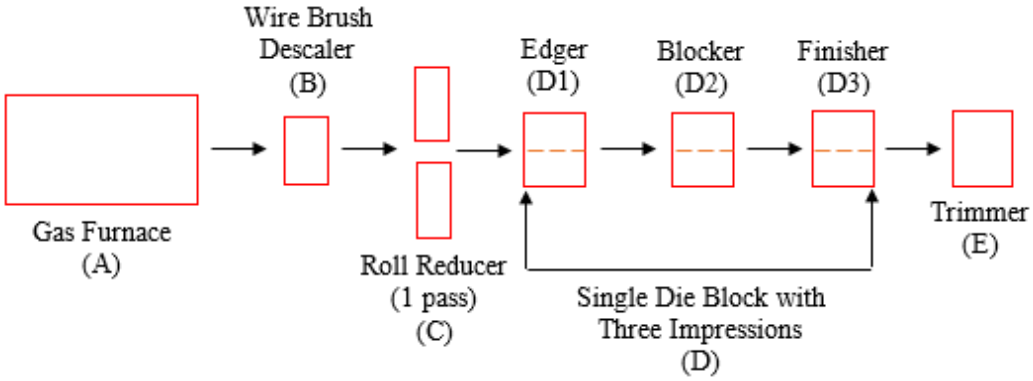

Figure 1.3.2 Flow schematic of the existing hammer forging process used at GBDF for an AISI 4047 large wrench

A summary description of the forging progression is as follows:

- A sheared billet having the desired volume is placed in a gas fired furnace which is set to an operating temperature of approximately 2300 ˚F. The billet is heated for approximately 10 – 15 minutes under atmospheric conditions (A)
- Once the billet has reached a uniform temperature of approximately 2200 ˚F - 2300 ˚F, it is manually removed from the furnace by the hammer operator using a pair of long tongs
- The billet is then placed in a wire brush descaler which is used to remove the surface scale build up resulting from heating in an air atmosphere (B)
- After the scale has been removed, the heated billet is passed through a set of roll reducers to produce a preform. This involves two rotating roll forging dies which compress and redistribute material by extending the length and reducing the thickness of the billet at specified locations (C)
- The preform is then manually transferred to a 3,000 lb drop hammer where it is forged on a single die block using three sets of impressions which consist of an edger, blocker, and finisher (D)
- A total of nine hammer blows are used in the existing process and the forging sequence can be broken down as follows:
    - The preform is placed in the edger impression and three hammer blows are used to further redistribute the metal needed to forge the individual sections of the large wrench (D1)

- The preform is then transferred to the blocker impression and three additional hammer blows are used to develop an approximate shape of the large wrench (D2)
    - Note: At this point the preform starts to take shape and the forged part is referred to as a platter
- The platter is finally moved to the finisher impression where three more hammer blows are used to obtain the final forged geometry (D3)

- Once the part has been forged, the platter is transferred to a trim press where the flash is removed by a shearing operation (E)

The problem with the existing forging process can be further understood by considering the finished forged platter of the large wrench as shown in Figure 1.3.3.

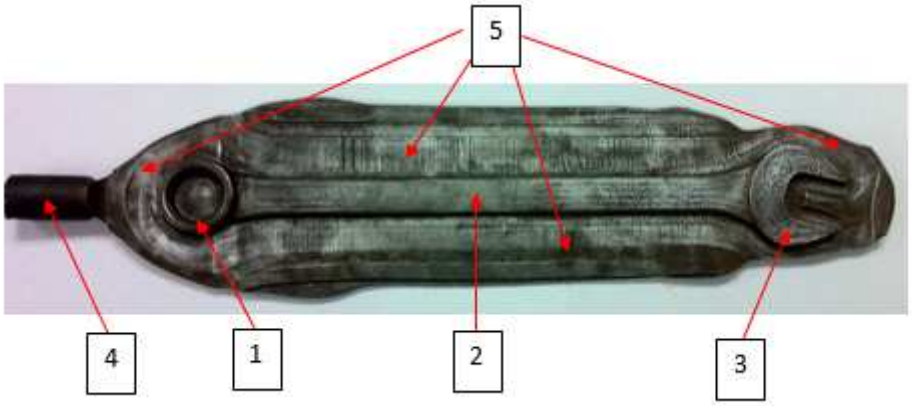

Figure 1.3.3 As – forged platter of the large wrench after nine hammer blows. (1) Wrench Closed End, (2) Wrench Handle, (3) Wrench Open End, (4) Platter Handle, (5) Flash

As seen in Figure 1.3.3 there is an excessive amount of flash around sections (1) and (2) of the forged platter while the amount of flash around section (3) is somewhat limited. The implication of the latter is that if the open end of the wrench is not positioned properly in the die, there is the possibility of incomplete die fill at the end of

the process causing the forged part to be scrapped. The total of nine hammer blows required to forge the part not only requires longer forging time but also increases the wear of the dies. In order to make the existing forging process more efficient, the amount of flash needs to be reduced and volume needs to be properly redistributed to obtain an improved metal flow and die fill. Also, the total number of hammer blows needs to be reduced in order to reduce forging time and die wear.

1.4 Objective of the Research – Optimization Approach Overview

The goal of this study was to optimize the existing hot forging progression for the large wrench manufactured at GBDF to improve forging process efficiency. The forging progression involved the use of roll forging to obtain a preform and subsequent impression – die forging using a drop hammer to obtain the final desired geometry. In order to accomplish the above goals, the proposed process strived to reduce the amount of flash present at the end of the forging process through good volume distribution and an improved metal flow. In order to accomplish this, a volume analysis for the different sections of the wrench, previously shown in Figure 1.3.1, was first conducted using the final forged platter in the cold condition and the results are presented in Table 1.4.1.

Table 1.4.1 Approximate volume distribution for different sections of the forged platter, after nine hammer blows (Cold Condition)

Section No.	**Section Name**	**Volume (in^3)**
1	Wrench Closed End	1.25
2	Wrench Handle	5.31
3	Wrench Open End	2.14
4	Platter Handle	2.00
5	Flash	5.95

The estimates presented in Table 1.4.1 helped to identify how much volume was needed for the main sections of the wrench and how much material could be removed from the flash. In doing so the approximate volume distribution analysis helped to determine possible geometry and dimensions of the proposed starting billet.

The proposed process also intended to reduce the total number of hammer blows required to forge the part. This was to be achieved through changes made to the roll forging segments and impression geometries of the die blocks used in the existing wrench forging process. Having an optimized set of die impressions would help obtain a good preform with improved volume distribution, and help reduce the total number of hammer blows needed to forge the part. The existing wrench forging process made one pass in the roll forging operation for initial volume distribution and the material was further redistributed in a subsequent edger operation.

Unlike the existing wrench forging process, the proposed process would make use of two different roll forging segment geometries. This would allow a larger diameter billet with a shorter length to be used, in order to achieve complete die fill at the end of the forging process. The proposed process would also make use of a redesigned edger impression with a new geometry and reduced impression depth. The depth of the blocker impression would also be reduced and the cavity of the open end section of the wrench would be enlarged, in order to obtain an improvement in die fill. The finisher impression would remain unchanged in order to maintain the overall part dimensions the same as specified in the forge drawing. A more detailed explanation of all the changes made and results is provided in Chapters 5 and 6.

Rather than spending significant time and money in an approach based on trial and error on the shop floor, finite element simulation software was used as the basis for redesigning the existing wrench forging process. Simulation or process modeling software has proved to be a useful tool in the design and validation of forging processes in the recent years. The use of computer software enables virtual representations of the existing and proposed processes, and made it possible to evaluate the effects of design changes on metal flow at a relatively low cost. The Computer Aided Design (CAD) and Finite Element (FE) based software programs used to analyze the forging progression were Unigraphics NX 8.5 and DEFORM V.10.2, respectively. The commercial CAD software NX 8.5 was used to generate solid model representations of the geometries of the roll forging and die block impressions. The commercial FE based software DEFORM was used to perform process modeling simulations of the existing and proposed wrench forging process using the solid model representations of the tools generated in NX 8.5. A more detailed explanation is provided in Chapters 4 and 5.

1.5 Summary of Analysis

Validation of the finite element model of the existing wrench forging process was of main importance in the first stages of the project. The geometric representations of the roll forging dies and die block impressions were modeled based on drawings supplied by GBDF. Since the wrench forging process at GBDF is largely operator based, it was important to identify the correct computer inputs needed for the process modeling simulation in DEFORM. This was important in order to ensure that the model accurately reflected the forging conditions seen during production.

The inputs were used to validate the models of the existing wrench forging process and to predict forging results of the proposed process. Inputs such as friction factor, heat transfer coefficients, boundary conditions, workpiece positioning, hammer blow efficiencies, and mesh size were approximated by performing a set of simulations in DEFORM and comparing the DEFORM workpiece model results to forged platters obtained from GBDF. Temperature plots from DEFORM were also compared to pyrometer temperature readings recorded during a wrench forging production run. Other inputs such as available energy, mass of the ram and die, dwell time, and number of hammer blows per operation were estimated based on information provided by GBDF.

The proposed forging process was performed using the same set of parameters used for the existing wrench forging process, once the DEFORM model of the existing wrench forging process was validated. The proposed process makes use of two passes in the roll forging dies rather than one pass, as used in the existing wrench forging process. Note that the proposed roll forging die segments contained a modified groove geometry. Changes were also made to the edger and blocker geometry and depth, while maintaining the finisher impression the same. Changes were not made in the finisher impression in order to meet customer specifications. The proposed changes suggested in this thesis, helped to reduce hammer forging time, flash, and total number of hammer blows, while improving metal flow and die fill. A detailed description of the proposed changes and results is provided in Chapters 5 and 6.

CHAPTER 2

OVERVIEW OF THE ROLL AND HAMMER FORGING PROCESSES

2.1 The Conventional Rolling Process

Roll forging plays an important role in the hot forging process being analyzed in this project. In order to have better insight of such operation it is essential to first discuss the conventional rolling process. The conventional rolling process is a compressive deformation process, which can either be continuous or stepwise and can be classified according to kinematics, tool geometry, and workpiece geometry [23]. The term kinematics in this case refers to the motion of the workpiece as it passes through the rolling dies. There are three basic rolling processes that affect the kinematic movements of the workpiece which include longitudinal, cross, and skewed rolling. In longitudinal rolling, there is only translational motion of the workpiece as it passes through the rolling gap perpendicular to the axis of the rolls, without rotating about its own axis. In cross rolling however, there is a rotational motion of the workpiece rather than the translational motion which occurs in longitudinal rolling. Finally skewed rolling, combines both rotational and translational motion of the workpiece as it passes through the rolling dies. Figure 2.1.1 has been provided to illustrate the kinematic behavior of each of the rolling processes that has been described.

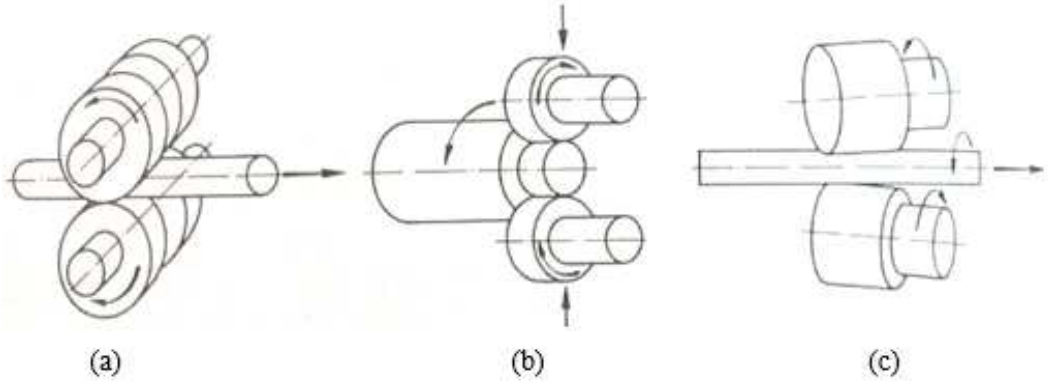

Figure 2.1.1 Schematic representation of kinematics associated with the rolling process. (a) Longitudinal, (b) Cross, and (c) Skewed rolling [23]

The rolling process can be further classified according to tool and workpiece geometry. For example, tool geometry can be divided into two categories based on the geometry of the roll gap, these two categories are termed flat and profile rolling. In flat – rolling, the segments of the roller dies have a cylindrical or conical shapes at the roll gap. In profile – rolling however, the shapes of the segments deviates from the typical geometries seen in flat – rolling. The rolling process can be divided into further subcategories depending on the workpiece geometry. In this particular case the geometry of the part refers to whether the workpiece being rolled is a solid or hollow shape. The conventional rolling process can be better understood by looking at the diagram shown in Figure 2.1.2.

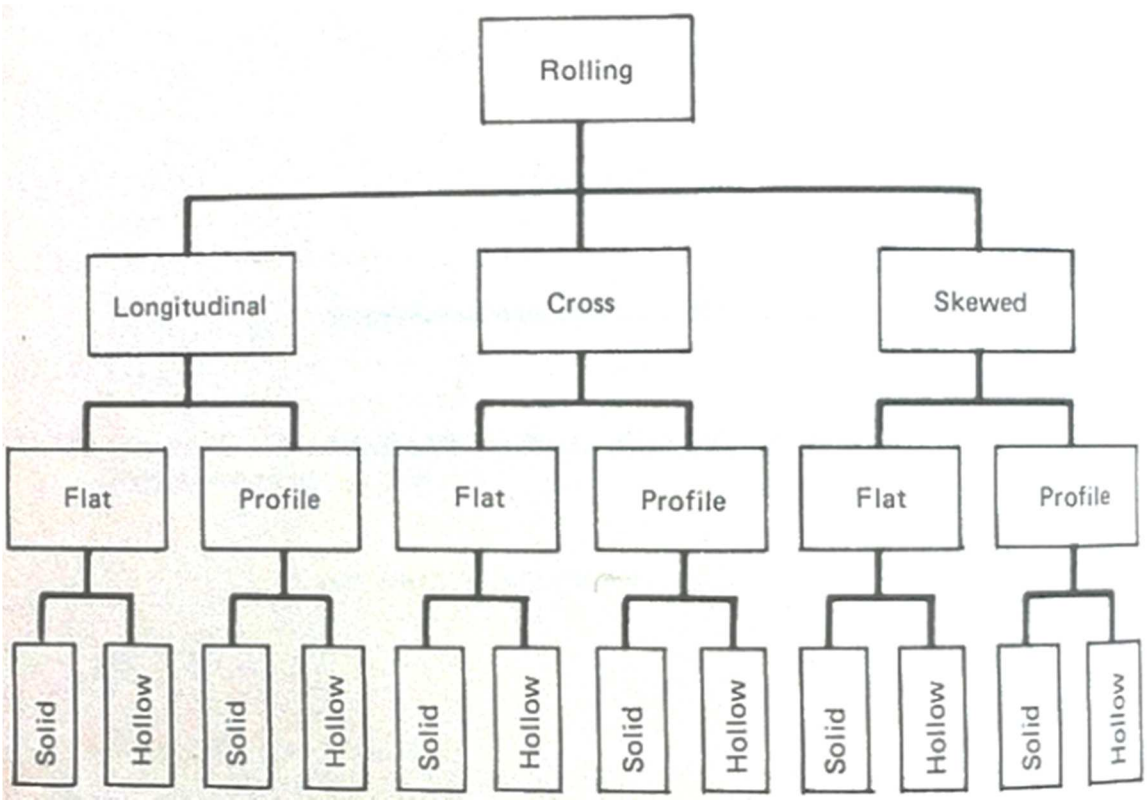

Figure 2.1.2 Diagram representation of the conventional rolling process [23]

2.2 The Roll Forging Process

Of the different rolling processes previously described, one type of rolling operation that is commonly used for preforms in the forging industry to aid in volume distribution required for forging sequences is the roll forging or roll forming process. Roll forging belongs to the kinematics and tool geometry categories of longitudinal and profile rolling, respectively. Roll forging is different than the conventional rolling processes in the sense that the rolls have variable segments along their circumference, which makes it possible to obtain variable workpiece cross – sections once rolling is complete. Roll forging also differs from the conventional rolling process with respect to tool size. For example, the rolls used for such operation are of relatively small diameter and serve as

arbors onto which the forging tools are secured [10]. Typically only a portion of the full circumference of the rollers come into contact with the workpiece, which tends to allow for better handling and positioning.

When using reducer rolls for the roll forging operations there are a few factors to keep in mind. Typically the roll forming operation is performed at warm or hot working conditions, which improves metal flow as the workpiece passes between the rollers. In these conditions however, it is important to pay attention to the spread of material in the roll segments in order to prevent unwanted flash, which can potentially cause defects in subsequent forging steps. Depending on the workpiece geometry at the start of the process, the segments in the roller dies can be appropriately designed to account for material spread as the height and length in the workpiece is reduced and elongated, respectively.

Another important factor to keep in mind when using reducer rolls, is the possibility of workpiece bending at the point of contact with the rollers. Note that since reducer rolls can have different segments along their circumference, their effective roll radius can vary. To avoid confusion, the term effective roll radius refers to the radius from the center of the reducer roll to the cavity of the segment where sticking of the workpiece can occur [23]. If the effective roll radius is different between the top and bottom rollers at the point of contact with the workpiece, then workpiece bending is more likely to occur in the direction of the smaller roll radius. Also, if the segment cavities in the rollers are not symmetrical in width, the probability of workpiece bending at the point of contact with the reducer rollers will also increase. In summary, workpiece bending is caused by the continuous translational motion of the workpiece as it passes between the

reducer rolls when there is a mismatch between the top and bottom roll forging die segments.

2.3 Functionality, Advantages and Disadvantages of the Roll Forging Process

In order to have better knowledge of the roll forging process, it is important to discuss its functionality before proceeding. The roll forging operation is carried out on a two – high rolling mill using a pair of forging or reducer rolls with varying segments and is controlled by the operator. At the beginning of the process the operator pushes the starting billet back against a stopper, located at a predetermined distance from the center of the rolls and aligned with the cavity of the roll forging die segment. Once proper workpiece positioning has been achieved, the operator starts the rolling machine by engaging the clutch, which cause the reducer rolls to make one full rotation. The operator holds the billet in position during rolling by using a long pair of tongs. As the rolling machine starts to operate, the surface of the reducer rolls grip the billet, pushing it towards the operator as the rolls complete one full rotation. The process is then repeated for multiple passes with varying roll segment geometries until the desired shape is obtained. An example of one pass in the roll forging operation is shown in Figure 2.3.1.

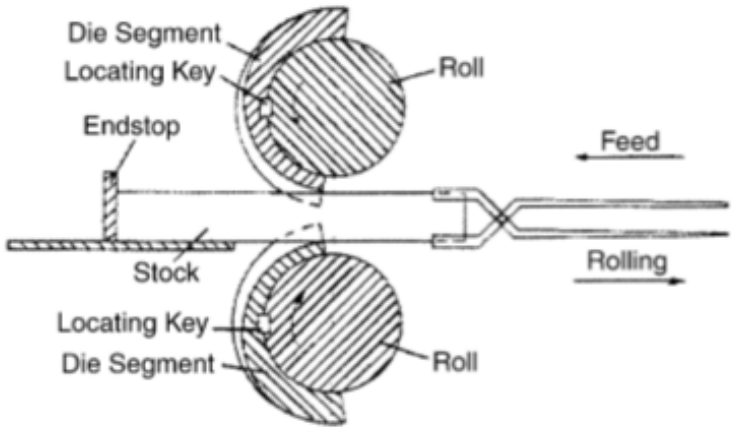

Figure 2.3.1 Schematic representation of the roll forging process [10]

Every process used for forming operations have many advantages and disadvantages that set them apart from one another, the ones for the roll forging process will be described in the this section. The roll forging process has many advantages such as high productivity, high utilization rate of material, good labor conditions, and long life of rolling dies [22]. The roll forging process also performs a certain amount of descaling, allowing the rolled part to have a smooth surface and be free of scale pockets [10]. Roll forming also has the advantage of serving as both a main operation and preforming operation. In cases were the roll forging process functions as the main type of operation, multiple passes with varying groove segments are utilized in order to obtain the semi – finished geometry. Examples of products made under these working conditions include airplane propeller blade half sections, tapered axle shafts, table knife blades, hand shovels and spades just to name a few [22]. Other detailing processes would be needed to obtain the final desired product. The roll forging process is also commonly used as a preforming operation, in which the volume of a starting billet is redistributed for further forging sequences in a hammer, hydraulic, or mechanical press. The simple, quick, and effective

results make the roll forging process more favorable than other preforming operations. Examples of this type of operation includes preforms rolled for crankshafts, connecting rods, and other automotive parts [22]. Disadvantages of this process however can include bending of the workpiece if the roll segments are not properly designed and proper precautions are not taken for the operation. Also, some process parameters such as temperature are difficult to control in roll forging, which prevents it from being used as a finish – forming process [23].

2.4 Brief History of Hammer Forging

The hammer forging process is the oldest commercial forging process in existence and dates back to the blacksmiths, whose revolutionary work has made many contributions to society over the centuries. Although the type of hammer forging equipment has changed over the years, the overall functionality and type of operation has remained the same. In its most basic form the hammer forging equipment is composed of an anvil and a hammer. In the United States the first hammer forging plant was opened up by a group of enterprising blacksmiths after the War of Independence as the nation's economy was becoming more industrially based [10]. In those times the blacksmiths made use of tilt hammers which were powered by water. Over the course of the years, the hammer forging industry began to expand significantly and this called for improvement in the hammer forging equipment that was being used. In 1839 the Scottish engineer and inventor, James Nasmyth, made a technological breakthrough when he developed the gravity drop hammer which was powered by steam. By the 1860's, drop hammer forging was already an established industry and new developments of hammer forging equipment

such as the board drop hammer, which was an American invention, continued to improve the capabilities of the industry. Hammer forging continues to play a major role in the forging industry of today and will likely continue to do so in the future. A graphic representation of the progression of the hammer forging equipment developed over the years is shown in Figure 2.4.1.

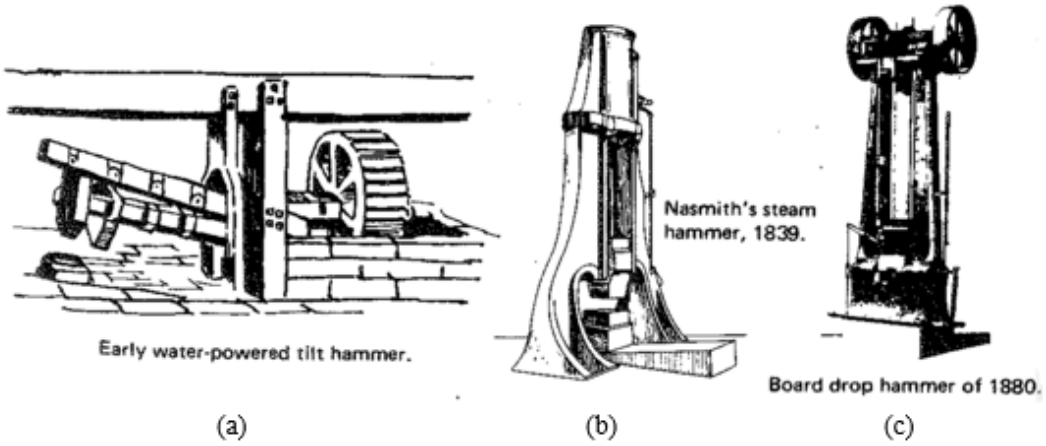

Figure 2.4.1 Progression of the hammer forging equipment over the years. (a) Water – powered tilt hammer, (b) Steam – powered drop hammer, and (c) Board drop hammer [10]

2.5 Overview of the Conventional Hammer Forging Equipment and Process

The hammer forging process has been widely used over the years due to its versatility and forging capabilities. In order to have more insight into the art of hammer forging, the characteristics of the conventional hammers equipment and its functionality need to be discussed. Hammer equipment in general is composed of a hammer ram, frame assembly, anvil, and anvil cap [12]. The upper die block for the forging process is attached to the ram of the hammer, the lower die is attached to the anvil cap, and the anvil is directly attached to the frame assembly. Hammers are energy – restricted machines, meaning that the deformation of a workpiece is caused by kinetic energy generated by the

ram and top die as it moves downward towards the workpiece. The total kinetic energy of the system is dissipated by plastic deformation of the material and by elastic deformation of the ram and anvil when opposing die faces come into contact with each other during a working stroke [13]. Since the amount of energy needed for complete plastic deformation of the workpiece might be more than the total amount available per machine, it is quite common to use multiple hammer blows to obtain the desired geometry at the end of the process. Hammers are primarily used in hot forging and coining operations, but some have been known to take part in manufacturing small quantity parts in sheet – metal forming. Note that coining is a form of precision stamping operation used to induce metal flow on the surface of a part to meet customer specifications.

As previously mentioned hammers are characterized by the amount of energy that can be provided to deform a workpiece. However, similar to other machines used in the forging industry, there are certain variations that distinguish hammer equipment apart from one another. Conventional hammers can be divided into two main categories which are gravity – drop and power – drop hammers. The functionality of the two types of forging equipment is the same in the sense that the ram is lifted to a specified height and then dropped on the workpiece located on the anvil. In gravity – drop hammers, the ram is accelerated by gravity, meaning that each blow contains roughly the same amount of total kinetic energy during the downstroke. In power – drop hammers however, in addition to gravity, the ram is accelerated by a piston that uses steam, cold or hot air pressure thus increasing the kinetic energy available [13].

2.5.1 Gravity – Drop Hammers

Gravity – drop hammers are further classified according to the way that the ram is lifted. For example, the ram can be lifted to a predetermined height via a board (board – drop hammer), a belt (belt – drop hammer), a chain (chain – drop hammer), or a piston (oil -, air-, or steam – lift drop hammer). A schematic representation of these variations in gravity – drop hammers is presented in Figure 2.5.1.1.

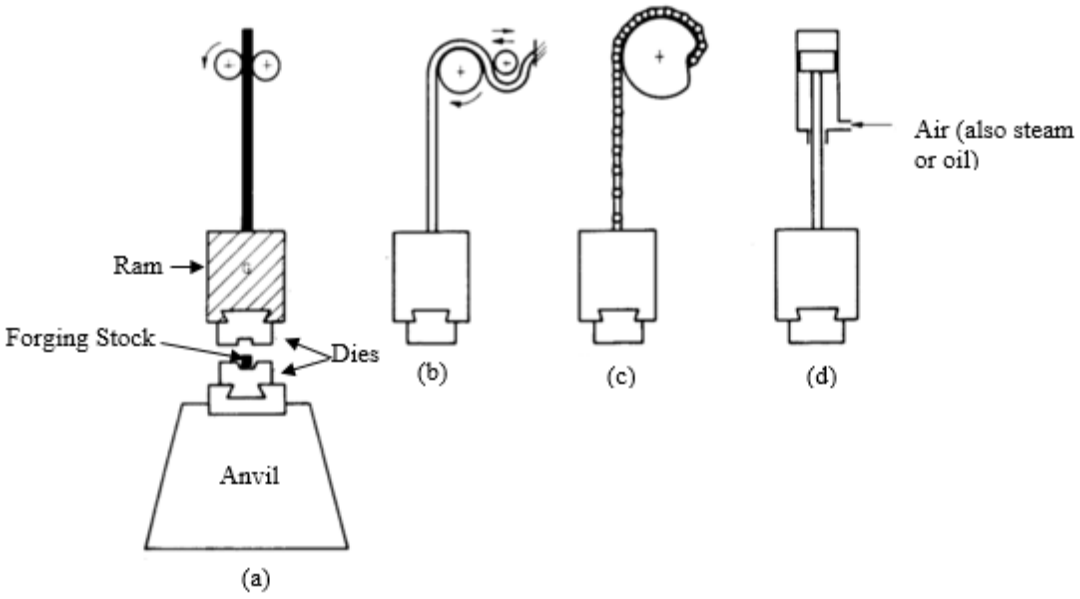

Figure 2.5.1.1 Various types of lift mechanisms used in gravity – drop hammers. (a) Board – drop, (b) Belt – drop, (c) Chain – drop, and (d) Air – drop [10]

The two most commonly used type of gravity – drop hammers in industry today are the board – drop and air – lift drop hammers. The board – drop hammer is capable of forging parts weighing no more than a few kilograms and have a falling weight or rated size ranging from 400 to 10,000 lb [12]. Standard sizes for this type of gravity – drop hammer range from 1000 to 5000 lb. Since the board – drop hammers have a predetermined drop height, the striking force for each hammer blow remains

approximately the same during the forging process. The striking force cannot be altered between forging steps such that in order to change the amount of energy generated by the board – drop hammer, the machine needs to be stopped and the drop height needs to be changed. Drop heights however, tend to vary with hammer size. Typical drop heights tend to range from approximately 35 to 75 in. for 400 lb and 7,500 lb hammers, respectively [12]. Board – drop hammers are capable of generating maximum blow energy, impact speeds, and number of blows per minute of approximately 35,000 ft-lb, 10-15 ft/s, and 45 – 60, respectively [12].

Air – lift drop hammers are similar to board – drop hammers, except that the ram is raised by action of air cylinders as previously mentioned. The air – lift drop hammer contains a device that makes it possible to have long and short strokes in a variable forging sequence. Typically air – lift drop hammers range in size of approximately 500 to 10,000 lb and the products forged are in the same weight range as that obtained in a board – drop hammer. Many air operated hammers are conversions from steam hammers and are capable of operating with both a power down and power up operation [5]. Air – lift drop hammers are capable of reaching maximum blow energy, impact speeds, and numbers of blow per minute of approximately 90,000 ft-lb, 12-16 ft/s, and 60, respectively [12]. For visual purposes, a schematic representation of a conventional board – drop hammer is shown in Figure 2.5.1.2.

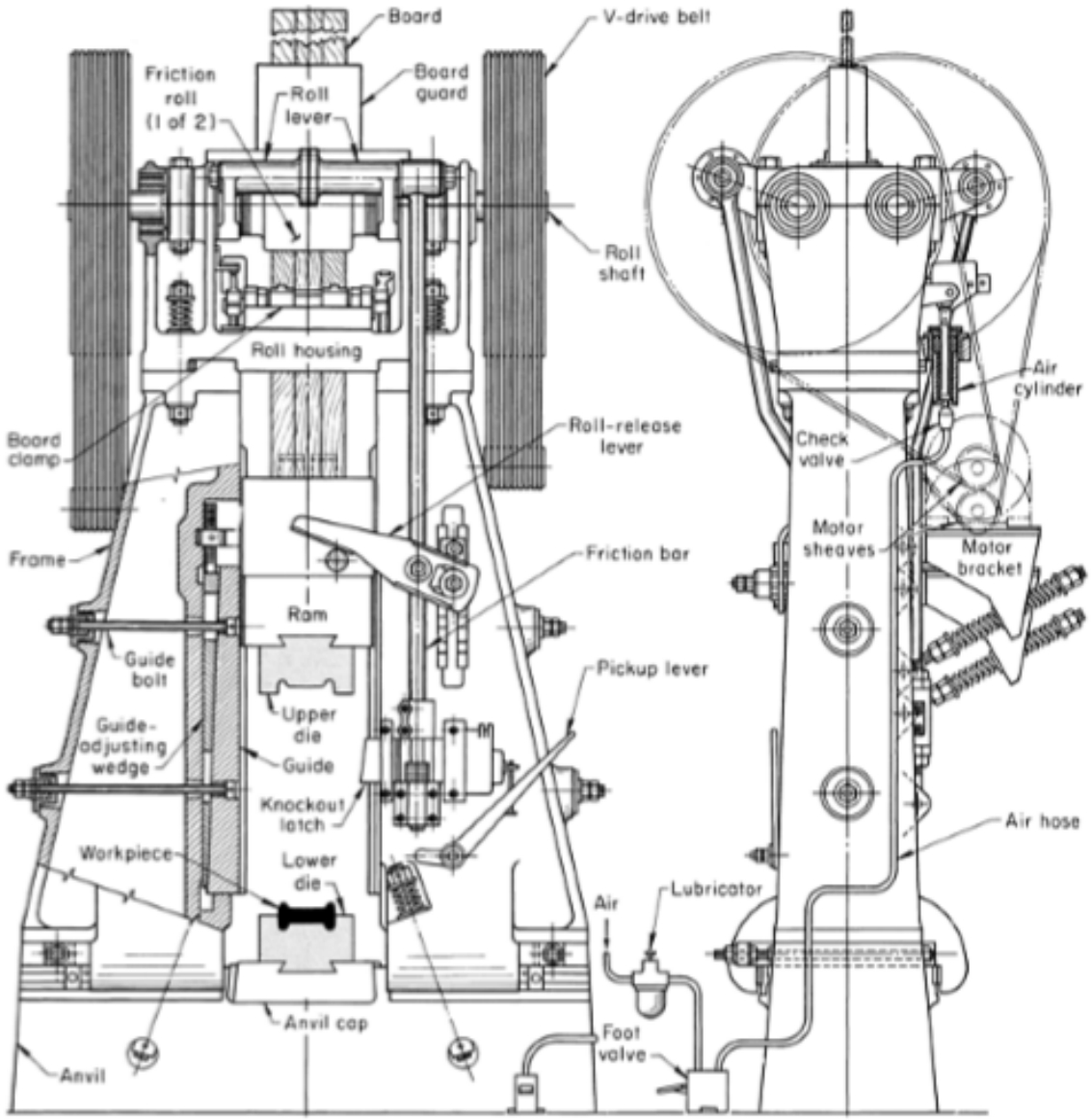

Figure 2.5.1.2 Schematic of the conventional board – drop hammer with its main components [12]

2.5.2 Power – Drop Hammers

Power – drop hammers as previously described are accelerated both by gravity and an additional source such as air, steam, or hydraulic pressure. Power – drop hammers are very powerful machines primarily used for closed die forgings and are used for the production of parts through impact pressures. The total energy generated in the system

can range from a slight tap to full power, depending on the type of part being forged in the process. In power – drop hammers the motion of the ram is controlled by a piston, which itself is controlled by a valve that admits air, steam, or oil to the upper or lower side of the piston [12]. Most modern power – drop hammers are equipped with electronic circuitry that enable the intensity of the hammer blows to be varied throughout the forging process without the need to stop the machine and adjust the drop height.

Conventional power – drop hammers tend to range in ram weight of 1,500 to 70,000 lb. Maximum blow energy, impact speed, and number of blows per minute for such machines are approximately 850,000 ft-lb, 15-30 ft/s, and 60-100, respectively [12]. As seen from the information provided, power – drop hammers are quite powerful machines with larger capabilities than basic gravity – drop hammers, but at the same time they require more experience and better care. A schematic of a conventional power – drop hammer is shown in Figure 2.5.2.1.

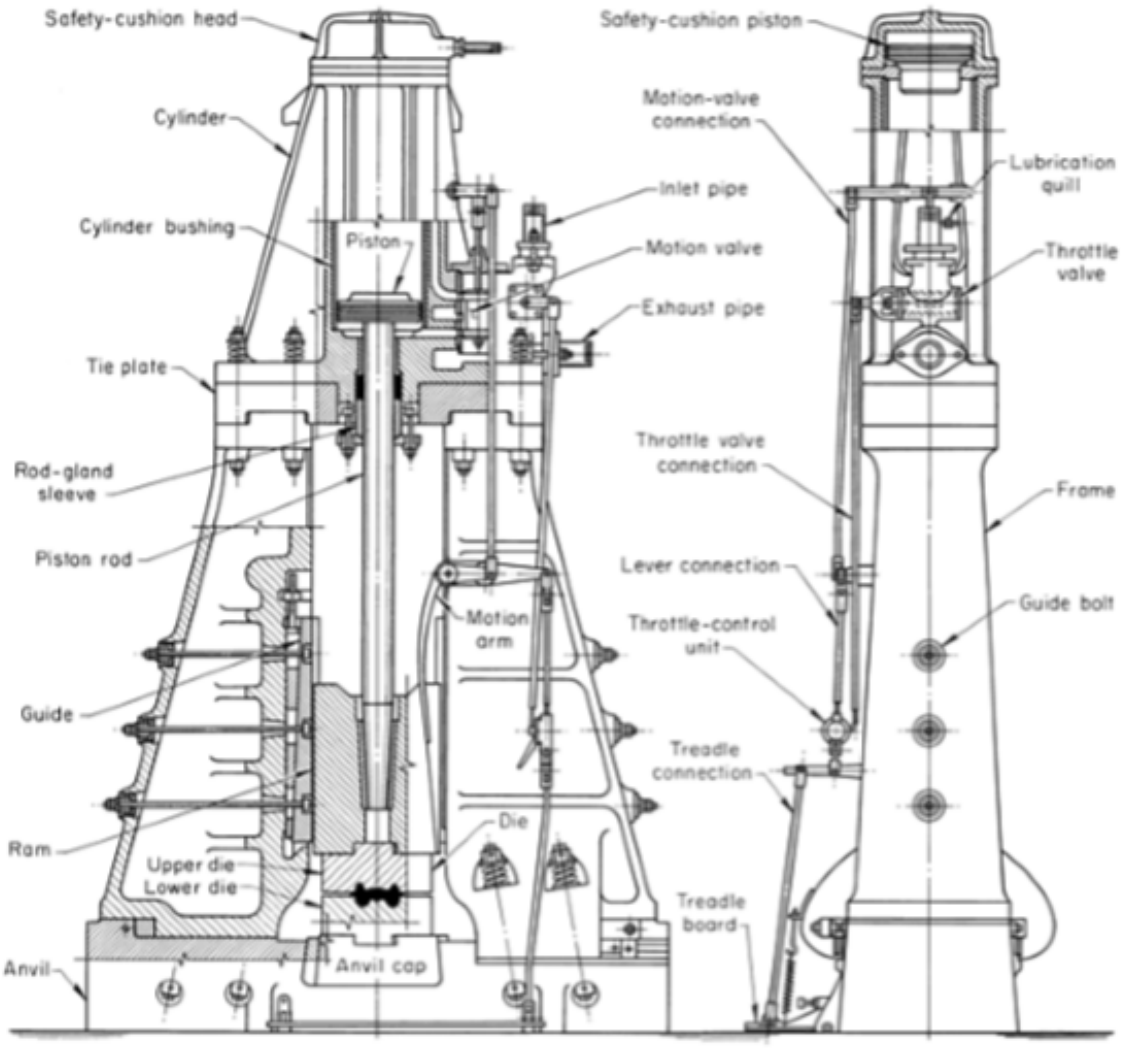

Figure 2.5.2.1 Schematic of the conventional power – drop hammer with its main components [12]

2.6 Other Types of Hammer Forging Equipment

Apart from the conventional hammer forging equipment already mentioned, there are still others that should be briefly discussed for completeness. Some of the other variations in the hammer forging equipment that exist, involve electrohydraulic gravity – drop, die forger, counterblow, open – die forging hammers and high energy rate forging (HERF) machines. The electrohydraulic gravity – drop hammer functions as combination

of both a gravity – drop and power – drop hammers. For example, in such equipment the ram of the hammer is lifted with oil pressure against an air cushion and then released. However as the air compresses, the upstroke speed of the ram is reduced, and in return the acceleration during downstroke is increased.

Die forger hammers on the other hand are more similar to power – drop hammers in operations, the difference however is that they have shorter strokes and faster striking rates [12]. Blow energy, efficiency, and forging sequence can be programed by the operator when using die forger hammers. Counterblow hammers are also similar to power – drop hammers, their use however is more common in Europe than in North America. Rather than having one ram and an anvil, counterblow hammers develop striking forces by making use of two rams simultaneously moving towards each other and meeting at a point midway. Some counterblow hammers can be pneumatically or hydraulically actuated, while others employ a mechanical – hydraulic or mechanical – pneumatic system [12]. The counterblow hammers can have a vertical or horizontal set – up, but their overall functionality remains the same. The rams of a counterblow hammer are capable of striking repeated blows, and by making use of two rams rather than a ram and an anvil, the impact vibrations are reduced. This feature found in counterblow hammers helps in delivering the full energy of the rams to the workpiece, improving plastic deformation of the workpiece and tool life as well.

Open – die forging hammers, can be made either with a single or double frame. Open – die forging equipment function in a similar manner as power – drop hammers, making use of steam or compressed air to drive the ram. Unlike the other hammer equipment mentioned, the die faces in open – die forging hammers do not make any

contact with one another. They are controlled by air or steam valves which are used to control the hammer piston [12]. Also open – die forging hammers are not directly attached to the frame which allow for heavier blows, without disrupting the frame assembly [12]. Finally high energy rate forging (HERF) machines, are essentially high – speed hammers that are capable of producing energy and striking forces well beyond those obtained by a standard power – drop hammer. HERF machines supply high energies for the forging process that would only be possible through the use of large size power – drop hammer, the machines themselves however are more complex and typically does not offer short cycle times [30].

2.7 Advantages and Disadvantages of the Hammer Forging Process

Fully understanding the capabilities of hammer forging machines is an important aspect that needs to be reviewed in order to achieve proper knowledge of the advantages and disadvantages of the hammer forging process. When compared to other forging machines, a hammer is the least expensive with the most versatile forging capabilities, which makes them somewhat unique. Hammer forging machines can be used for both small quantity and large quantity productions. Since hammer forging equipment are energy – restricted machines, the amount of energy used for different forging operations can be easily altered through changes to the drop height and extra power exerted during a downstroke. Some of the disadvantages of hammer forging however involve excessive vibrations and operators need to have a significant amount of experience to use the equipment. Due to the large striking blows generated by the hammers, a large amount of vibrations are generated in the system and in the shop floor as the energy that is not fully

used in the deformation of the workpiece is dissipated by the surroundings. In most cases the hammer forging process is performed by an experienced and highly trained operator. However, finding individuals with such experience is difficult and training them to obtain such level of skill can be costly and time consuming.

CHAPTER 3

LITERATURE REVIEW

As previously mentioned, the analysis of this thesis consists of an optimization approach for a manufacturing process using roll forging and hammer forging equipment. To facilitate the design process and minimize time and cost, process modeling simulations were performed prior to shop trials. The redesign process proposed in this study makes use of finite element simulations in an effort to develop an optimized forging process. For such reason it is important to review and identify how finite element simulations have been used in the past and how it has influenced the forging process design of today. Roll forging is an important part of the forging sequence being analyzed, as such, it requires a thorough understanding of the process to perform accurate simulations. Similarly, hammer forging simulations done in the past need to be reviewed in order to identify proper process modeling techniques. Relevant die design and process optimization techniques also need to be reviewed in order to obtain an efficient optimization approach to use in the analysis.

3.1 Finite Element (FE) Based Computer Simulations

Over the past 40 – 50 years, the use of finite element modeling (FEM) has become an integral part of processing control and product quality in forging. An article written by Howson and Delgado [21] in the late 1980's discusses the importance of using FEM in forging applications and how metal flow can be closely approximated through the software. Metal flow observed from computer simulations can be used to identify die

filling, forging defects such as laps, and metal flow patterns that would be undesirable during forging. Based on sample simulations performed, it was noted that workpiece heat up was common, however such increases in temperature could affect the microstructure of the parts being forged. Other sample simulations were performed in order to identify die filling and lap formation. For example, tools which were known to cause laps in the part being forged were modeled and simulated to validate the software. Once occurrence of a lap was predicted, die geometries were changed and simulated to evaluate how the modifications improved metal flow and part quality. Due to the limited computational capabilities of the time, three dimensional (3D) modeling was too complex and therefore not available when the research was done. The type of equipment used, such as hammers or press, for the simulations was not mentioned, however the investigation proved that the use of FEM for process modeling in forging was essential.

Although 2D models used for process modeling simulations have been considered state – of – the art in the past decades, increasing complexity of part geometry has led to the need for 3D modeling to achieve better accuracy. An article written by Ngaile and Altan [26] details the impact that 3D FEM has had in the forging industry in the recent years. As stated by Howson and Delgado the use of FEM for forging process modeling has been essential in the past, similarly Ngaile and Altan confirm its importance in the present day. The possibility of optimizing metal flow, forging sequences and conducting die stress analysis before actual testing has been made possible through FE simulations. By modeling the forging process in a computer before conducting physical trials on the shop floor, manufacturing engineers are able to reduce part development time and cost. At the same time, quality and productivity is also improved. Ngaile and Altan note that

the use of 3D process models has gained wide acceptance in the forging industry. This has led to the improvements of computer algorithms and developments of user friendly interfaces making simulations more practical for a variety of different applications. In their research Ngaile and Altan also emphasized the need to use correct data inputs and suggested selecting such inputs carefully.

When discussing the use of input data for FE simulations, it is important to keep in mind that the validity of the results heavily depends on the quality of the input parameters used. Inputs for material data like flow stress and other variables such as temperature, strain, strain rate, and friction are crucial. However, most current forging softwares contain detailed information based on past research and experience that make it less challenging for a user to identify the correct data to use. Ngaile and Altan [26] provided suggestions for friction factor values to use, most of these suggestions however pertained to specific lubricants, while the current research involves a dry forging process. Whenever a friction factor for computer simulations was not known, the use of ring tests was suggested.

Examples of case studies analyzed in the article by Ngaile and Altan, include the hot forging simulation of aerospace components and tool life in cold forging of bevel gears. In the former, the 3D FEM simulation was performed using the commercial software program DEFORM to obtain a better understanding of the temperature and strain distribution during forging. In the process, metal flow and die filling was studied, furthermore die stress analysis was conducted to verify the design proposed. In the latter, a numerical process simulation and stress analysis was used to predict the pressure distribution on the forging tools at the material – die interface. In doing so the FE model

was used to predict how changes to the die design would affect the pressure on the dies and improve the die life. As demonstrated by Howson, Delgado, Ngaile, and Altan, the use of FE process modeling simulations is instrumental in achieving further improvements in the forging industry.

Prior to the development of computers, analyses made regarding plastic deformation of parts involved the use of simple theoretical calculations. The simple theoretical procedures as mentioned by M. Math [24] prior to the development of FEM involved closed form calculation rules or theories, based on bounding theorems such as the slip line theory. It is for that reason that the parts used for analyses were simple and symmetrical. However, the assumptions and simplifications used did not provide accurate results and led to the development of computer modeling techniques in the 1950's. It further expanded upon in the 1970's with the finite element method making use of higher plasticity theories than previously used. Over the years many FE based forging softwares have been developed making use of 2D and 3D models. Examples of these include softwares such ABAQUS, Autoforge, DEFORM and FORGE2/3.

3.2 Simulating the Roll Forging Process

Metal flow in roll forging is a complex process though computer simulations have enabled designers to obtain more insight. Due to the lack of symmetry, most simulations have been based on 3D models in order to obtain accurate results. Biba, Vlasov, and Stebounov [14] used FE simulations to predict how changes to the roll profile and pass sequence would affect the material spread during deformation. In their simulations, roll forging was used as a preforming operation, for the forging of a crankshaft in a

mechanical press. Due to its ability to properly distribute volume, the roll forging operation is commonly used to develop preforms in forging processes. To model the roll forging dies Biba and co – workers used a special program known as VeraCAD, which was developed from empirically based forging rules. The program had the capability of calculating flash, calibration sequences, size of raw material, and the number of necessary passes for the dies. Once modeling of the rolling dies was completed the finite element simulations were carried out using the commercial forging software of QForm.

Biba and co – workers simulated two passes through the roll forging dies, as expected the billet was affected by elongation and cross spreading. It was noticed that in order to prevent the formation of a large flash during the roll forging process, the width of the groove needed to be large enough to allow for proper cross spreading. Properly dimensioning the width of the groove in the roll forging dies would allow for multiple passes without defects. Interestingly, some defects such as slugs were observed during the simulation when the billet was not positioned correctly for the second pass. Slug defects are partial formations of flash between the roll forging dies and develop when the groove widths are too small for the cross spread caused by the deformation of the billet. Biba and co – workers, suggest that such defects could be eliminated by proper positioning of the billet prior to the start of a roll pass. The work done by these researchers provide good recommendations for avoiding defects in the roll forging process that can be used in related FEM simulations.

In the early 2000's, Karacaovali [22] simulated the roll forging process to study the accuracy of using symmetry assumptions. His goal was to determine how the model predictions compared to parts obtained from experimental tests. It was observed that

when using symmetry conditions the time needed to complete the simulations for multiple passes through rolling dies, was quite short, roughly 40 minutes. Due to the simplifying assumptions only one quarter section of the billet was used which required a smaller mesh size, reducing the computational time needed to complete the simulation. Also, a total of four passes were simulated for the analyses. Due to the geometry of the billet after each pass, modified groove segment geometries were used to continue decreasing and increasing height and length of the billet, respectively.

Karacaovali also performed simulations using a full model of the billet geometry without symmetry assumptions, and found that computational time increased greatly. It was observed that when using the full billet model, simulation of four passes through the roll forging dies took approximately six hours to complete. This however was expected since a much larger number of elements in the mesh size was needed for the process. Similar trends were observed in both cases, such as increases in temperature at the point of contact between dies and workpiece, as well as increase in mesh size caused by remeshing after each pass through the roll forging dies.

When comparing both cases to the actual parts obtained from experimental tests, Karacaovali observed that the full model demonstrated better agreement with the experimental parts than the symmetry model. It was suggested by Karacaovali that misalignment of the dies during set up might have caused the differences between the symmetry model and the parts from the experiment. Although the full model was in better agreement, some notable differences were still present when the comparison was made. Perhaps one of the main reasons for such variations might have been due to the mesh size and mesh type used during the finite element simulation. The mesh used for the

simulation contained approximately 2772 elements at the start of the process and roughly 5666 elements at the end of the process. Also, the mesh type used was hexahedral eight node brick elements. Using a finer mesh and different mesh type might have provided more accurate modeling results even though computational time would have been greatly increased.

3.3 Simulating the Hammer Forging Process

Computer simulations of the hammer forging process based on the FE method have been done in the past, however, there has been difficulty in obtaining accurate results. Studies such as the one done by Park [27] in the 1980's attempted to make use of FEM to simulate a hammer forging process. In his work, Park provided a thorough explanation of the theory behind the hammer forging process, providing more insight into the computational methods used during the simulation. The simulations were performed using a modified version of the process modeling software program A.L.P.I.D (Analysis of Large Plastic Increment Deformation) version 1.4 which was developed at Battelle Laboratories in Columbus, Ohio. The simulations performed made use of a gravity – drop and a power – drop hammer, however the results obtained were not very accurate. The approach consisted of using 2D models under isothermal conditions for the simulations in the case studies being analyzed.

Perhaps the reason for why such an approach was taken in Park's research was due to the complexity of remeshing during process modeling simulations. At the time of the study, remeshing of the workpiece and dies was rather time consuming and had to be performed manually. Such conditions made the study difficult, preventing more detailed

simulations with more accurate results. In reality, the hammer forging process is complex, regardless of the type of equipment used. Improvement of the accuracy of a virtual hammer forging process requires the use of 3D models under non – isothermal conditions. This is crucial in order to properly account for heat loss throughout the process and have a better understanding of the metal flow as well. Although an isothermal process can be used as an initial approach, the non – isothermal process provides more accurate predictions of a forging process and the effects of die design.

The development of automatic re – meshing algorithms enables complex process modeling simulations to be performed in a timelier manner than manual remeshing. A research done in the late 1990's by Yang and Yoo [32] sought to develop an efficient 3D elastic – plastic finite element formula and code to study the dynamic behavior of impact forging that could be applied to simulate industrial parts. Two simulation methods were analyzed, one was an explicit FE method which incorporated the Johnson – Cook yield model and the Central Difference method for the development of the mesh. The other was an implicit FE method which made use of the Newmark and Newton – Raphson method in the development of the mesh. In order to compare the two re – meshing algorithms, Yang and Yoo performed an experimental test.

The validity of the proposed algorithms were compared and verified through a copper blow test. The copper blow test, made use of a copper cylinder specimen that was upset between two flat dies. Once completed the simulation results were compared to the results of the copper blow test by looking at height reduction percent vs forging load. The results obtained for the two methods analyzed were in good agreement with the results obtained from the copper blow test which justified their use in industrial applications.

Yang and Yoo proceeded to perform a simulation of a turbine blade using a multi – blow, hammer forging process. The dies used for the process simulation were assumed to be elastic. The assumptions used by Yang and Yoo were more realistic than the ones Park used, however, some errors were still encountered. Issues regarding volume loss during remeshing were observed and it was suggested that increasing mesh size could help correct the problems seen. In the analysis it is not clear if a hammer forging template was used for the simulations, taking into account dwell time and heat loss during transfer, which is an important aspect of the process that should not be dismissed. The study performed on the FE remeshing codes has allowed for more accurate approximations using 3D models which can be further improved by taking into account heat transfer between workpiece, dies, and environment.

Identifying the correct data inputs that should be used for process modeling simulations can be difficult. However, with improved software developments, identifying proper data has become slightly less challenging. In the late 1990's, Hallstrom [20] analyzed the influence of friction on die filling using a counterblow hammer. Typically FE based forging softwares such as FORM2D, in this case, make use of friction factor values for their simulations. Identifying the correct friction factor value to use is difficult, especially for a hammer forging process in which impact occurs at relatively fast speeds. In his study of friction, Hallstrom used 2D models to analyze how different values of friction affected die fill and final tool closure. He did this by performing multiple simulations in which different variations of friction factors were used for the top and bottom die. It is for such reason that multiple models were needed and hence the less time consuming 2D models were preferred.

The study done made use of an oil/graphite mixture lubricant for the top die and no lubricant for the bottom die. When compared to actual parts, the friction factor values that matched the best were that of $m = 0.2$ for the upper die containing an oil/graphite mixture lubricant and of $m = 1$ for the lower die containing no lubricant. The friction factor value used for an oil/graphite mixture lubrication in Yang and Yoo's study, was noted to be the same as that of Hallstrom. The friction factor value suggested for dry forging however, could be applied to the simulations in the study of this thesis. Hallstrom's simulations contained some errors such as underfill, which he suggested could have been caused by temperature gradients due to dwell time. Interestingly, it was observed that the final tool distance seemed to remain somewhat unaffected with different friction factor values.

Although the research done by Hallstrom did take into account dwell time for the hammer forging process simulations, it did not specify the use of hammer blow efficiency. Taking into account the blow efficiency would have significantly changed the process modeling results. In the work done by Park, a constant hammer blow efficiency of 0.85 was used. Even though the value recommended by Park is functional to a certain extent, it is perhaps more reasonable to use different hammer blow efficiencies for multiple operations. In closed die forging these operations would make use of an edger, blocker, and finisher impression.

Other studies similar to the one done by Hallstrom have been done in efforts to identify proper inputs needed to simulate hammer forging processes. The work done by De Arizon, Filippi, Barboza, and D'Alvise [15] considered this topic in order to obtain more realistic results. Mechanical properties of the workpiece, properties of the tool –

workpiece interface, initial shape of the workpiece, tool geometry, tool speed, and energy required for deformation of the part are all basic information needed for process modeling. Boundary conditions such as contact between the workpiece and dies during the deformation process are also important as well as thermal conditions. Thermal conditions are discussed and noted that during a hot forging process the workpiece is heated to high temperatures in order to reduce compression efforts during forging. Similarly, dies are preheated in efforts to reduce thermal shocks and cracking during the forging process.

For the analysis of the forging process performed by De Arizon and co – workers, the software code Morfeo (Manufacturing ORiented Finite Element tOol), developed in Belgium was used. A 2D model along with simplifying assumption such as symmetry of the workpiece were used. An upset operation was performed using a mechanical press simulation, and subsequent forging was done using a hammer forging simulation. The results showed that by reducing the total number of blows in the hammer forging process, an increase in finish die life was observed. In their 2D model, De Arizon and co – workers assumed circumstances that are somewhat questionable such as an isothermal process and frictionless conditions. It is not very clear whether the actual process made use of any lubrication or if it was performed under dry conditions. Such forging conditions would have altered the results of the simulations if taken into account. At the time that the paper was written, there was an attempt being made to perform 3D model simulations. The new simulations would provide better insight through more realistic results. The paper written by De Arizon and co – workers suggest that 2D models can be

used for the initial stages of FE simulations of simple geometries, however 3D models are necessary for a more significant analysis.

In recent years, more work has been done involving the use of 3D FE models taking into account important parameters to replicate forging processes as closely as possible. In 2013, Gontarz, [17] analyzed the hammer forging process of an AZ31 magnesium alloy rim through theoretical analysis and experimental testing. The analysis performed was due to unfavorable conditions identified during the forging process such as large strain rates and low tool temperatures. The study made use of the commercial FE based software of DEFORM 3D for the simulations and a steam – air – hammer for testing. Heat transfer between the workpiece and tool as well as with the environment was taken into account. The friction factor value used for an oil/ graphite based lubricant was compared and noted to be consistent with the one used by Hallstrom.

In contrast to other researchers mentioned in this section, Gontarz utilized the FE forging software to investigate the possible causes of overlapping during a forging process. To do this he performed two sets of forging sequences, one set involved a blocker and finisher impressions while the other involved an upset, blocker, and finisher impressions. The DEFORM models demonstrated that the forging sequence not involving an upsetting operation would cause overlapping in the forged part. The forging sequence involving an upset operation however, did not shown signs of overlapping when the part was reduced to a specified height of 2.8 in. (70mm). It was noted that if the part was upset to a height larger than the one mentioned, the possibility of overlapping became apparent. Based on the process modeling software it was predicted that a total of five hammer blows would be needed to forge the part without any overlaps.

For validation and comparison purposes, both forging sequences analyzed by Gontarz were tested through physical experiments. As predicted, the forging sequence not involving an upset operation showed overlapping, whereas the other did not. A deviation however from the latter forging sequence showed that when forging the part, a total of seven hammer blows were needed rather than five as initially predicted. Additional blows were needed in the blocker and finisher impressions. The results seen in the study demonstrated the importance of using an upsetting operation that should not be easily dismissed. Unlike Gontarz, the simulations in this thesis involve a forging process containing no lubricant. This is why the friction factor of m = 1 as recommended by Hallstrom was initially assumed. Also, in contrast to the project of this thesis, the analysis performed by Gontarz was done for a warm forging process whereas the former is performed for a hot forging process.

3.4 Die and Process Optimization for Improved Material Yield

The need for improvement of forging processes such as roll forging and hammer forging, is constantly looked upon in order to produce better quality parts in a more efficient manner. An example of this can be seen in the work done by Zhou, Jia, Liu, and Wang [33] for the optimization of roll forging dies. In their work, Zhou and co – workers discussed the common rectangular groove design used in roll forging dies and proposed a new design that could help improve material flow. The proposed design would also help reduce the damage experienced by the roll forging dies. The new design consisted of an oval and diamond combined groove geometry. Note that the simulations and experiments consisted of two passes through the roll forging dies. The first pass made use of the

proposed or traditional groove dies, while the second pass made use of hat groove geometry dies as shown in Figure 3.4.1.

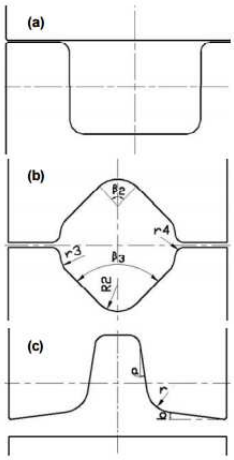

Figure 3.4.1 Cross sections of the roll forming dies, showing groove geometry. (a) Traditional, (b) Proposed, and (c) Hat groove geometry [32]

The analysis of the proposed geometry was done by FE model simulations and was later verified through experimental tests. From the simulations it was observed that using the proposed groove design for the first pass in the process, caused a more uniform material distribution in the cross section. A reduction in stress and strain at the contact area was also observed. The proposed groove design provided a smaller wear depth distribution in the simulation models as well. When comparing the experimental results to the FE models, it was concluded that there was good agreement. When comparing the results of the experimental tests for the traditional rectangular – hat groove rolling sequence with that of the proposed special shaped – hat groove rolling sequence, it was observed that an improved metal distribution was obtained as predicted. The proposed design suggested by Zhou and co – workers for the groove geometry was observed to produce good results that could potentially be utilized in this thesis.

Similar to the work done by Zhou and co – workers, other research has been done on the subject of improving metal flow through die design. In 2008, Ervasti [16] performed a series of analyses attempting to improve material yield. Here, the term "material yield" represents the amount of material correctly utilized in the forging of a part through proper volume distribution. One of the analyses performed by Ervasti involved the use of the roll forging process. Ervasti, points out that by increasing material yield in the forging of a product, the amount of material scrapped at the end of a process would be decreased. In order to optimize the preform geometry in his work, Ervasti decided to start the process by looking at the final forged part and dividing it into different sections. Once the final forged part was divided, it was easier to identify how much volume was needed per section. For better understanding, Figure 3.4.2 has been provided illustrating the critical sections that were analyzed.

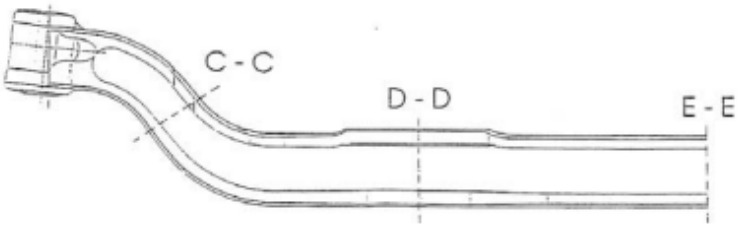

Figure 3.4.2 Critical sections for a front axle beam [16]

It was noted that after one pass in the roll forging dies and bending, section C – C from Figure 3.4.2, contained a circular cross – section, while sections D – D and E – E contained rectangular cross – sections. Through FE simulations it was determined that material yield was improved when all cross – sections in the preform were changed to circular rather than a mixtures of circular and rectangular cross – sections. It was suggested that by using the new set of cross – section geometry, the material yield for

sections C – C, D – D, and E – E, would improve by 4.5%, 7.6%, and 2.6%, respectively. The proposed changes by Ervasti were accepted and used in production. The analysis done provided great insight in terms of approaching a solution by first analyzing the finished product.

Apart from optimizing preforms in roll forging processes, Ervasti, also performed an analysis involving material yield in a closed die forging using a hammer forging process. The analysis of the material yield in closed die forging was performed for heavy crown wheels. For improving the material yield in the process, a new die design was proposed. The concept of hammer blows were briefly discussed and it was noted that during finishing operations, only a small amount of the total energy available is transferred to the workpiece. This means that there is a larger amount of plastic deformation of the workpiece during initial blows than final blows. By improving die design however, the number of hammer of blows used to forge a part could be reduced. In the proposed die design, Ervasti made use of larger draft angles and added new features, which improved the load while reducing the total number of hammer blows needed. Figure 3.4.3 has been provided, to show a comparison between the old and the initial proposed die design and demonstrate the impact it has on pressure.

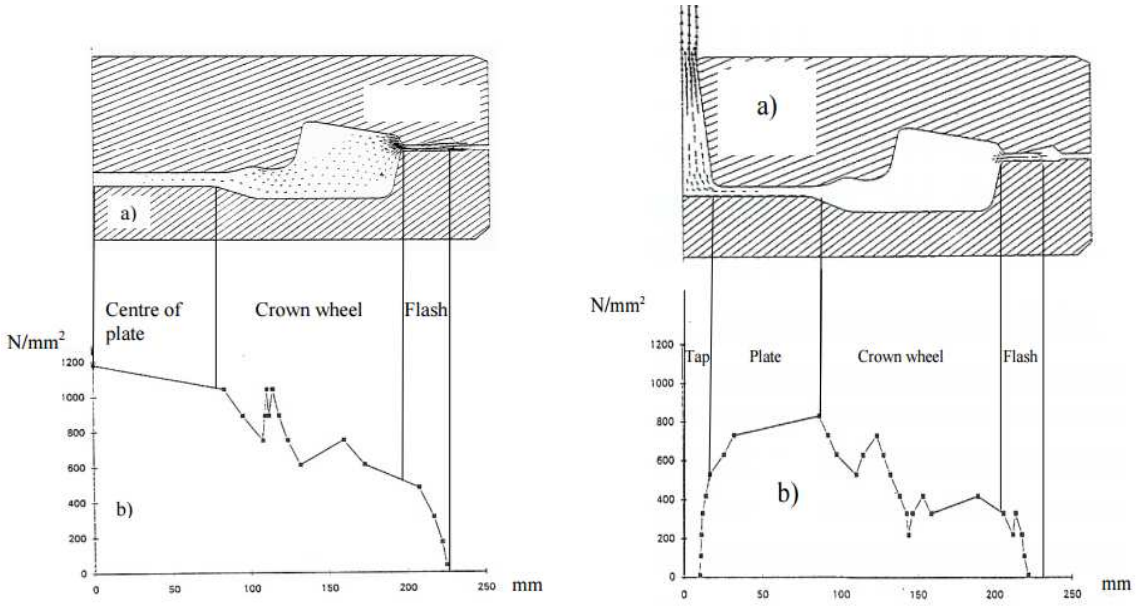

(1) (2)

Figure 3.4.3 Die design and corresponding pressures. (1) Old design and (2) First iteration of proposed design [16]

Multiple iterations were made before reaching an optimal design. The final proposed design by Ervasti made use of two tap features similar to the one seen in Figure 3.4.3. The taps however, were included in both the top and bottom dies. With the final proposed design, it was predicted that the total number of hammer blows needed to forge the part would be reduced. Through experimental testing it was confirmed that the proposed design did reduce the number of hammer blows by approximately 33%. The die design used by Ervasti, is quite different than the one analyzed in this thesis. However, a similar approach can be used for optimization.

Although the investigation of this thesis involves the use of hammer forging equipment and flash, analysis of flashless forgings with press equipment can be of help in the optimization process. The work done by Takemasu, Vasquez, Painter, and Altan [29] investigated metal flow and preform optimization in the flashless forging of a connecting

rod. Unlike operations involving flash, a flashless operation needs to be carefully analyzed for accurate volume distribution in the process. By examining the approach taken by Takemasu and co – workers, the volume distribution in the analysis of this thesis can be more effective.

Similar to the approach taken by Ervasti, Takemasu and co – workers divided the preform used in the process into different sections which could be optimized independently. The analysis was done using a 3D FE model in DEFORM due to the complexity of the part geometry. The type of workpiece material and forging equipment used for the simulation process was aluminum and a hydraulic press, respectively. For validation purposes the first set of simulations were performed using the original preform to see how well the FE model compared to the forged part. In order to save cost in physical trials, plasticine billets and aluminum tooling were used. Once a good agreement was reached the optimization took place. As mentioned, the crankshaft was divided into three sections termed, large end, connecting I – Beam, and small end sections. For each section, different geometries were modeled and simulated to see what combination would provide the best results. An example of the changes made to the geometry of the large end of the crankshaft is shown in Figure 3.4.4 and the simulations results in Figure 3.4.5. Note that the terms BT0, BT1, and BT2, represent the original geometry, proposed geometry # 1, and proposed geometry # 2, respectively.

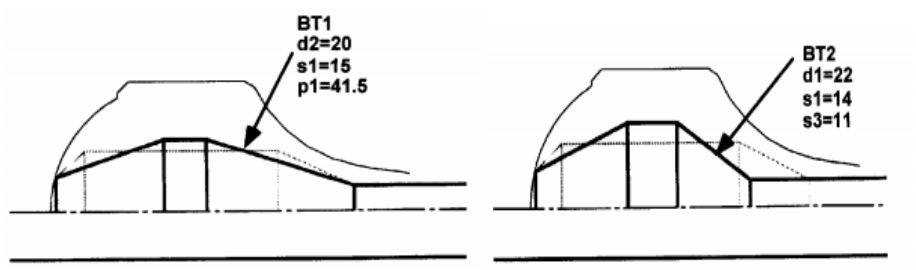

(a) (b)

Figure 3.4.4 Proposed geometry changes for the large end of the crankshaft analysis. (a) Proposed change # 1 and (b) Proposed change # 2 [29]

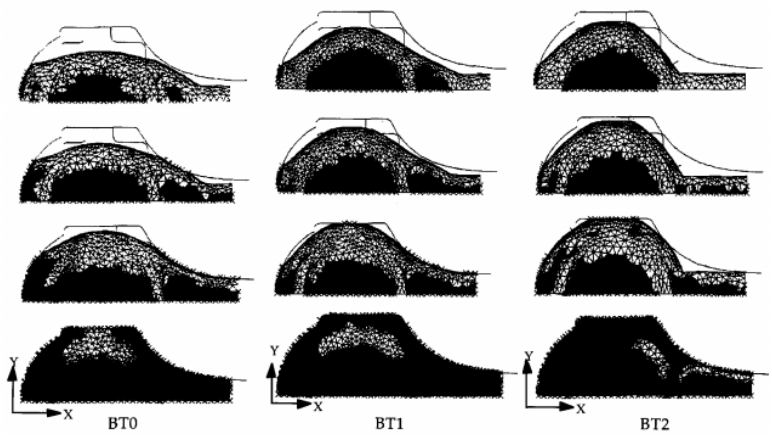

Figure 3.4.5 Simulation results for the large end of the crankshaft analysis. BTO – original, BT1 – proposed changes #1, BT2 – proposed changes #2. Black regions represent contact areas with the die [29]

Similarly the same approach was taken for the small end section optimization, and is shown in figures 3.4.6. In this case the terms TP1, TP2, and TP3, represent the original geometry, proposed geometry # 1, and proposed geometry # 2, respectively.

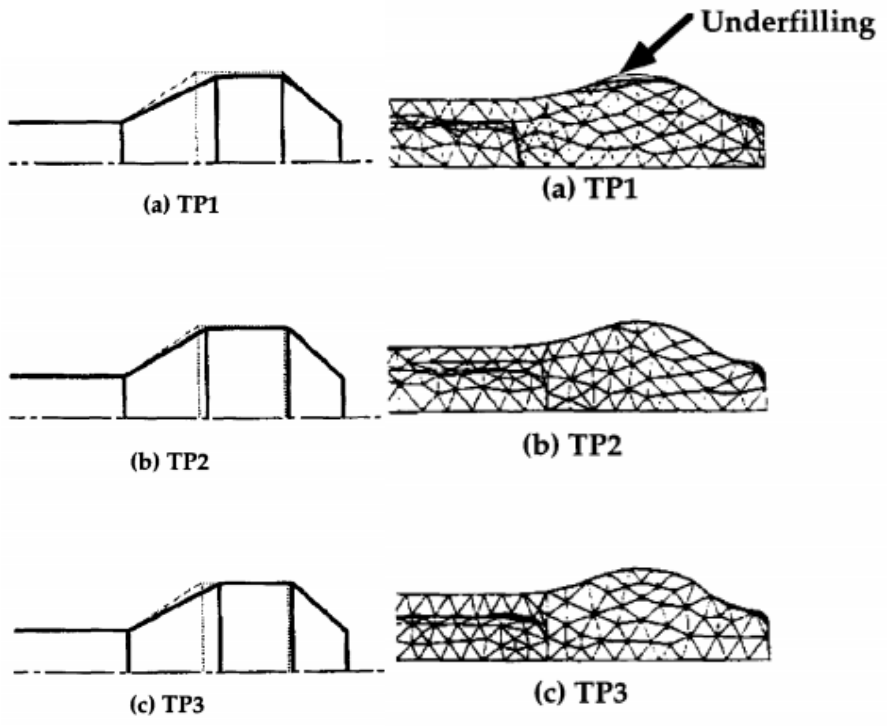

(1) (2)

Figure 3.4.6 Geometry and simulation results for the small end of the crankshaft analysis. (1) Geometry models and (2) FEM results [29]

A similar approach was taken for the connecting I – Beam section, however drastic changes were not observed sinnce the geometry of the section was simple in comparison to the others. After analysis of the individual sections was completed, a new preform geometry was proposed. When compared to the original preform it was observed that there was a higher peak load with the proposed preform, however better contact between dies and workpiece was achieved, improving material flow as expected. Due to the positive results seen, the ideas suggested by Takemasu and co – workers could potentially be implemented to the optimization of the preform being done in this thesis.

The design of the preform plays an important role in the optimization of a forging process as previously seen, other factors however can also have a large impact as well. The work done by Movrin, Plancak, Vilotic, Milutinovic, Shakun, Luzanin, and

Trbojevic [25] analyzed the optimization and design of multistage hot forging processes through FE simulations and experimental verification for a wheel hub and joint socket. In both sets of simulations a hammer forging process was modeled. The objective of the research was to obtain complete die fill, reduce the amount of contact stress, and potentially minimize the number of steps used in the forging process. For the simulations, the commercial software of Simufact.Forming 9.0 was used prior to experimental trials.

The optimization of the wheel hub forging was simple in comparison to the joint socket, due to its geometry. It was observed that by reducing the amount of top die traveled in the upset operation of the wheel hub forging process, better die fill and less stress was seen in subsequent forging operations. Similarly for the joint socket, a free upset operation was used on one end of the billet which helped to improve die fill and stress values than previously seen. The predictions made by Movrin and co –workers were confirmed by experimental tests. The study done by Movrin and co –workers helped to understand that optimization of a forging process entails more than die design itself. By analyzing different optimization approaches used in the past, the modifications needed for a more efficient process of the project of this thesis become much clearer.

CHAPTER 4

SOFTWARE AND INPUT PARAMETERS FOR PROCESS MODELING SIMULATIONS

4.1 Modeling Software Used

Prior to performing the FEM simulations, solid model representations of the tool geometries used in the roll forming and hammer forging processes were developed. The commercial 3D solid/surface modeling software Siemens NX PLM version 8.5 (NX 8.5) was used to model the roll reducer and die block impressions. Once 3D geometric representations of the tool geometries were completed the part files were converted to STereoLithography (STL) file formats. STL file formats are compatible with a variety of process modeling software such as DEFORM, and are also used for rapid prototyping, 3D printing, and computer aided manufacturing. The converted STL files were then imported into the DEFORM process modeling software to perform simulations of the existing and proposed wrench forging processes.

The process modeling software used for simulations of the existing and proposed wrench forging processes was the commercial forging software DEFORM V.10.2 from Scientific Forming Technologies Corporation (SFTC). The process modeling simulations performed in DEFORM V.10.2, made use of the software's 3D module for better accuracy of the asymmetric part geometries. The 3D module of DEFORM, for forging operations is an "open system" which contains and supports user defined routines and variables for advanced simulation problems. Also, the software module enabled the possibility of non – isothermal simulations for the roll and hammer forging operations

needed for the analysis. The use of the DEFORM V.10.2, 3D module helped evaluate tool redesign as well as forging sequences. After various iterations, the best redesign and forging sequence capable improving metal flow, die fill, reduction of flash and reduction of total number of hammer blows required to forge the part was selected.

4.2 Overview of Input Parameters for Process Modeling in DEFORM

4.2.1 Workpiece and Die Material

Selecting the correct workpiece material was important in order to obtain accurate simulation results. However, due to the limited amount of data available, there is a limited amount of materials within the program that can be selected for process modeling simulations. In cases like these a close approximation based on the chemical composition of the material is reasonable. At GBDF the actual workpiece material used for the production of the large wrench being analyzed is an AISI 4047 low alloy steel. Some of the common elements present in AISI 4047 steel include carbon, iron, manganese and molybdenum. Alloying elements such as manganese and molybdenum are added to improve the workability, toughness and hardenability of the steels required by the forged wrench. As DEFORM's material library does not contain data for an AISI 4047 steel, an alternative material was selected for the process modeling simulations. An AISI 4140 steel was selected as the workpiece material for the simulation trials, as its chemical composition in weight percentages, is close to that of an AISI 4047 steel as shown in Table 4.2.1.1.

Table 4.2.1.1 Comparison of chemical composition in weight percent (% wt.) for AISI 4047 and AISI 4140 Steel [1], [6]

Composition Elements	AISI 4047 Steel	AISI 4140 Steel
Carbon, C	0.45 - 0.50	0.380 - 0.430
Iron, Fe	97.87 - 98.51	96.785 - 97.77
Manganese, Mn	0.70 - 0.90	0.75 - 1.0
Molybdenum, Mo	0.20 - 0.30	0.15 - 0.25
Phosphorous, P	<= 0.035	0.035
Silicon, Si	0.15 - 0.35	0.15 - 0.30
Sulfur, S	<= 0.040	0.04
Chromium, Cr	--	0.80 - 1.10

Also, AISI 4140 steel was readily available for experimental testing, which helped to narrow down the selection of an alternative material for simulation trials. It is important to note that part materials such as the ones for a large wrench are specified by the customer. However, using a close alternative material for simulation purposes can nonetheless produce satisfactory approximations of actual forging results when data of the desired material is not available.

Similarly, the die material selected was dictated by the limited available data in the DEFORM material library. Based on discussions with the staff of GBDF, it was mentioned that the die material used for the wrench forging process is a Finkl FX – XTRA forming die steel. Hammer forging dies are exposed to high impact loads and elevated temperatures during usage. Consequently it is important that forging tools be made of materials having high hardenability and fracture toughness like Finkl FX – XTRA, in order to achieve reasonable die life. A combination of nickel, chromium, and molybdenum alloying elements provide a good balance between fracture toughness and wear resistance that are needed in hammer forging dies. Based on past research and forging practice it was noted that H – 13 is commonly used in hot forging operations and

was available in the DEFORM database. It was for such reason that H – 13 was selected as the die material for the simulations. It is important to point out that the chemical composition between the two die steels showed some large differences. For simulation purposes however, it was concluded that the thermal properties of H – 13 would suffice as die stress was not a primary focus. Table 4.2.1.2 has been included to show a comparison between the chemical compositions of the two die steels.

Table 4.2.1.2 Chemical composition comparison of FX –XTRA and H – 13 die steel [3], [4]

Composition Elements	FX - XTRA Die Steel	H - 13 Die Steel
Carbon, C	0.5	0.38
Manganese, Mn	0.85	0.3
Silicon, Si	0.25	1
Nickel, Ni	0.9	--
Chromium, Cr	1.15	5.2
Molybdenum, Mo	0.5	1.35
Vanadium, V	0.05	1

When comparing some of the mechanical and thermal properties of the two die steels, it was observed that there were some differences. Once again due to the given circumstances, it was concluded that H – 13 would suffice for simulation purposes. Table 4.2.1.3, has been provided to show some of the differences between the mechanical and thermal properties of the two die steels.

Table 4.2.1.3 Comparison of mechanical and thermal properties of FX –XTRA and H – 13 die steel [2], [4]

	Properties	FX Die Steel	H - 13 Die Steel
Mechanical	*Tensile Strength (Ksi)*	196	289
	Yield Strength (Ksi)	166	239
	Modulus of Elasticity (Ksi)	29000	30500
Thermal	*Specific Heat Capacity (BTU/lb˚F)*	0.11	0.11
	Thermal Conductivity (BTU/ft^2/in/hr/˚F)	205	169

It is important to mention that the Finkl FX – XTRA die steel is available in different temper designations, designated as T1, T2, T3, T4, H and XH which refers to the maximum hardness values that can be achieved. Brinell hardness values for the mentioned tempers range from 277 – 534 BHN. Note that as die temperature increases, the hardness value decreases. The temper of the Finkl FX – XTRA die steel used at GBDF is a T1 temper, which has a brinell hardness range of 401 – 429 BHN. Higher hardness tempers like T1 are good for higher temperatures and cavity pressures [4] which are commonly experienced in drop hammer forging operations.

4.2.2 Workpiece and Die Temperatures

Isothermal and non – isothermal simulations can be performed in DEFORM V.10.2. In isothermal simulations the temperature of the workpiece remains the same throughout the simulation process. In non – isothermal simulations, the temperature of the workpiece is constantly changing due to influences of die and environment temperatures in the model. Depending on the type of simulation performed, the computational time and results will be affected. Using isothermal conditions for process modeling simulations are reasonable only for the initial stages of hot forging simulations.

Using isothermal conditions for a hot forging process simulations reduces the computational time significantly since heat transfer calculations between dies, workpiece and the environment are eliminated. Note that an approximate design can be obtained when using isothermal conditions for a hot forging process, but it is refined when the simulations are performed again using non – isothermal conditions. The same approach has been done in the past for forging optimization purposes, as described in Chapter 3. Using both methods can help improve simulation time for the optimization process. In this analysis, simulations of the existing and proposed wrench forging process were initially performed using isothermal conditions. This allowed for multiple iterations to be performed in a timely manner and the final design iteration was simulated using non – isothermal conditions to obtain more accurate results.

In an effort to obtain accurate results, heat transfer between workpiece, dies and environment needed to be accounted for in the simulation model. From a discussion with GBDF personnel, it was established that billets at ambient temperature are place in a gas fired furnace set to a temperature of approximately 2300 ˚F, for 10 minutes. The simulations performed in DEFORM involved a variety of heat transfer simulations to maintain consistency with the actual forging process as closely as possible. As such, the starting workpiece temperature in the simulations was set to an approximate ambient temperature of 70 ˚F. Heat up to a forging temperature between 2200 – 2300 ˚F was achieved through a heat transfer simulations with the environment for 10 minutes.

Unlike the workpiece temperature, die temperatures were set to a starting temperature of 300 ˚F. The staff from GBDF mentioned that die surfaces are typically pre – heated for the forging processes. For this specific operations the pre – heat was done at

a temperature of 300 ˚F. Similar to the workpiece, a variation of temperature changes was expected for the dies due to heat transfer and heat generated from impact pressures.

4.2.3 Mesh Size

The mesh size selected for the simulations performed in this analysis played a key role in obtaining good simulation results. Note that a smaller mesh size is typically used in 2D simulations due to the simplicity of the models and the less time consuming calculations. When using complex 3D geometry however, it is important to use a larger number of elements and nodes to obtain better accuracy and resolution. A mesh size that makes use of small number of elements and nodes is termed a coarse mesh, while a mesh size involving a larger number of elements and nodes is termed a fine mesh. Some issues that might occur when using a coarse mesh for 3D simulations are mesh degradation, excessive volume loss, and remeshing problems. Although a finer mesh helps to improve the mentioned issues, the amount of time needed to perform the simulations is greatly increased. Figure 4.2.3.1 shown below demonstrates the difference between using the two mesh types described. Note that the coarse mesh contains 26650 number of elements and 6146 number of nodes, while the fine mesh contains 204619 number of elements and 44154 number of nodes.

Top View

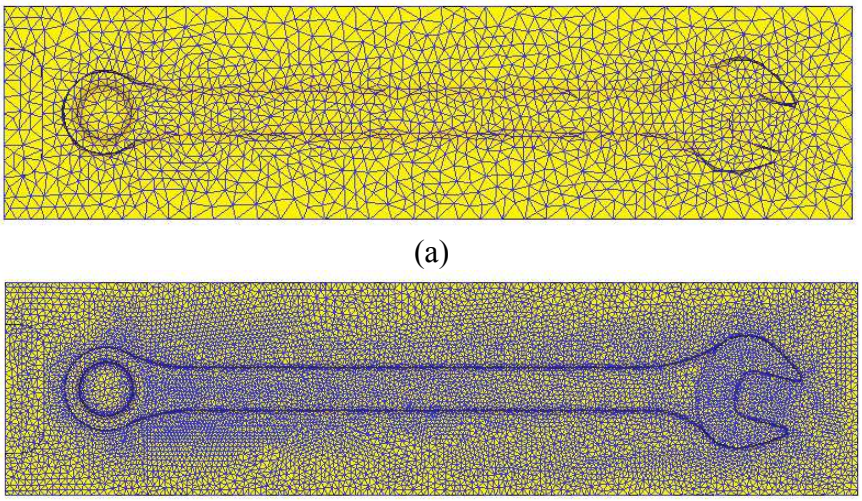

(a)

(b)

Figure 4.2.3.1 Coarse and fine mesh comparison for the blocker die impression. (a) Coarse and (b) Fine mesh

4.2.4 Friction Factor

The use of friction in forging simulations, is also important to obtain good modeling results regarding metal flow and die fill. Friction models can be divided into two categories known as shear friction and coulomb friction in which:

Shear Friction: $f_s = mk$ EQN (4.2.4.1)
Coulomb Friction: $f_s = \mu p$ EQN (4.2.4.2)

Where:
f_s is the frictional stress
m and μ are friction factor and coefficient of friction, respectively
k is the shear yield stress of the material
p is the interface pressure between two bodies

Constant shear friction is used mostly for bulk – forming simulations, whereas coulomb friction is mostly used in simulations where contact occurs between two elastically deforming bodies or between an elastic and rigid body, such as sheet forming. It should be noted that the input variable needed for simulations is either the friction

factor or coefficient of friction, depending on the type of simulation being performed. In this case the simulations were performed for a bulk – forming process, which involved roll and hammer forging operations. It is for such reason that a constant shear friction factor was used. Past researchers have recommended using friction factor values of 0.7 and 1.0 for processes involves dry forging conditions, as in this case. Such range of values was verified by looking at the DEFORM user manual which suggested using friction factor values ranging between 0.7 – 0.9 for unlubricated forging conditions.

For comparison purposes a variety of forging simulations were performed to identify how changing the friction factor value would affect the simulation results. Two sets of simulations were performed for a roll forging operation using friction factor values of 0.7 and 1.0. It was determined that there was better agreement between the DEFORM models and forged platters when a value of 0.7 was used for the friction factor. Similarly, four sets of hammer forging simulations for one hit in the edger impression were conducted. The friction factor values used in the comparison were 0.1, 0.3, 0.7, and 1.0. The simulations consisted of a constant die movement, using a calculated velocity for the hammer forging process being analyzed and deforming the workpiece to a specified height previously measured on the forged platter. The amount of energy needed for the deformation of the workpiece in each simulation was compared to the total kinetic energy available in the hammer forging equipment. The total kinetic energy available in the hammer forging equipment was calculated as a function of mass, ram and top die, and drop height, more details will be provided in a later sub – section. It was observed from the simulation results that the amount of energy used for the deformation of the workpiece when using a friction factor of 0.1, 0.3, 0.7, and 1.0 were all larger than that

calculated energy available for the given hammer forging equipment. The friction factor of 0.7 however, seemed to provide the best results and therefore was selected for the hammer forging simulations.

4.2.5 Heat Transfer Conditions

Performing non – isothermal simulations in DEFORM involved the use of heat transfer coefficients in order to obtain results that closely resemble the actual forging process. One method of estimating correct values to use can be made through the use of pyrometer readings. The pyrometer is a non – contacting device that intercepts and measures thermal radiation, which in turn determines the surface temperature of an object. A set of simulations were be performed using a variation of heat transfer coefficients and compared to pyrometer temperature readings. Although pyrometer readings are not exact, it is useful in providing close approximations of surface temperatures during hammer forging processes. Note that pyrometers can only give feedback which helps to decide if the proper coefficients are being used in the simulation model.

Two types of heat transfer coefficients were needed in the DEFORM simulations of the hammer forging process, which involved free resting and forming conditions. In this study, free resting conditions pertain to situations where the workpiece sits on top of the bottom die prior to hammer blows. This occurrence is commonly known as dwell time in the forging industry. In forming conditions however, a larger heat transfer between the workpiece and dies occurs due to high pressures encountered during plastic deformation of the workpiece. Note that these heat transfer coefficients only pertain to

the forging process such as the roll forging and hammer forging operations in DEFORM. Based on the DEFORM user manual, two sets of values for heat transfer coefficients were suggested when such data was not known. The values suggested were the following:

Free resting condition: $0.0003 \frac{Btu}{(\text{sec})(in^2)(^\circ\text{F})}$ EQN (4.2.5.1)

Forming condition: $0.002 \frac{Btu}{(\text{sec})(in^2)(^\circ\text{F})}$ EQN (4.2.5.2)

These values were used in the simulations and temperature plots of the workpiece model observed at the end of each operation were compared to pyrometer readings taken during a production run of the large wrench forging. The temperature values observed were in good agreement, and therefore used for the simulations of the existing and proposed wrench forging process.

4.2.6 Boundary Conditions

Another set of parameters that were important to identify for process modeling, were boundary conditions. Depending on the simulation performed, the type of boundary conditions used would vary. In this analysis the two types of boundary conditions used were thermal and velocity boundary conditions. Thermal boundary conditions involved heat exchange with the environment which was set to an approximate ambient temperature of 70˚F. A constant convection coefficient of 7.7 x 10^{-6} Btu/(s∗in^2∗F) suggested by DEFORM and confirmed by their staff was also used. In order to obtain good results, the thermal boundary conditions were applied to all elements of the object's mesh. This was done by enclosing the DEFORM workpiece within a rectangular prism which would allow the selection of all elements in the mesh as shown in Figure 4.2.6.1.

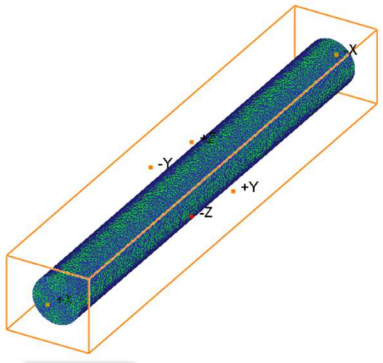

Figure 4.2.6.1 Selection of mesh elements for thermal boundary conditions

Velocity boundary conditions were also used for both heat transfer and forging simulations. In heat transfer simulations which involved heat exchange with the environment, the program required a free distortion boundary condition to be selected when no movement was taking place. The free distortion boundary condition essentially fixed the workpiece in order for the simulation to take place and served as a reference point. It was mentioned by the DEFORM staff, that the free distortion boundary condition was typically selected at one end of the workpiece being analyzed as shown in Figure 4.2.6.2.

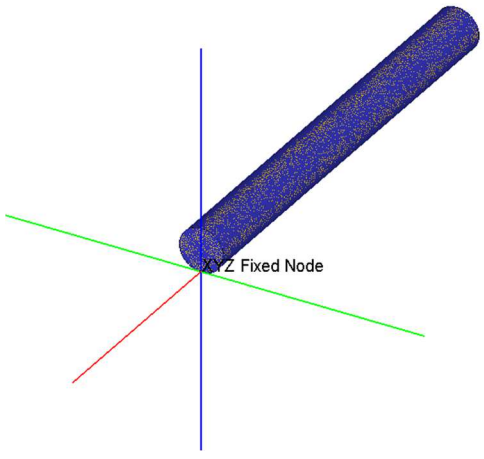

Figure 4.2.6.2 Velocity boundary conditions used for heat transfer simulations

Velocity boundary conditions were also applied to one end of the workpiece during roll forging and edger impression operations to account for the tongs used during the actual forging process. For the roll forging operation, four nodes were selected in order to maintain the workpiece as straight as possible as is done in actuality, as the workpiece passes through the roll forging dies. It was observed that when selecting too many nodes the model became too restricting and with too little nodes there was more room for misalignment. In the edger impression however, it was observed that selecting the end face where the tong would grip the part, provided better results in comparison to the forged platters provided by GBDF. Figure 4.2.6.3 shows how the number of nodes selected for each operation differs from one another, for the roll forging and edger impression operations.

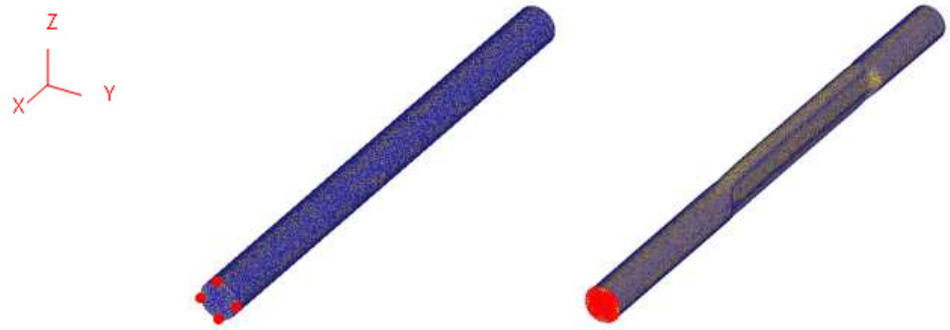

(a) (b)

Figure 4.2.6.3 Velocity boundary conditions for roll forming and edger impression operations. (a) Roll forming operation, fixed ends in the y and z direction (b) Edger impression operation, fixed ends in the x and y direction

It should be noted that during the actual forging process a 90 degree rotation of the part occurs when the workpiece is transferred from the roll forging dies to the edger impression by the operator. Due to the 90 degree rotation and workpiece positioning in the edger impression, rotation of the workpiece can occur during initial hammer blows if

no boundary conditions are used, which is why they are needed in the FE model. In the blocker impression, the workpiece begins to shape into the predetermined geometry and tends to remain fixed in the impression after an initial hammer blow that prevents the need for boundary conditions. Similarly, no boundary conditions were added during the finisher impression operation due to the nesting of the workpiece in the die impression. It was observed that there was better agreement between the DEFORM models and the forged platters when the mentioned velocity boundary conditions were used.

4.2.7 Angular Velocity of Roll Forging Dies

The angular velocity of the roll forging dies also known as reducer rolls was important when performing the roll forging simulations. A specific value for this input was not provided, which meant a calculation was required. In order to calculate the angular velocity, the time required for the reducer rolls to complete one revolution needed to be identified. This was done by using a video camera to record the rotation of the reducer rolls during the actual forging process for multiple passes. It was observed that on average, it took the reducer rolls approximately 0.7 seconds to complete one full revolution. Note that the units required for DEFORM were in radians per second and therefore the following conversion was used:

$$\omega = \frac{1\ rev}{0.7\ sec}\left(\frac{2\pi\ rad}{1\ rev}\right) = 9\ rad/sec \qquad \text{EQN (4.2.7.1)}$$

It should be noted that due to the mesh size selected and the need to reduce simulation errors, a small constant time step was used. This was done for both the simulations of the existing and the proposed processes. For clarity, based on the right

hand rule, the motion of the top reducer roll revolved around the – y axis, while the bottom reducer roll revolved around the + y axis as shown in Figure 4.2.7.1.

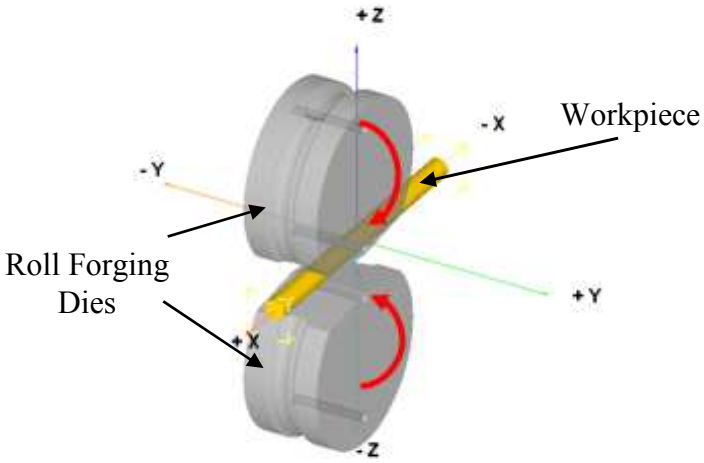

Figure 4.2.7.1 DEFORM model of the existing roll forming operation, depicting the rotation of the dies

Based upon discussion with GBDF personnel, and the forged platter after the roll forging operation, a 0.060 in. gap was discovered between the two roll forging dies, which was accounted for in the simulation process.

4.2.8 Hammer Blow Energy and Mass

When performing the forging sequence using the hammer equipment it was important to identify the total kinetic energy available at the point of impact when the hammer blows occur. Note that this kinetic energy is equivalent to the potential energy available at the start of the process, defined by drop height and the mass of ram and top die. For clarification, the hammer used was a 3,000 lb_m drop hammer. Note that the mass of the hammer, represented the mass of the ram. Energy values needed to be estimated and converted into the right units to be compatible with the DEFORM software. Since the

hammer forging equipment used was a gravity drop hammer, gravity also needed to be accounted for in the calculation. Based on the DEFORM user manual and previous research, the following equation was used to calculate the total energy available of the system:

$$E_T = m_T g h \qquad \text{EQN (4.2.8.1)}$$

Where:

$E_T = Total\ energy\ available$
$m_T = Total\ combined\ mass\ of\ ram\ and\ top\ die \approx 3{,}817\ lb_m$
$g = Gravity\ constant \approx 32.2\ ft/s^2$
$h = Drop\ height \approx 34\ in$

Note that DEFORM uses units of $klb_f * in$ for energy and $(klb_f * s^2)/in$ for mass, therefore the following conversion factors were used in the calculations:

$$1\ slug = 32.2\ lb_m \qquad \text{EQN (4.2.8.2)}$$
$$1\ slug = \frac{1\ lb_f * s^2}{ft} \qquad \text{EQN (4.2.8.3)}$$
$$1\ klb_f = 1000\ lb_f \qquad \text{EQN (4.2.8.4)}$$
$$1\ ft = 12\ in \qquad \text{EQN (4.2.8.5)}$$

Using the known values provided along with equations 4.2.8.1 – 4.2.8.5, the calculated values for the total mass and energy available in the hammer equipment were the following:

Total combined mass of top die and ram

$$m_T = (3817\ lb_m)\left(\frac{1\ slug}{32.2\ lb_m}\right)\left(\frac{1\ \frac{lb_f * s^2}{ft}}{1\ slug}\right)\left(\frac{1\ klb_f}{1000 lb_f}\right)\left(\frac{1\ ft}{12\ in}\right) \qquad \text{EQN (4.2.8.6)}$$

$$m_T = 0.00988\ klb_f * \frac{s^2}{in}$$

Total energy available

$$E_T = \left(0.00988\ klb_f * \frac{s^2}{in}\right)\left(32.2\ \frac{ft}{s^2}\right)(34\ in)\left(\frac{12\ in}{1\ ft}\right) \qquad \text{EQN (4.2.8.7)}$$
$$E_T = 129.8\ klb_f * in$$

4.2.9 Hammer Blow Efficiency

The hammer blow efficiency affects the amount of energy transferred from the hammer equipment to the plastic deformation of the workpiece, and therefore was an important parameter to be considered when performing hammer forging simulations. For clarity, the term "blow efficiency" refers to the ratio between the energy required to plastically deform a part and the total energy available in the hammer forging equipment, as shown in equation 4.2.9.1.

$$\eta = \frac{E_R}{E_T} \qquad \text{EQN (4.2.9.1)}$$

Where:

$\eta = Hammer\ blow\ efficiency$
$E_R = Energy\ required\ for\ plastic\ deformation$
$E_T = Total\ energy\ available$

From past research and forging practice it was observed that hammer blow efficiency is typically divided into three categories which are termed soft, medium, and hard blows. During soft blows larger amounts of energy are supplied to the workpiece rather than the surroundings which results in larger plastic deformations and die movement. During medium and hard blows, less energy is transferred to the workpiece and more is dissipated to the surroundings, in the form of vibration through the forging equipment and noise in the shop floor. Based on past research as described by Altan [13]

the range of typical recommended values for soft, medium, and hard blows are 0.8 – 0.9, 0.5 – 0.8, and 0.2 – 0.5, respectively.

The first step in identifying the correct hammer blow efficiency to use in the simulations, was to characterize the hammer blows heard for the existing forging process as being soft, medium, or hard blows. This was done by listening to the tonal quality of each blow per operation on the shop floor, during a production run of the wrench forging process. The type of blows heard during the forging process were mainly soft to medium blows. Typically the louder the tone, the harder the blow, since less plastic deformation takes place and more contact between the die surfaces occur. In order to approximate a value however, a series of simulations were performed with suggested values such as 0.8 – 0.9 for soft blows, 0.5 – 0.8 for medium blows. The simulations results for the existing wrench forging process were then compared to the GBDF forged platters. Since the intensity of the hammer blows varied throughout the actual forging process, it was hypothesized that the hammer blow efficiency during each blow in the simulations would vary as well. Results of the hammer blow efficiencies used for the simulations are presented in Chapter 5.

4.2.10 Workpiece Positioning

Workpiece positioning was another important factor that needs to be discussed, since it could greatly impact the simulation results. During the initial set up of the current roll and impression die forging operations, workpiece positioning was identified by looking at the forged platters provided by GBDF. It was informed by the GBDF staff that prior to the roll forging operation, the workpiece was fed between the reducer rolls until it

hit a stop, located approximately 11.4 in. from the center of the reducer rolls as shown in Figure 4.2.10.1.

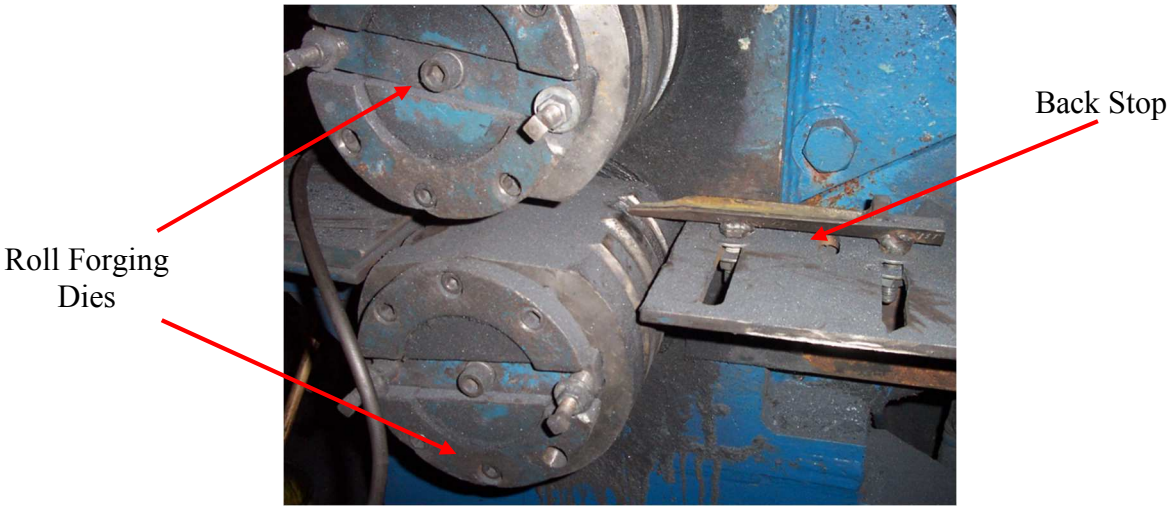

Figure 4.2.10.1 Roll forming die set – up for the existing wrench forging process

An example of the model set – up in DEFORM is shown in Figure 4.2.10.2. Note that the examples shown only correspond to the simulations of the existing wrench forging process.

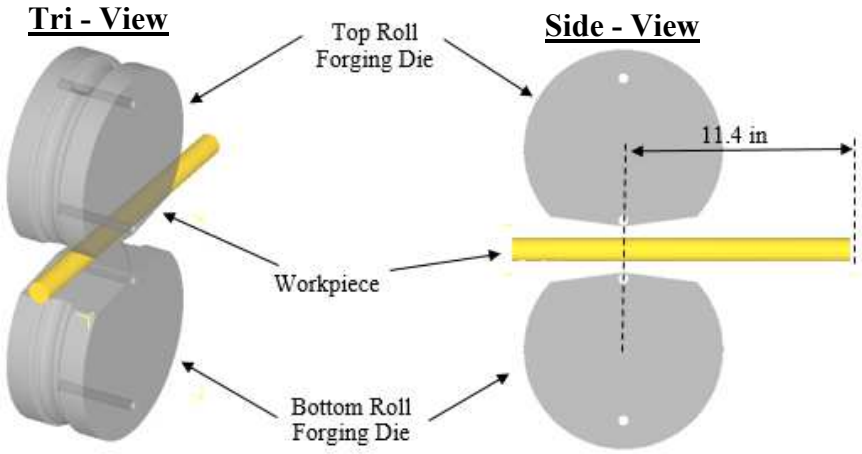

Figure 4.2.10.2 Workpiece positioning for the roll forming operation of the existing wrench forging process, showing distance from the center of the reducer rolls to the end stopper

It is important to keep in mind that workpiece positioning for the forging process being analyzed is heavily dependent on the experience of the operator. This is especially important during workpiece positioning for the hammer forging sequence to maintain consistency of the forged parts. Unlike the roll forging operation there are no specific end stops for the hammer forging sequence, which means that there could be some slight variations between each forged platter. From the forged platters provided by GBDF it was observed that the length of the platter handle which is gripped by tongs remained consistent throughout all platters. This length was approximately 2 in. which was used to help locate the workpiece in the edger and blocker impressions for the simulations. Note that after the completion of the hammer blows in the blocker operation, the workpiece is shaped into an approximate wrench geometry, and as such it becomes easier to locate the workpiece in the finisher impression. Also note that the operators try to center the workpiece in the die impressions as closely as possible for all parts being forged. An example of workpiece positioning for an edger operation is shown in Figure 4.2.10.3.

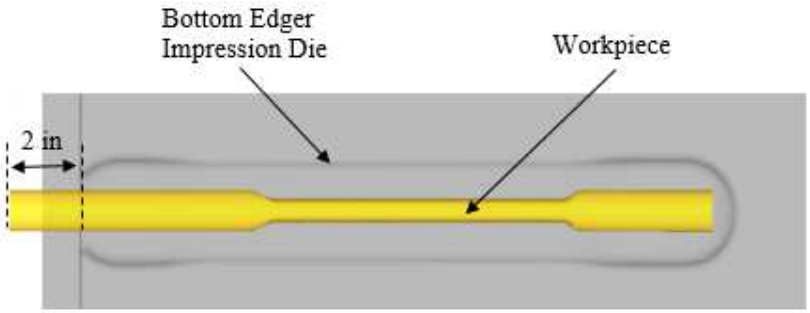

Figure 4.2.10.3 Workpiece positioning for the edger impression operation of the existing wrench forging process

CHAPTER 5

FEM SIMULATIONS OF THE ROLL FORMING AND HAMMER FORGING PROCESSES

The optimization approach for this project involved the use of computer aided design and FEM process modeling softwares of NX 8.5 and DEFORM, respectively, to propose changes to the existing wrench forging process used at GBDF. Validation of the DEFORM process model was obtained by simulating the existing wrench forging process and comparing selected measurements between the DEFORM workpiece model and forge platters obtained from GBDF. Proposed changes were made to billet and impression die geometries, and DEFORM was used to predict forging results. An in depth analysis of the optimization approach described, is provided in this chapter.

5.1 FEM Simulations of the Existing Wrench Forging Process

5.1.1 Tool and Billet Geometry

The existing wrench forging process makes use of roll forming dies, a single die block with three sets of impressions and a round starting billet. The dimensions of the diameter and width of the roll forming dies are 10 in. and 8 in., respectively. The roll forming dies also contain three sets of impressions referred to as roll forming die segments. However, during the wrench forging of the existing process, only one roll forming segment is used. One set of roll dies are typically used for different forging processes, however in some cases passes through multiple roll forming segments is required to achieve the desired material redistribution. The typical roll forming die used

at GBDF and the three dimensional model representation of the die segment used in the existing wrench forging process is shown in Figure 5.1.1.1.

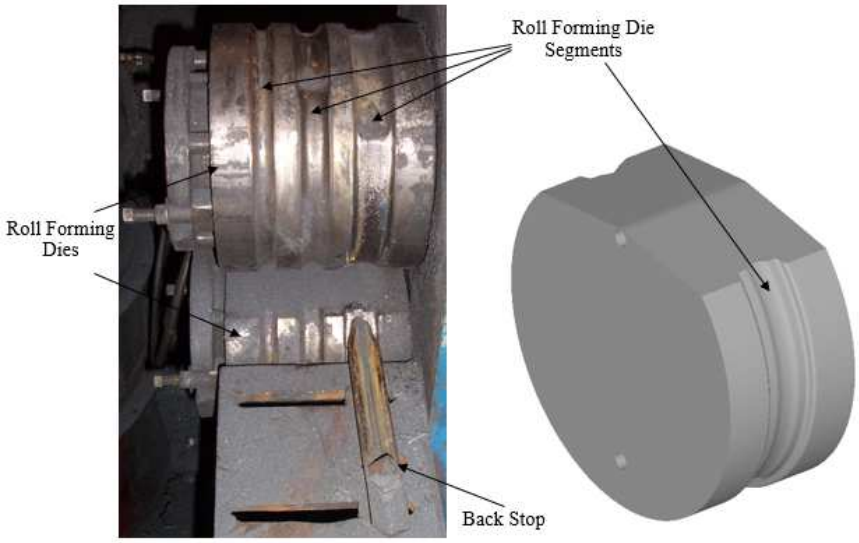

Figure 5.1.1.1 Roll forming dies used in the existing wrench forging process. (a) Actual roll forming die set used at GBDF and (b) Three dimensional geometry representation of one segment used in DEFORM

For the existing wrench forging process, the hammer forging die block contained three sets of impressions termed edger, blocker, and finisher. The edger impression is used to achieve further material redistribution after the roll forming operation, while the blocker impression is used to shape the forge part into an approximate wrench geometry. Finally, the finisher impression is used to forge the part to its final dimensions as specified by the forge drawing. Three hammer blows are typically required per operation and a total of nine hammer blows are required to forge one wrench. In order to minimize model size and simulation time significantly, it was decided to simulate each forging operation separately. Saving the simulations of all operations in one database would cause the program to slow down or even keep the program from responding due to all the

data saved in one file. A comparison of the GBDF die block and the three dimensional geometry representation from NX 8.5 is shown in Figure 5.1.1.2.

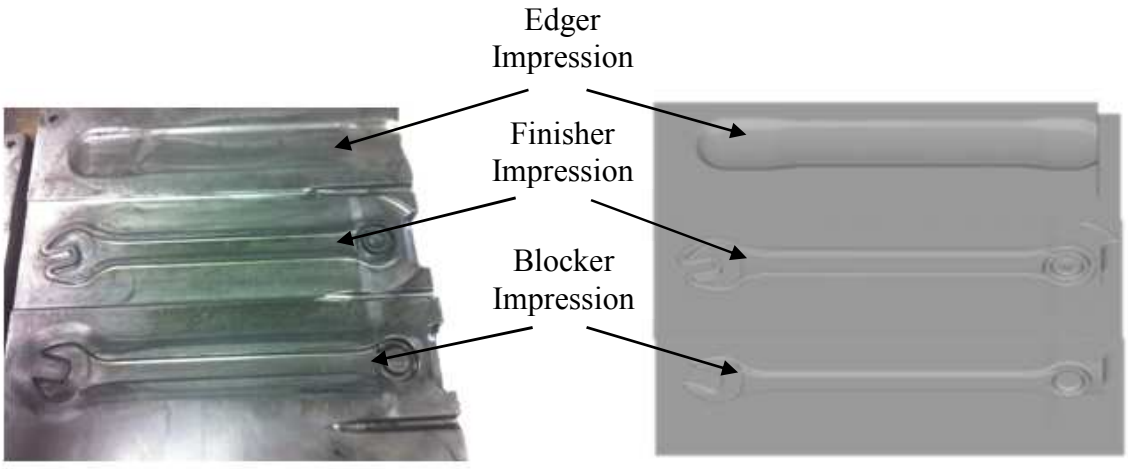

Figure 5.1.1.2 Bottom die block of the existing wrench forging process. (a) Actual die block used at GBDF and (b) Three dimensional geometry representation used in DEFORM

A round starting billet was used for the large wrench forging considered in the study. The diameter and length of the billet was 1.125 inches by 16.75 inches, as shown in Figure 5.1.1.3.

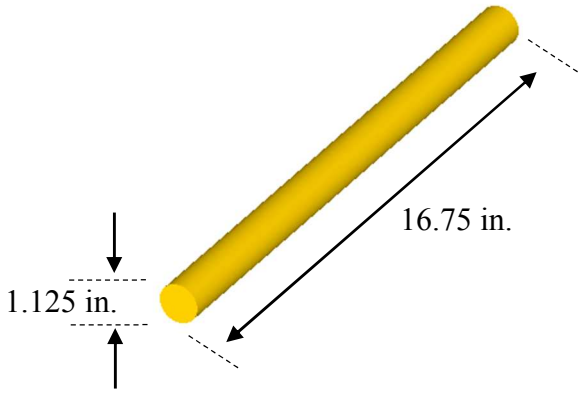

Figure 5.1.1.3 Starting billet dimensions of the existing wrench forging process

5.1.2 FE Model of the Existing Wrench Forging Process

Simulations of the hammer forging process consisted of five different operations. The operations involved heat transfer, roll forming, edger impression, blocker impression, and finisher impression forging. The forging sequence used at GBDF, not including trim, as discussed in Chapter 1 is shown in Figure 5.1.2.1.

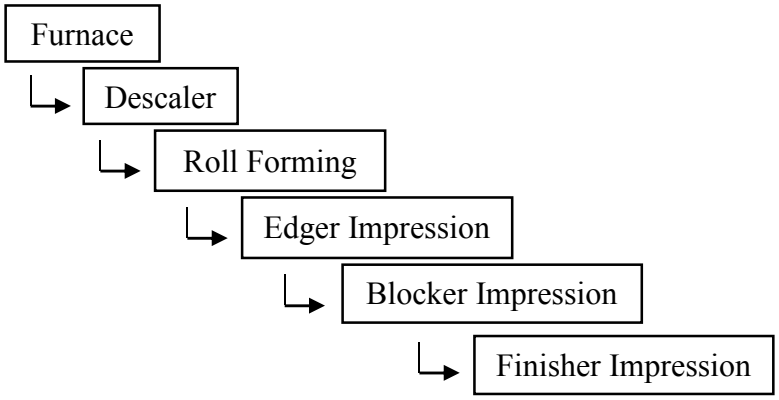

Figure 5.1.2.1 Forging sequence used at GBDF

All heat transfer simulations were performed using boundary conditions of "Heat exchange with the environment" as described in Chapter 4. For furnace heat up, the environment temperature was set to 2300 ˚F, whereas 70 ˚F was used for all other heat transfer simulations. During a production run of the wrench forging, a stopwatch was used to keep track of the time the workpiece spent in each operation. From such data, heat transfer times for the process model simulations were identified and is shown in Table 5.1.2.1.

Table 5.1.2.1 Heat transfer times for the existing wrench forging process simulations

	Operation	Time (sec)
Heat Up	*Furnace*	600.0
Heat Loss	*Furnace to Descaler*	1.2
	Descaler	0.6
	Descaler to Reducer Rolls	0.8
	Reducer Rolls to Die Block	2.0

The roll forming simulation was performed after the descaler operation shown in Table 5.1.2.1. For the simulation, the roll forming dies were assigned a temperature of 300 ˚F, which was a heat up die temperature used by GBDF prior to the wrench forging process. Other main parameters needed to perform the simulation were angular velocity of the dies, friction, and heat transfer coefficient for forming conditions as described in Chapter 4. A small time step was also noticed to improve simulation results by reducing possible remeshing errors in the model. The constants used for the different roll forming parameters is shown in Table 5.1.2.2.

Table 5.1.2.2 Roll forming parameters for the existing wrench forging process simulation

Roll Forming Parameters	Input
Angular Velocity (rad/sec)	9
Shear Friction Factor	0.7
Heat Transfer Coefficient (BTU/sec/in^2/˚F)	0.002
Solution Time Step (sec)	0.006

Forging simulations of the edger, blocker, and finisher impression followed the roll forming operation. Similar to roll forming, the hammer forging model required specific inputs to perform the simulation. Inputs such as mass of the ram and energy of the system remained constant throughout the edger, blocker, and finisher impression

forging. The hammer blow efficiencies however, were hypothesized to vary with each blow per operation as shown in Table 5.1.2.3. Note that recommended values for soft and medium blows, as identified for the existing forging process, were 0.8 - 0.9 and 0.5 – 0.8, respectively.

Table 5.1.2.3 Initial hammer blow efficiencies used for the existing wrench forging process simulations

Operation	Blow Sequence	Efficiency
Edger	Blow 1	0.9
	Blow 2	0.9
	Blow 3	0.8
Blocker	Blow 1	0.9
	Blow 2	0.8
	Blow 3	0.7
Finisher	Blow 1	0.9
	Blow 2	0.8
	Blow 3	0.7

After a few simulation trials with the given constraints of mass of the ram and energy of the system, 0.00988 Klb-s^2/in and 129.8 Klb-in, respectively, it was observed that a constant blow efficiency of 0.9 provided better results. Although the differences observed were small, the DEFORM model results using a constant efficiency of 0.9 gave a better comparison with the GBDF forged platters. It is believed that other factors such as hammer stiffness could have affected die deflection and hence the hammer blow efficiencies used. Such details however were not readily available during the time of the study and could not be easily calculated during the given time frame.

FEM simulations of the existing wrench forging process were conducted once all modeling parameters were established. The results of the process modeling simulation is

shown in Figure 5.1.2.2. Note that for simplicity, the top dies were excluded and only the deformed workpiece geometry at the end of each operation is shown.

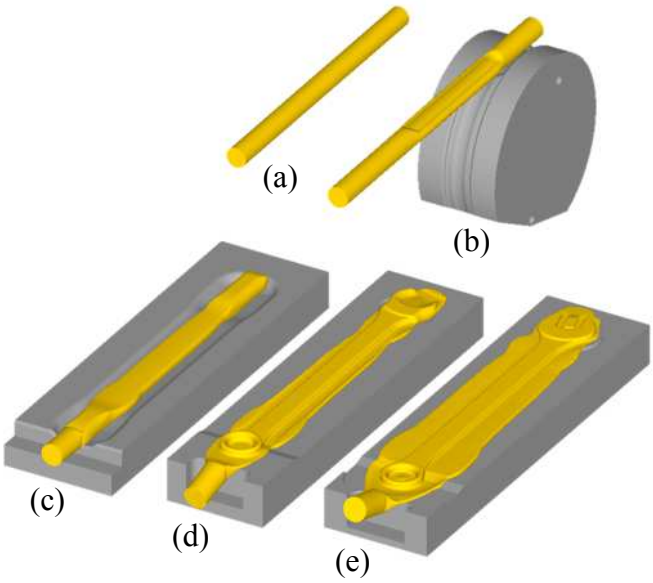

Figure 5.1.2.2 Simulation workpiece model results at the end of each operation, for the existing wrench forging process. (a) Starting billet and (b) Roll forming (c) Edger (d) Blocker (e) Finisher operation

A more detailed representation of the simulation results at the end of each hammer blow per operation can be found in Appendix C. Based upon the results observed from Figure 5.1.2.2 it was apparent that the forge geometry from the DEFORM model resembled the GBDF forged platters shown in Figure 5.1.2.3.

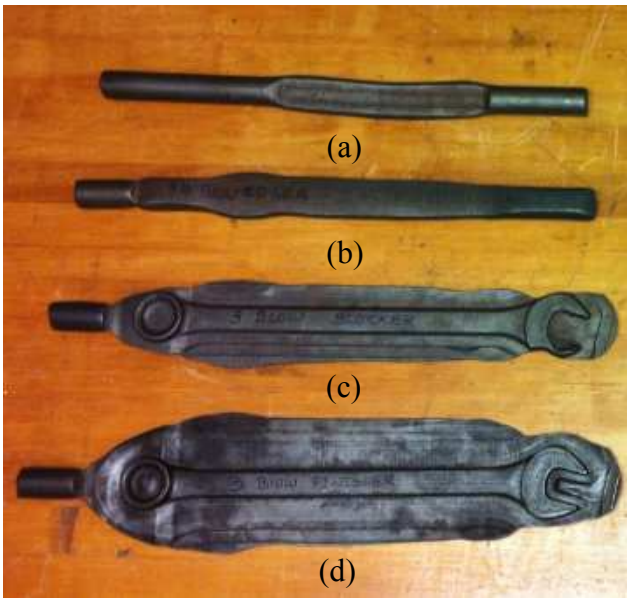

Figure 5.1.2.3 GBDF forged platters at the end of each operation for the existing wrench forging process. (a) Roll forming, (b) Edger, (c) Blocker, and (d) Finisher operation

It was hypothesized that some differences would be observed due to any remeshing errors that could have occurred during the simulations. In finite element simulations, a mesh is typically generated for any object being analyzed. A mesh consists of a finite number of elements and nodes, which are used to predict the behavior of the object during a process such as forging. The predictions of the model are approximated at the nodes through complex mathematical calculations performed by a computer as the simulation takes place. When plastic deformation is involved, remeshing of the workpiece is required whenever the mesh becomes excessively deformed. . However, in some cases remeshing errors can occur when the geometry of the workpiece being analyzed is too complex or if the time step selected for the simulation process is too large. A time step is essentially the incremental change in time for which the calculations in the system are being solved.

For the simulations of the existing wrench forging process, a fine mesh size, which included a large number of elements and nodes was selected. For simulations involving plastic deformation of the workpiece such as impression die forging, the mesh size was increased to reduce the risk of remeshing errors. In some cases however, when the mesh size became too large, the size needed to be reduced in order to prevent computational overload. Computational overload was noticed to cause simulation failure, and had to be avoided. The average mesh size of the workpiece used for the existing wrench forging process is shown in Table 5.1.2.4.

Table 5.1.2.4 Average mesh size of the workpiece used for simulations of the existing wrench forging process

Operation	**Blow Sequence**	**Mesh Size**	
		Number of Elements	**Number of Nodes**
Furnace Heat Up	N/A	103956	23436
Furnace to Descaler Transfer	N/A	103956	23436
Descaler Heat Loss	N/A	103956	23436
Descaler to Reducer Roll Transfer	N/A	103956	23436
Roll Reduction/Roll Forming	N/A	103956	23436
Roll Reducer to Die Block Transfer	N/A	103956	23436
Edger	Blow 1	124553	28159
	Blow 2	153647	31529
	Blow 3	154152	34748
Blocker	Blow 1	168750	38178
	Blow 2	182158	41629
	Blow 3	195960	44915
Finisher	Blow 1	188104	43707
	Blow 2	179413	42112
	Blow 3	185208	43884

5.2 DEFORM Model Validation

In the process of validating the DEFORM model, a variety of measurements were made using the DEFORM results of the workpiece and the GBDF forged platters. It is important to note that due to thermal condition effects, the workpiece material expands during a hot forging process due to the heat it is exposed to and contracts during cool down. The DEFORM model accounted for heat expansion of the workpiece throughout the simulations. The GBDF forged platters however, were in a cold state, meaning at ambient room temperature after cool down of the part was completed. For such reasons the following linear thermal expansion equation was used for the DEFORM model and GBDF forge platter comparison.

$$\Delta L = (\alpha)(\Delta T)(L_o) \qquad \text{EQN (5.2.1)}$$

Where:

$\Delta L = Change\ in\ length$
$\alpha = Thermal\ expansion\ coefficient$
$\Delta T = Change\ in\ temperature$
$L_o = Original\ length$

The thermal expansion coefficient used for AISI 4047 steel was 8.6 x 10^{-6} in/(in$*^{\circ}$F), a value used for low alloy steels as suggested by Lucas Milhaupt Global Brazing Solutions [7]. The change in temperature was calculated as the difference between the average hot temperature of the workpiece, at the end of each operation in DEFORM, and ambient room temperature.

In an effort to maintain consistency during the comparison process, the workpiece was divided into measurement sections where the largest differences would be observed.

Measurements at the selected locations as shown in Figure 5.2.1 would be performed after each forging operation.

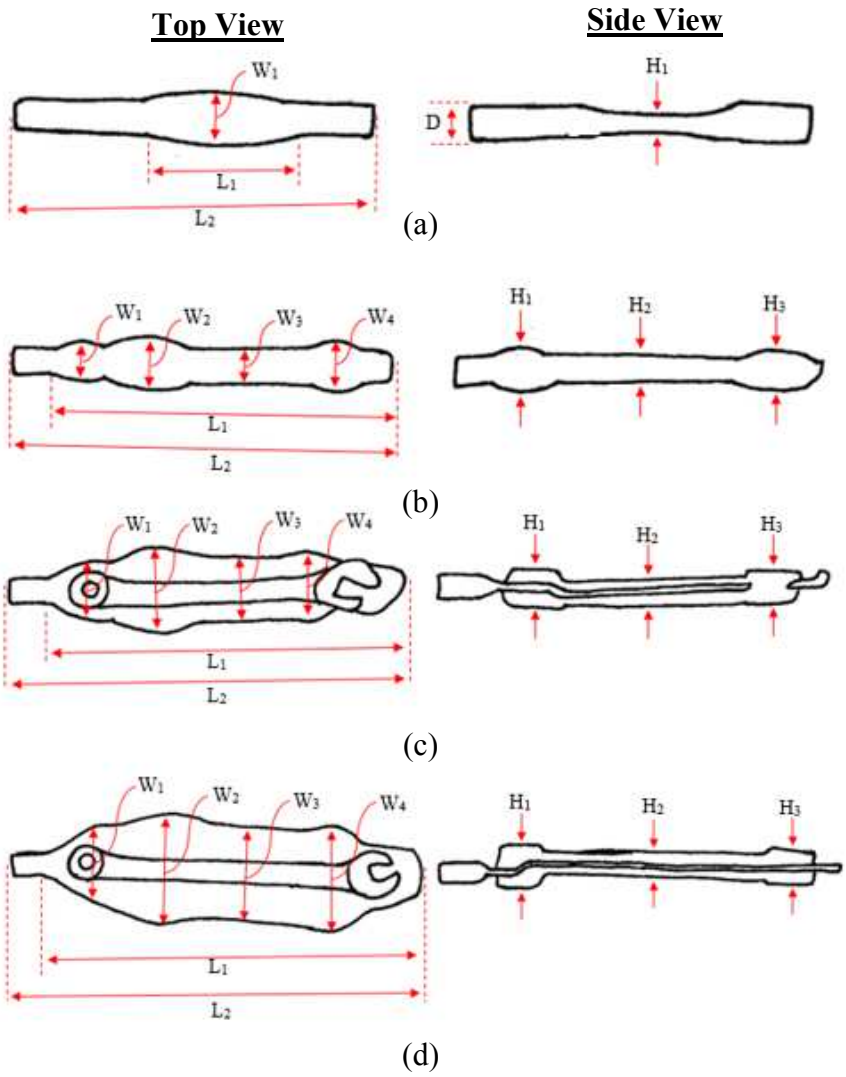

Figure 5.2.1 Workpiece measurement locations for process model validation. (a) Roll forming, (b) Edger, (c) Blocker, and (d) Finisher operation

Measurements of GBDF forged platters were done using a caliper and measuring tape, taking into account material heat expansion. Measurements of the DEFORM workpiece model however, were done using the built – in measuring tool of the software.

An example of the measurements performed is shown in Table 5.2.1 for the third blow of the finisher operation.

Table 5.2.1 Forged Platter and DEFORM workpiece model comparison for the 3rd blow in the finisher operation for the existing wrench forging process

	Measurement (in)	**Heat Expansion (in)**	**Measurement w/ Heat Expansion (in)**	**DEFORM (in)**
W1	4.125	0.071	4.196	3.628
W2	5.125	0.089	5.214	4.158
W3	4.563	0.079	4.641	3.311
W4	4.375	0.076	4.451	3.181
L1	19.500	0.337	19.837	19.333
L2	21.750	0.376	22.126	21.623
H1	0.742	0.013	0.755	0.776
H2	0.420	0.007	0.427	0.453
H3	0.570	0.010	0.580	0.597
Flash Thickness Average	0.056	0.001	0.057	0.077

Once all measurements were concluded, a percent difference was calculated between the dimensions of the GBDF forged platter, taking into account heat expansion, and the DEFORM workpiece model. The percent difference calculated at the end of each operation is shown in Tables 5.2.2 – 5.2.3.

Table 5.2.2 Percent difference comparison between the GBDF forged platter and the DEFORM workpiece model, at the end of the roll forming operation, for the existing wrench forging process

Measurement	**Roll Forming (%)**
D	0.79
W1	6.76
L1	1.16
L2	1.24
H1	3.21

Table 5.2.3 Percent difference comparison between the GBDF forged platters and the DEFORM workpiece model, at the end of each impression die forging operation, for the existing wrench forging process

Measurement	**Edger (%)**	**Blocker (%)**	**Finisher (%)**
W1	9.47	2.82	14.53
W2	2.50	16.34	22.53
W3	5.92	26.18	33.46
W4	6.92	20.72	33.27
L1	0.92	1.43	2.57
L2	1.36	0.99	2.30
H1	1.39	2.41	2.77
H2	3.26	4.52	5.85
H3	1.93	1.65	2.83
Flash Thickness Average	N/A	20.57	30.49

Based upon the results shown in Table 5.2.2 it was observed that the GBDF forge platters and the DEFORM workpiece model were in very good agreement for the roll forming operation of the existing process, since the largest percentage difference calculated was less than 7 %. The comparison was also in very good agreement with the results for the edger operation since the largest percentage difference calculated was less

than 10 %. As measurements proceeded to the results of the blocker and finisher operations, it was noticed that while some percentage differences remained less than 10 %, others were noticeably larger.

The larger percentage differences between the GBDF forge platters and the DEFORM model results for the blocker and finisher operations could have been a result of various factors. One factor that is very common in simulation processes is volume loss due to remeshing errors. As the geometry of the workpiece in the DEFORM model gets more complex with multiple operations, remeshing of the workpiece occurs more often. With frequent remeshing, the possibility of errors occurring in such a small time frame while trying to adopt a more complex shape is very high, and hence volume loss of the workpiece begins to take place.

Another factor that could have affected the percentage difference results for the blocker and finisher operations are the handling techniques used by an operator that could not be easily simulated. Operators performing the wrench forging process use techniques for handling and positioning the workpiece based on practice and past experience. Although positioning of the workpiece in the DEFORM software is achievable, it is never exactly the same as what happens in actuality. Therefore certain deviations between the GBDF forged platters and DEFORM model results were to be expected.

The largest percentage difference seen in the comparison of the GBDF forged platters and the DEFORM workpiece model was approximately 33 %. Therefore, it was decided that the forged platter and DEFORM workpiece model comparison for the final proposed process was required to maintain a percentage difference less than 33% at the end of the blocker and finisher operation. Note that larger percentage differences were to

be expected for widths 2, 3, 4 and the flash thickness in the comparison of the forged platters and DEFORM workpiece model of the final proposed process.

Temperature comparisons of the forged platters and the DEFORM workpiece model for the existing wrench forging process were also conducted to validate the heat transfer coefficients used for the process modeling simulations. Surface temperature readings of the forged platters were measured using a handheld pyrometer with an emissivity of 0.85, during a production run of the wrench part. Averages of the measured values were compared to temperature plots generated in DEFORM as the example shown in Figure 5.2.2 and are presented in Table 5.2.4.

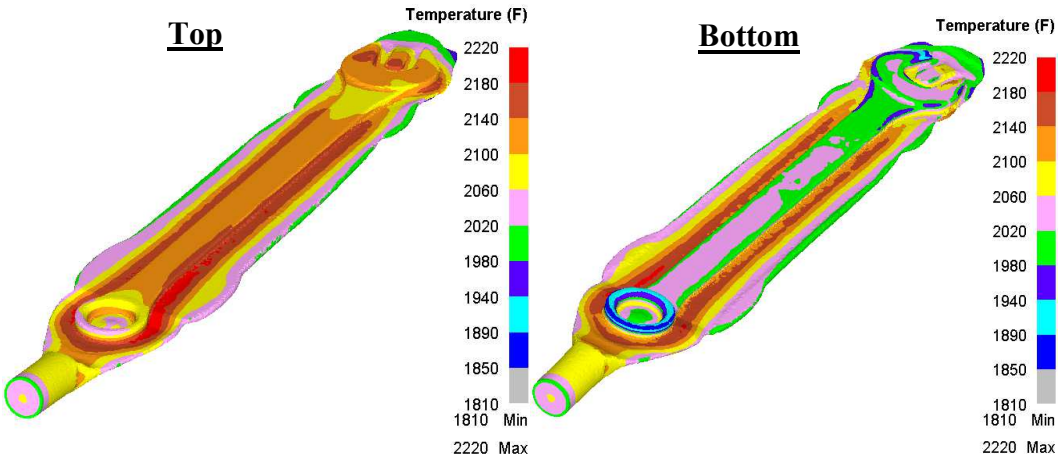

Figure 5.2.2 Temperature plots of the DEFORM workpiece model at the end of the finisher operation for the existing wrench forging process

Table 5.2.4 Temperature measurement comparison for the GBDF forged platters and the DEFORM workpiece model at the end of each operation for the existing wrench forging process

Operation	Forged Platter (˚F)	DEFORM Model (˚F)	% Difference
Roll Forming	2186	2200	0.62
Edger	2164	2175	0.49
Blocker	2148	2110	1.79
Finisher	2079	2040	1.86

Note that core temperature of the part is typically hotter than the surface temperature, and therefore only the surface temperature of the DEFORM workpiece model was used to calculate the average for comparison. As seen from Table 5.2.4, the heat transfer coefficients suggested in Chapter 4, for the process modeling simulations of the existing wrench forging process had an excellent correlation with the forged platters maintaining a percentage difference less than 2%. This correlation justified the use of the heat transfer conditions for simulations of the final proposed process. Temperature plots of the DEFORM workpiece model at the end of each operation can be found in Appendix B.

5.3 Initial Proposed Process DEFORM Model

Simulations of the initial proposed process were carried out in a similar manner as the existing wrench forging process. This meant that all input parameters used in the DEFORM model were kept the same. However, modified die impressions and billet geometry were used for the initial proposed process and are described in the following sub – sections.

5.3.1 Billet and Tool Geometry Proposed Changes

The billet geometry used for the wrench forging was the first set of changes made in an effort to improve the existing forging process. It was hypothesized that the use of a slightly larger diameter billet would improve the flow of the material in difficult to reach areas to obtain better die fill. Changing the shape of the starting billet to a square, instead of a circle was investigated, but was discovered that a new geometry shape would require

new forming equipment. Using a billet with a square cross – sectional shape in a roll forming operation would not be ideal. Therefore, it was concluded that the shape of the billet would remain circular, the same as the existing process.

The existing wrench forging process uses a 1.125 x 16.75 in., diameter and length billet. For optimization, a diameter of 1.25 in. was initially proposed and the starting volume was to be reduced. In order to reduce the starting volume using the proposed billet diameter, the length of the billet could not exceed the length of 16.75 in. used in the existing wrench forging process. From initial volume calculations, for the various sections of the wrench, it was established that material from the flash could be reduced. A 10 % reduction of material was initially proposed by using a starting billet, 1.25 x 12.75 in., in diameter and length.

Following the changes to the billet geometry, was the optimization of the roll forming dies. Based on the volume analysis of the final forged platter discussed in Chapter 1, it was apparent that more material was needed towards the open end of the wrench than the closed end, as seen in Figure 5.3.1.1.

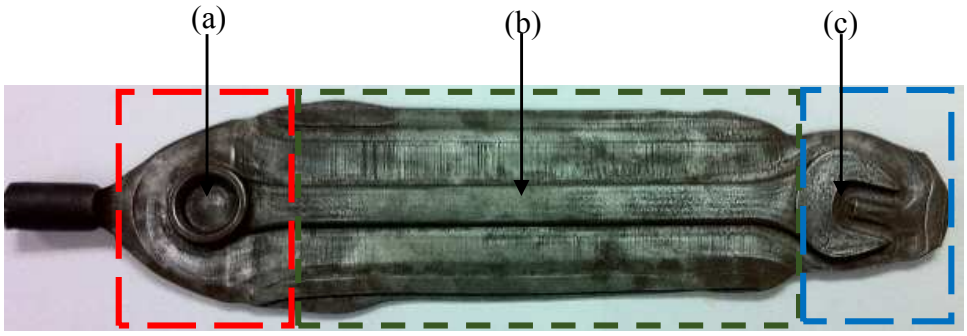

Figure 5.3.1.1 GBDF final forged platter for the existing wrench forging process. (a) Closed end, (b) Handle, and (c) Open end

An improved material distribution was to be achieved by making changes to the groove geometry of the roll forming dies. Due to the selection of the proposed billet geometry, the proposed roll forming operation would require two passes through different groove segments. This was necessary in order to obtain the desired metal distribution for the forging. The first roll forming die segment was kept simple as a rectangular cross sectional shape. The second roll forming die segment however contained a diamond cross – sectional shape. The use of the two proposed cross – sectional shapes used in sequence for the roll forming operation gave the best results. While the first pass in the proposed segment initialized the workpiece deformation, the second pass allowed the material to be further reduced in the middle section and elongated the overall length of workpiece. A comparison of the existing and proposed roll forming dies is shown in Figures 5.3.1.2 – 5.3.1.3 as well as in Table 5.3.1.1.

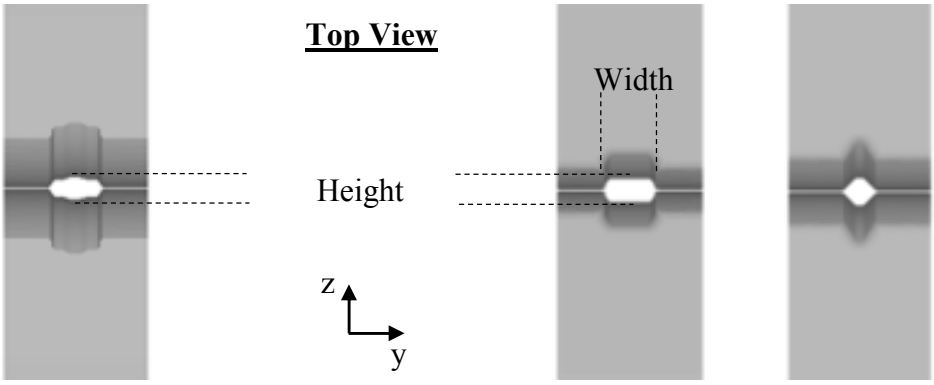

Figure 5.3.1.2 Roll forming die model comparison. (a) Existing, (b) 1st pass initial proposed, and (c) 2nd pass initial proposed geometries

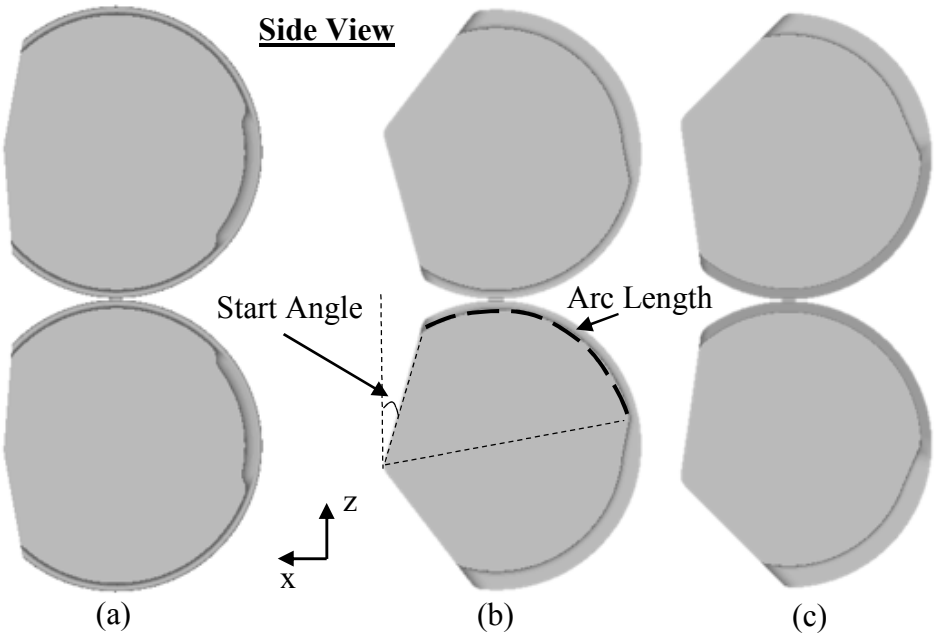

Figure 5.3.1.3 Cross – section of the roll forming die model comparison. (a) Existing, (b) 1st pass initial proposed, and (c) 2nd pass initial proposed geometries

Table 5.3.1.1 Roll forming groove geometry comparison, of the existing and initial proposed wrench forging process

		Initial Proposed Process	
Groove Segment Dimensions	**Existing Process**	**1st Pass**	**2nd Pass**
Start Angle (Deg)	7.50	26.5	26.50
Width (in)	1.47	1.50	0.97
Height (in)	0.66	0.70	0.86
Arc Length (in)	7.87	10.2	10.76
2nd Pass Chamfer z – dir. (in)	N/A	N/A	0.40
2nd Pass Chamfer y – dir. (in)	N/A	N/A	0.40

After analyzing the edger impression of the existing wrench forging process it was concluded that a few modifications to the impression geometry could improve metal flow. It was hypothesized that reducing the depth of the edger impression would allow material to fill the cavity with a reduced number of hammer blows. Therefore it was proposed to reduce the depth of the edger impression and adjust the sections to obtain

better die fill. A comparison of the edger impression geometries between the existing and initial proposed process is shown in Figure 5.3.1.4.

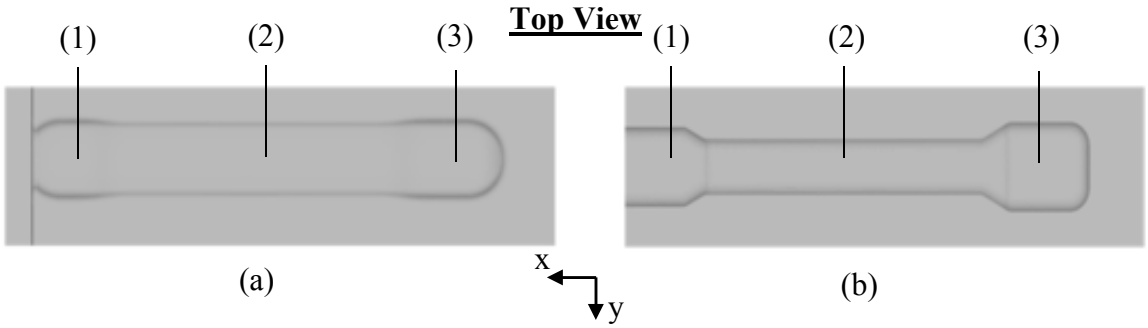

Figure 5.3.1.4 Edger impression model comparison. (a) Existing and (b) Initial proposed geometries

The numerical values for the changes made is presented in Table 5.3.1.2. Note that widths, lengths, and impression heights for each section of the wrench is denoted by *W*, *L*, and *H* in Table 5.3.1.2. Also, *Chamfer 1* is located near the closed end section, while *Chamfer 2* is located near the open end section of the wrench.

Table 5.3.1.2 Edger impression geometry comparison, of the existing and initial proposed wrench forging process

Impression Dimensions	Existing Process	Initial Proposed Process
W_1 *(in)*	3.00	2.50
W_2 *(in)*	2.70	1.75
W_3 *(in)*	3.00	2.80
L_1 *(in)*	2.75	2.30
L_2 *(in)*	11.5	10.7
L_3 *(in)*	3.75	3.10
H_1 *(in)*	0.45	0.30
H_2 *(in)*	0.25	0.23
H_3 *(in)*	0.45	0.30
Chamfer 1x	NA	0.75
Chamfer 1y	NA	0.38
Chamfer 2x	NA	1.10
Chamfer 2y	NA	0.53

In a similar manner, the depth of the proposed blocker impression was slightly reduced with the hopes of reducing the number of hammer blows for this operation as well. Changes were also made to the open end of the blocker impression in order to improve metal flow in that section. This included enlarging the cavity and rounding the sharp edges with a larger radii. A comparison of the blocker impression for the existing and proposed process is shown in Figure 5.3.1.5.

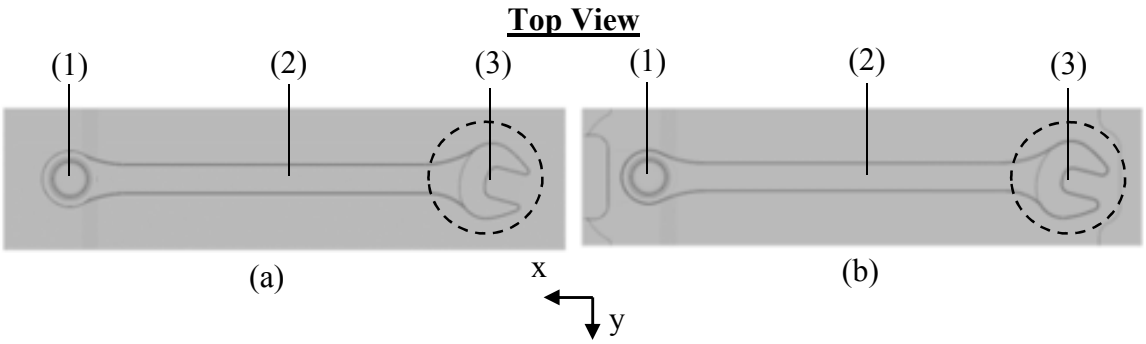

Figure 5.3.1.5 Blocker impression model comparison. (a) Existing and (b) Initial proposed geometries

The numerical values for the changes made is presented in Table 5.3.1.3. Note that widths, lengths, and impression heights for each section of the wrench is denoted by *W*, *L*, and *H* in Table 5.3.1.3.

Table 5.3.1.3 Blocker impression geometry comparison, of the existing and initial proposed wrench forging process

Impression Dimensions	Existing Process	Initial Proposed Process
W_1 *(in)*	2.00	2.00
W_2 *(in)*	1.00	1.00
W_3 *(in)*	2.70	2.80
L_1 *(in)*	2.00	2.00
L_2 *(in)*	12.86	12.86
L_3 *(in)*	2.50	2.50
H_1 *(in)*	0.38	0.32
H_2 *(in)*	0.22	0.16
H_3 *(in)*	0.29	0.23

The geometry of the finisher impression was proposed to remain the same as the existing forging process. This would ensure that the workpiece would be forged to the dimensions specified on the forge drawing. Dimensions of the finisher impression geometry can be found in Appendix A.

5.3.2 Initial Proposed Process DEFORM Model Results

For the DEFORM model of the proposed process, input parameters such as friction factors, hammer blow efficiencies, hammer mass, energy, and boundary conditions were kept the same as the model of the existing process. Note that an additional pass was used in the roll forming operation of the initial proposed process. The DEFORM model results for the initial proposed process is shown in Figure 5.3.2.1. Note that for simplicity, the top dies have been excluded and only the deformed workpiece geometry at the end of each operation is shown.

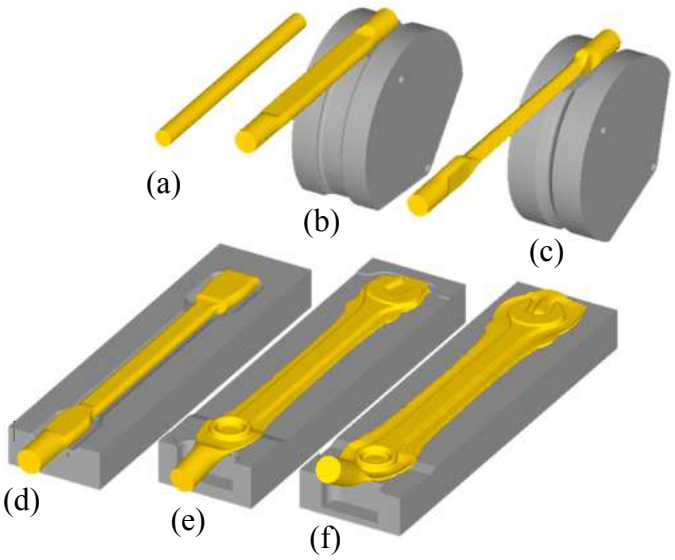

Figure 5.1.2.2 Simulation workpiece model results at the end of each operation, for the initial proposed wrench forging process. (a) Starting billet and (b) Roll forming – 1st pass, (c) Roll forming – 2nd pass, (d) Edger (e) Blocker (f) Finisher operation

A more detailed representation of the results for the initial proposed process can be found in Appendix D. From the DEFORM model results it was observed that only six hammer blows were needed to forge the part when using the initial proposed process. In

doing so the total number of hammer blows used by the process was reduced by 33 %. One hammer blow was needed for the edger, three for the blocker, and two for the finisher operation. When analyzing the amount of material remaining in the flash, it was observed that the starting volume proposed by the optimized process reduced the amount of flash by approximately 27 %. When discussing die fill, it was observed that for the edger impression, complete die fill was not achieved, however the material distribution at the end of the operation was useful for the blocker and finisher operations. Complete die fill were achieved for the blocker and finisher impressions for the proposed process. Although the DEFORM model results of the proposed process seemed promising, a trial in the GBDF forge shop was needed for verification.

CHAPTER 6

DISCUSSION OF RESULTS

6.1 Initial Proposed Process Trial Results

Trials of the first design iteration took place in the forge shop of GBDF after a design review was conducted. In preparation for the first forge trials, it was noticed that machining of the proposed roll forming dies presented some problems. As discussed in Chapter 5, the proposed start angle of the groove segment in the roll forming dies was set to be 26.50˚, however this was problematic as the operator would have a difficult time locating the workpiece in the dies. A simple solution was to maintain the start angle of the groove segments the same as in the existing process, with an angle of 7.50˚. The groove geometry of the second segment in the proposed roll forming dies presented a challenge due to machining equipment availability in the shop floor. However, such issues were resolved in a timely manner. Unlike the proposed roll forming dies, machining of the die blocks with the proposed impression changes were completed without any issues.

During trials of the initial proposed process, it was observed that some flash formation in the workpiece was present after the second pass through the roll forming dies. Due to the positioning of the workpiece in the edger impression of the die block, the presence of flash at the end of the roll forming operation was not ideal. The flash would cause folds in the part during subsequent forging in the hammer equipment and therefore needed to be resolved. For such reasons it was decided that a second design iteration of the roll forming dies was needed. Note that trials of the impression forging in the hammer

equipment were to be performed once the issues with the initial proposed roll forming dies were resolved.

Based upon the results of the first trial and discussions with GBDF personnel, a set of simple solutions to the flash formation problem were suggested. One suggestion was to use a slightly smaller diameter billet. Note that the initial proposed billet diameter was 1.25 in. while the existing process uses a 1.125 in. diameter billet. Therefore, the final diameter billet proposed would need to be between 1.125 and 1.25 in. A second suggestion was to increase the width of the groove geometry in the second segment of the roll forming dies. Finally a third suggestion was to increase the distance between the roll forming dies, which would increase the height of the groove geometry in the second segment. Note that increasing the distance between the roll forming dies would also increase the height of the groove geometry of the first segment.

6.2 Final Proposed Process DEFORM Model Results

For the final process design, a second set of simulations were performed with the modification suggestions from Trial 1 results. It was decided that implementing the three suggestions made would be less time consuming and cost effective than proposing an entirely new roll forming die design. For this set of simulations a 1.1875 in. diameter billet, readily available at GBDF was used. Due to the change in the diameter of the billet, the length was adjusted to 15 in. to maintain the starting volume the same as the existing process. Also, the inner groove width of the second segment in the roll forming dies was increased by 25%. This was done by reducing the horizontal lengths of the chamfers shown in Figure 6.2.1.

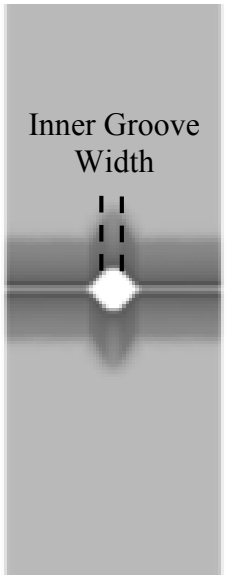

Figure 6.2.1 Second groove segment geometry of the final proposed roll forming dies, for the wrench forging process

As suggested, the spacing between the roll forming dies was also increased. Initially the distance between the dies was set to 0.060 in. for both the simulations and the first set of forging trials. During the first set of trials it was observed that the maximum spacing achievable between the roll forming dies was 0.180 in. Therefore, it was decided to use the maximum allowable distance between the roll forming dies to perform the second set of simulations. This would allow the increase height of the groove geometry without any extra machining. Since the height of the groove geometry for both segments were increased, the arc lengths for both needed to be reduced in order to allow a 15 in. length billet to be used. Note that as the height of the groove geometries were increased, more volume of the material would be maintained within the cavities. Reducing the arc lengths would eliminate the need for a longer length billet. A comparison of the existing, initial, and final proposed roll forming die segment geometries is shown in Table 6.2.1.

Table 6.2.1 Final roll forming die segment groove geometry comparison, for the wrench forging process

Groove Segment Dimensions	Existing Process	Initial Proposed Process		Final Proposed Process	
	1 Pass	1st Pass	2nd Pass	1st Pass	2nd Pass
Start Angle (Deg)	7.50	26.50	26.50	7.50	7.50
Width (in)	1.47	1.50	0.97	1.50	0.97
Height (in)	0.66	0.70	0.86	0.82	0.98
Arc Length (in)	7.87	10.20	10.76	8.00	10.28
Side Chamfer Vertical (in)	N/A	N/A	0.40	N/A	0.40
Side Chamfer Horizontal (in)	N/A	N/A	0.40	N/A	0.30

The second set of simulations were performed using the final proposed billet geometry and roll forming die segments. The first design iterations of the die block impressions were also used for the simulations. The results of the process modeling simulation for the second design iteration/final proposed process is shown in Figure 6.2.2. Note that for simplicity, the top dies were excluded and only the deformed workpiece geometry at the end of each operation is shown.

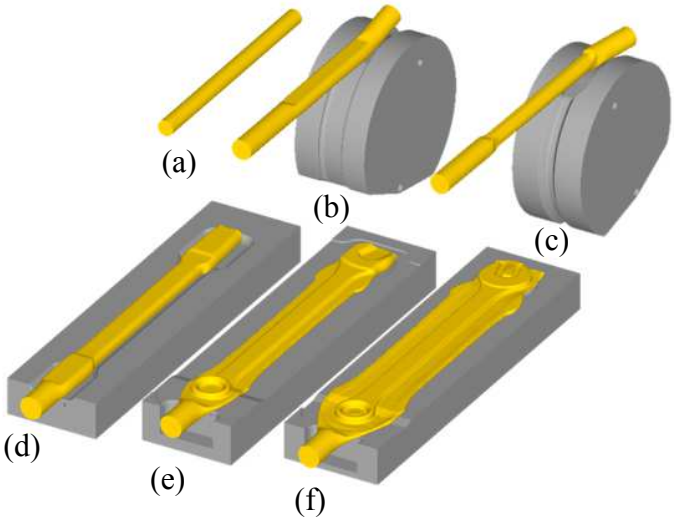

Figure 6.2.2 Simulation workpiece model results at the end of each operation, for the final wrench forging process. (a) Starting billet and (b) Roll forming – 1st pass, (c) Roll forming – 2nd pass, (d) Edger (e) Blocker (f) Finisher operation

A more detailed representation of the results for the initial proposed process can be found in Appendix E. Based on the DEFORM model results of the second design iterations, it was apparent that more material was kept within the groove segments of the first and second pass of the roll forming dies. No signs of possible flash formation were observed. It was noticed however, that there was going to be a larger amount of flash than originally intended at the end of the forging process. The model also predicted that a total of seven hammer blows would be required to forge the part. Keeping in mind that the existing process required a total of nine hammer blows, any reduction of such, was an improvement. The DEFORM model also predicted an improvement in die fill for the open end of the wrench for the blocker and finisher operations. However in order to verify the predictions made by the process modeling software, a second trial was needed.

6.3 Final Proposed Process Trial Results

The trial for the second design iteration was performed without any complications and noticeable changes for the forged part were observed. The flash formation along the length of the workpiece seen during the first trial, was eliminated due to the final adjustments made to the groove segments of the roll forming dies. It is important to mention that when the part was not positioned correctly, a slight amount of flash formed at the initial point of contact between the dies and workpiece for the second pass. However, due to the orientation of the workpiece in the edger impression, the small amount of flash would not affect the integrity of the part. The small amount of excess material would end up in the flash anyway, therefore it was not considered to be a concern to GBDF personnel.

For the hammer forging sequence, the die blocks of the first design iteration containing the edger and blocker impression as well as the unchanged finisher impression were used. The results observed in the hammer forging trial were as predicted in DEFORM. The total number of hammer blows needed to forge the part was seven. This was a 22 % reduction from the existing process. As anticipated, a larger amount of flash than originally desired was present at the end of the process. A set of forged platters of the final proposed process were collected for comparison and is shown in Figure 6.3.1.

Figure 6.3.1 GBDF forged platters of the final proposed wrench forging process

6.4 Final Proposed Process DEFORM Model and Forged Platter Comparison

In order to verify the predictions made by the process modeling simulation, a comparison between DEFORM workpiece model and the final forged platters were made. All measurements followed the same process as the comparison made for the existing process, described in Chapter 5. The percentage differences observed at the end of each forming and forging operation is shown in Tables 6.4.1 – 6.4.2. Note that a more detailed comparisons for each operation can be found in Appendix G.

Table 6.4.1 Percent difference comparison between the GBDF forged platter and the DEFORM workpiece model, at the end of the roll forming operation, for the final proposed wrench forging process

Measurement	1st Pass (%)	2nd Pass (%)
D	0.55	0.55
W1	1.60	3.00
L1	0.83	0.63
L2	0.58	2.57
H1	0.66	0.32

Table 6.4.2 Percent difference comparison between the GBDF forged platters and the DEFORM workpiece model, at the end of each impression die forging operation, for the final proposed wrench forging process

Measurement	Edger (%)	Blocker (%)	Finisher (%)
W1	3.05	11.10	1.40
W2	17.42	28.74	17.71
W3	5.55	25.75	14.40
W4	17.08	1.47	22.92
L1	1.11	3.02	2.06
L2	4.35	14.64	4.70
H1	7.15	3.98	1.21
H2	8.55	6.72	3.13
H3	5.72	5.98	2.09
Flash Thickness Average	N/A	21.10	5.14

The comparison of the final forge platter and the DEFORM workpiece model showed that there was an excellent agreement for the roll forming operation. All percentage difference values observed were less than or equal to 3 %. This meant that the final prediction made by DEFORM was extremely close to the results of the final forging trial. Note that recalling from the first set of comparisons made for the existing process,

the largest percentage difference calculated for the roll forming operation was approximately 7 %.

When analyzing the percentage differences at the end of each die impression forging operation, it is important to discuss what type of variations were expected. This was based on the comparisons made for the existing process. In Chapter 5, a discussion was presented on what type of factors might have caused large percentage differences between the forged platers and DEFORM workpiece models. Based on the comparisons made for the existing process, percentage differences ranging from 15 % - 33 % were expected for widths 2, 3, 4 as well as the average flash thickness. The goal for the final comparison, was to maintain all percentage differences less than 33 % for all the sections. Doing so, would allow for a better agreement between the forge platter and DEFORM workpiece model as well as an improvement of the DEFORM model itself.

As seen from Table 6.4.2, the largest percentage difference observed was in fact less than 33 %. All percentage differences for the height of each section of the wrench were less than 10 %, and the final flash thickness was approximately 5%. Overall, keeping in mind the larger variations expected, there was a good agreement between the forged platters and the DEFORM workpiece model for the final proposed process.

6.5 Final Forged Platter Comparisons

A final comparison between the forged platters of the existing process and the final proposed process was needed to identify any improvements in metal flow and die fill. As mentioned, an improvement in the total number of blows was achieved with a reduction of 22 %. However, it was also important to obtain an improvement in the metal

flow of the part. Before analyzing any specifics, a comparison of the forged platters at the end of each operation is shown in Figure 6.5.1. Note that the operations consisted of the roll forming, edger, blocker, and finisher impression forging.

(a) (b)

Figure 6.5.1 Final forged platter comparison. (a) Existing and (b) Final proposed wrench forging process

As seen from the comparison shown in Figure 6.5.1, an improvement in material distribution was apparent as more was gathered near the open end section of the wrench, for the final proposed process. Note that the open end of the wrench typically took longer to fill and less flash was formed around its sides. If the workpiece was not positioned correctly in the die block impressions, there was a risk of scrapping the part due to underfill in the open end section at end of the forging process.

From the different forge platters provided by GBDF for the existing and final proposed process, the most noticeable differences were observed after the last blow in the edger operation, the second blow in the blocker operation, and the first blow in the finisher operation. Looking at the workpiece at the end of the edger operation, it is clear that more material was gathered near the open section of the wrench with the final proposed process as shown in Figure 6.5.2. Note that material was also removed near the

closed end section of the wrench, and a more uniform distribution was achieved for the wrench handle section.

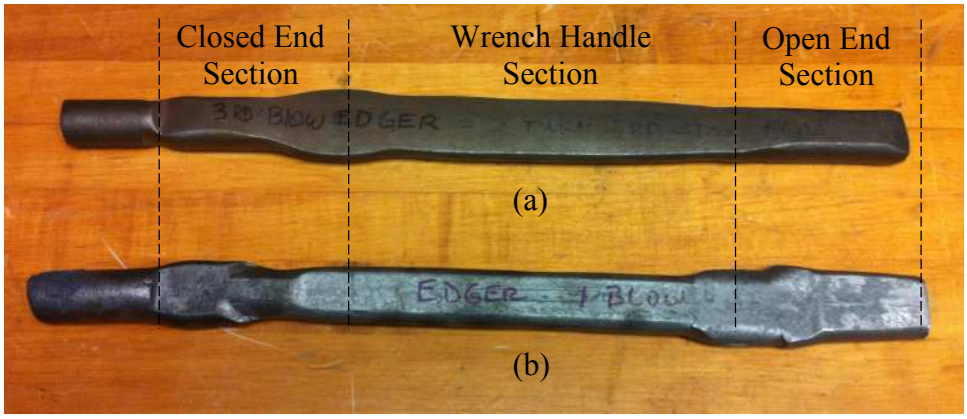

Figure 6.5.2 GBDF forged platter comparison at the end of the edger operation. (a) Existing and (b) Final proposed wrench forging process

When looking at the forged platters of the blocker operation it was observed that an improvement in metal flow for the open end section of the wrench was achieved. The observations were made after the second blow in the blocker operation as shown in Figure 6.5.3.

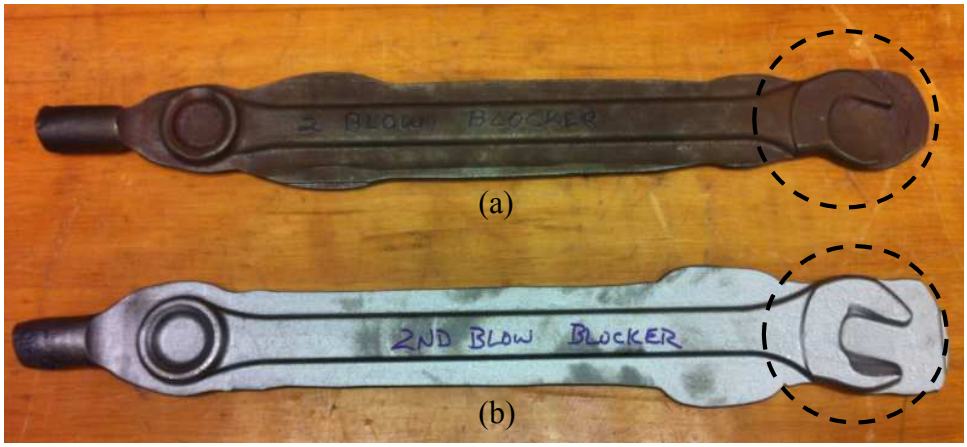

Figure 6.5.3 GBDF forged platter comparison after the second blow in the blocker operation. (a) Existing and (b) Final proposed wrench forging process

In Figure 6.5.3, it is shown that an improvement in metal flow was indeed achieved. The closed end and the wrench handle sections for the final proposed process showed signs of an improved die fill with a good amount of flash formation. Most importantly, with the final proposed process, there was more material contained in the cavity for the open end section. This improvement helped to obtain better die fill in the finisher operation as well.

As predicted, a better die fill was achieved for the open end section of the wrench after the first blow in the finisher operation. In the existing process some underfill was observed, however after the trials with the final proposed process, there were no signs of the underfill seen before. The comparison between the two forged platters after the first blow in the finisher operation is shown in Figure 6.5.4.

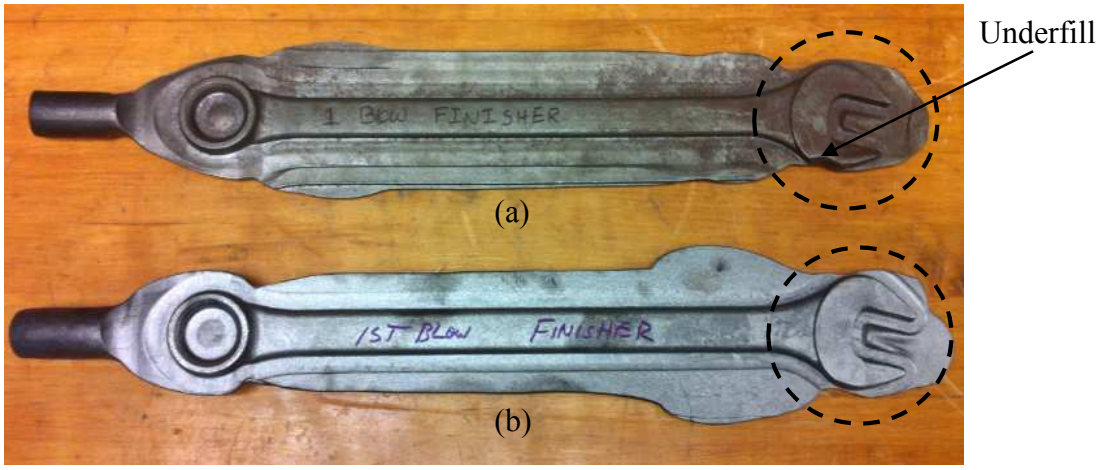

Figure 6.5.4 GBDF forged platter comparison after the first blow in the finisher operation. (a) Existing and (b) Final proposed wrench forging process

The overall results of the final proposed process were good, in the sense that improvements were made, making the forging process more efficient. As mentioned previous times, the total number of hammer blows was reduced from nine to seven, a

total of 22 % reduction and the amount of flash reduced was 4 %. An improvement in metal flow was achieved as more material was gathered near the open end section of the wrench, rather than the closed end. An improvement in die fill was also observed for the open end section of the wrench as seen in the forged platter comparisons. More specifically, the underfill in the finisher operation seen in the existing process was eliminated with the changes made for the final proposed process

CHAPTER 7

CONCLUSION AND FUTURE WORK

7.1 Conclusion

The objective of the research discussed in this thesis was to improve the forging process for a large hand tool manufactured at Green Bay Drop Forge. A large wrench, to be specific, was noticed to contain a large amount of flash, an excessive amount of hammer blows needed to forge the part, and a lack of good material distribution. Note that the forging process consisted of a roll forming operation and impression die forging in a single die block. Rather than spending time and money on trial and error on the shop floor, an optimization approach was applied through the use of computer design softwares for process modeling simulations. Forging trials were performed and the final results were compared to the predictions made by the process modeling software. Note that for this analysis the three dimensional software of NX 8.5 was used to generate the geometric representations of the dies needed to perform simulations. Also, the FEM modeling software used to perform the simulations and make forging predictions was DEFORM.

For the analysis, a virtual process model was established using known conditions for the existing forging process. Once validated, changes were proposed to the billet and impression geometry in an effort to improve metal flow, as well as reduce the total number of hammer blows and the amount of flash at the end of the forging process. A total of two design iterations were needed for the final roll forming dies and one design iteration for the impressions in the die block. The predictions made by the process

modeling software and the forging trials of the final proposed process showed that the total number of hammer blows needed to forge the wrench were reduced from nine to seven blows. This was a 22 % percent reduction, which is useful in improving die life. The amount of flash around the wrench was reduced by 4 %, and an improved metal flow in the cavity for the open end section of the wrench was observed in both the blocker and finisher operations.

The optimization approach used in the analysis, helped to reduce time and money spent on trial and errors on the shop floor in an effort to make the wrench forging process more efficient. Although there were some limitations due to the equipment used, an improvement in the forging process was achieved. Overall the results of the final forging trials were considered to be a good improvement by Green Bay Drop Forge and the new process was to be implemented for the next set of production parts.

7.2 Future Work

During the time of the study it was noticed that certain limitations in the preforming equipment used, prevented greater improvements in the preform shapes that could be achieved. As such it would be ideal to continue the current study by analyzing alternative preforming operations that could further improve the material distribution in a preform shape. Examples of these would be cross – wedge rolling, and heading operations. Although these other preforming operations might increase production time, they might help improve the forging process as a whole. When performing the analysis, the following questions should be answered:

- Does the alternative preforming operation provide any further improvements to the shape of the preform and material distribution?
- Is it worth investing time and money on new equipment for alternative preforming operations?
- How does the preform obtained through the alternative preforming operation help improve die life?
- Does the material distribution achieved through the alternative preforming operations help reduce scrap material? If so, does this outweigh the extra time spent in the production process?

In an effort to improve modeling accuracy, it is recommended that an in depth study be performed on the effects of die deflection on hammer blow efficiencies. It is believed that hammer blow efficiencies used in process modeling simulations vary with each blow in a hammer forging process. However, this needs to be analyzed by studying the forging equipment used for the hammer forging process as well as any deflections that might be observed in the dies. A good set of reference data would significantly improve modeling accuracy in the future. It is also recommended that a study be performed on the effects of die life based upon changes made to preforming operations and impression geometries as the ones seen in this analysis. Results of die stress and die wear should be provided along with any recommendations for further improvement.

References

[1] "AISI 4140 Alloy Steel (UNS G41400)." AZO Materials. Web. 5 Dec. 2013.

[2] "AISI Type H13 Hot Work Tool Steel." MatWeb - Material Property Data. Web. 2 Mar. 2014.

[3] "DC + DC XTRA Die Steel." *Press Die Steels*. A. Finkl & Sons Co. Web. 2 Mar. 2014.

[4] "FX-XTRA Forging Die Steel." *Hammer Die Steels*. A. Finkl & Sons Co. Web. 01 Mar. 2014.

[5] "Manufacturing Processes." *Product Design Guide for Forging*. Cleveland: Forging Industry Association, 1997. 85 - 89. Print.

[6] "AISI 4047 Steel." MatWeb - Material Property Data. Web. 15 Nov. 2013.

[7] "Coefficients of Thermal Expansion Chart." Lucas Milhaupt Global Brazing Solutions. Web. 10 Nov. 2014.

[8] "DEFORM V10.2 User Manual." Scientific Forging Technology Corporation.

[9] "Impression Die Forging Process Operations." Forging Industry Association. Web. 5 Aug. 2014.

[10] "Introduction and Applications" *ASM Forging Handbook*. Ed. Thomas G Byrer, S.L. Semiatin, and Donald C. Vollmer. Ohio: Forging Industry Association, 1985. 11 – 24. Print.

[11] "Open Die Forging Process." Forging Industry Association. Web. 5 Aug. 2014.

[12] Altan, Taylan. "Hammers and Presses for Forging." *ASM Handbook: Forming and Forging*. Vol 14. P, 1993. 24 – 36. Print.

[13] Altan, Taylan. "Selection of Forging Equipment" *ASM Forging Handbook*. Ed. Thomas G Byrer, S.L. Semiatin, and Donald C. Vollmer. Ohio: Forging Industry Association, 1985. 203 – 215. Print.

[14] Biba, Nikolay, Alexey Vlasov, and Sergei Stebounov. "Automated Design and Finite Element Simulation of Reducer Rolling Technology." Moscow, Russia. Web. 16 Oct. 2014.

[15] De Arizon, J., E. Filippi, J Barboza, and L. D' Alvise. "A Finite Element Simulation of the Hot Forging Process." Gosselies, Belgium. Web. 20 Nov. 2014.

[16] Ervasti, Esa. *Closed – Die Forging and Slab Hot Rolling with Focus on Material Yield*. Diss. Kunglila Tekniska Hogskolan, Stockholm, Sweden, 2008. Web. 1 Mar. 2015.

[17] Gontarz, A. "Theoretical and Experimental Research of Hammer Forging Process of Rim from AZ31 Magnesium Alloy." *Metalurgija* 53 (2014): 645 – 648. Web. 2 Feb. 2015.

[18] Groover, Mikell P. "Forging." *Fundamentals of Modern Manufacturing: Materials, Processes, and Systems*. 4th ed. Hoboken, NJ: J. Wiley & Sons, 2010. 405 - 416. Print.

[19] Groover, Mikell P. "Other Deformation Processes Related to Forging." *Fundamentals of Modern Manufacturing: Materials, Processes, and Systems*. 4th ed. Hoboken, NJ: J. Wiley & Sons, 2010. 417 - 418. Print.

[20] Hallstrom, Jonas. "Influence of friction on die filling in counterblow hammer forging." *Journal of Material Processing Technology* 108 (2000): 21 – 25. Web. 5 Dec. 2014.

[21] Howson, T.E. and H.E. Delgado. "Computer Modeling Metal Flow in Forging." *JOM: The Journal of the Minerals, Metals and Materials Society* 41.2 (1989): 32 – 34. Web. 3 Mar. 2015.

[22] Karacaovali, Hakan. *Analysis of Roll – Forging Process*. MS thesis. Middle East Technical University, 2005. Web. 15 Oct. 2014.

[23] Lange, Kurt. "Rolling." *Handbook of Metal Forming*. New York: McGraw-Hill, 1985. 12.2 – 12.16. Print.

[24] Math, Miljenko. "Simulation and Virtual Reality – A Key Factor in Future Development of Metal Forming Processes." University of Zagreb. Web. 10 Jan. 2015.

[25] Movrin, D., Plancak M., Vilotic D., Milutinovic M., Skakin P., Luzanin O., and Trbojevic I. "Optimization and Design of Multistage Hot Forging Processes by Numerical Simulation and Experimental Verification." *Journal for Technology of Plasticity* 35.1 – 2 (2010): 75 – 89. Web. 11 Apr. 2015.

[26] Ngaile, Gracious and Taylan Altan. "Computer Aided Engineering in Forging." *ERC for Net Shape Manufacturing, The Ohio State University*. Web. 15 Dec. 2014.

[27] Park, Joon Boo. *Computer Simulation of the Hammer Forging Process*. MS thesis. Ohio University, 1986. Web. 20 Sep. 2014.

[28] Shirgaokar, Manas. “Process Design in Impression – Die Forging.” *ASM Handbook: Cold and Hot Forging Fundamentals and Applications*. Ed. Taylan Altan, Gracious Ngaile and Gangshu Shen. P, 2005. 159 – 183. Print.

[29] Takemasu, Teruie, Victor Vazquez, Brett Painter, and Taylan Altan. “Investigation of Metal Flow and Preform Optimization in Flashless Forging of a Connecting Rod.” Journal of Materials Processing Technology 59 (1996): 95 – 105. Web 5 Sep. 2014.

[30] Tlusty, Jiri. "Basic Machines for Metal Forming." *Manufacturing Processes and Equipment*. Upper Saddle River, NJ: Prentice-Hall, 2000. 185 - 190. Print.

[31] Walters, John, Taylan Altan, and Manas Shirgaokar. “Simulation Based Process Design for Improvement of Profitability in the Hot Forging Industry.” *Engineering Research Center for Net Shape Manufacturing (ERC/NSM)* (2008). Web. 5 Jan. 2015.

[32] Yang, D. Y. and Y. H. Yoo. “Analysis and Design of Multiblow Hammer Forging Processes by the Explicit Dynamic Finite Element Method.” *Annals of the CIRP* 46.1 (1997): 191 – 194. Web. 15 Jan. 2015.

[33] Zhou, Jie, Zhi Jia, Hao Liu, and Mengham Wang. “A Study on Simulation of Deformation During Roll – Forging Process Using System of Special Shaped and Hat Groove.” Reviews on Advanced Material Science 33 (2013): 354 – 359. Web. 15 Mar. 2015.

APPENDIX A

FINISHER IMPRESSION GEOMETRY DIMENSIONS

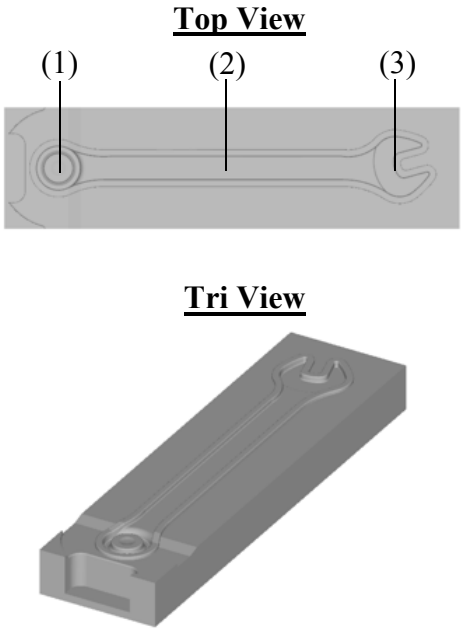

Figure A.1 Finisher impressions geometry of the existing/final proposed wrench forging process

Table A.1 Dimensions of finisher impression geometry for the existing/final proposed wrench forging process

Impression Dimensions	Existing/ Proposed Process
W_1 (in)	2.00
W_2 (in)	1.00
W_3 (in)	2.64
L_1 (in)	2.00
L_2 (in)	12.89
L_3 (in)	2.44
H_1 (in)	0.35
H_2 (in)	0.19
H_3 (in)	0.26

APPENDIX B

SIMULATION WORKPIECE TEMPERATURE PLOTS FOR THE EXISTING WRENCH FORGING PROCESS

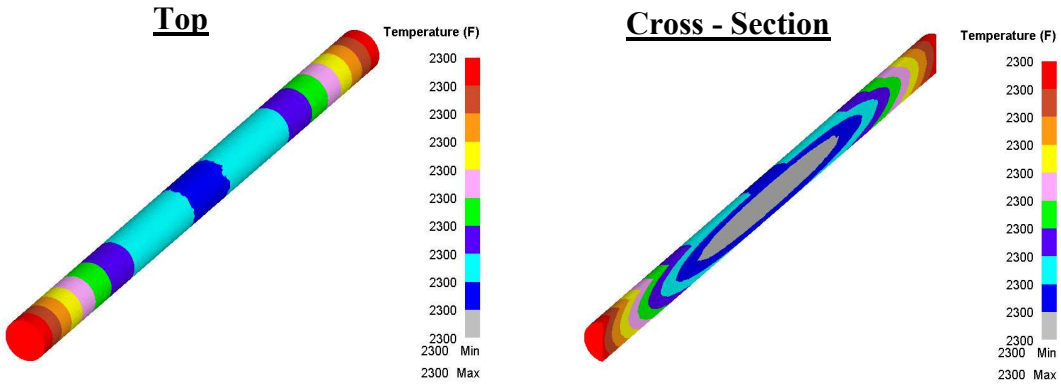

Figure B.1 Workpiece temperature plots at the end of furnace heat up, for the existing wrench forging process

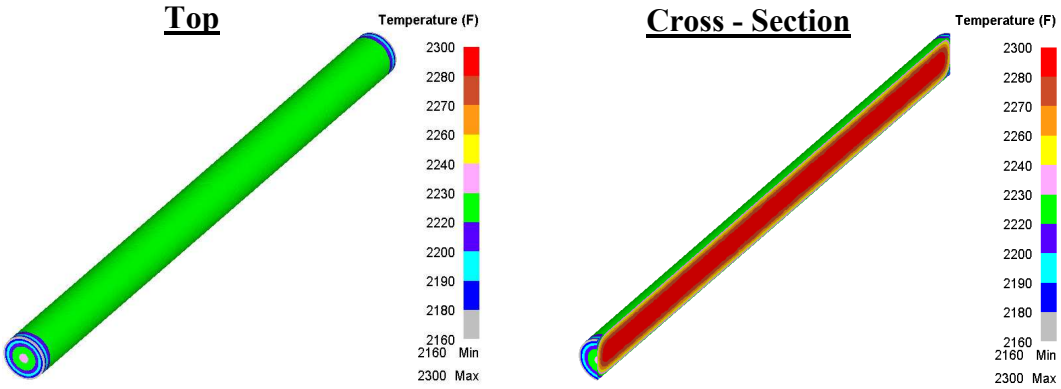

Figure B.2 Workpiece temperature plots at the end of transfer from furnace to roll forming dies, for the existing wrench forging process

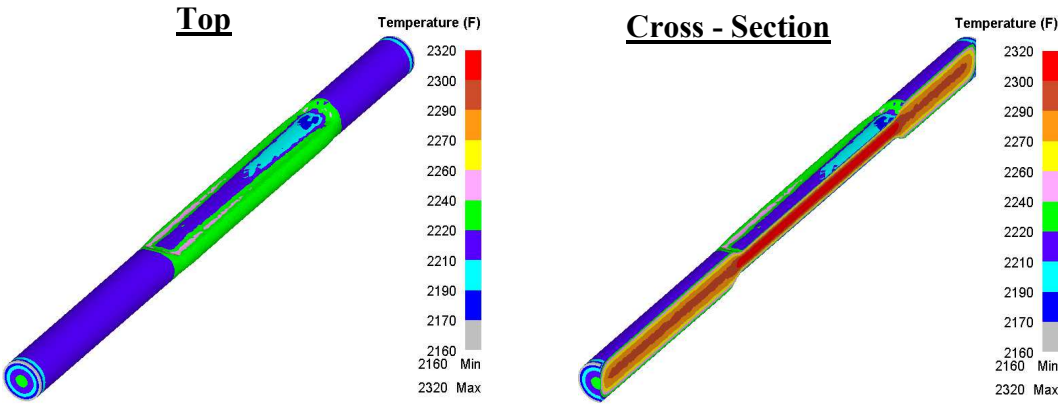

Figure B.3 Workpiece temperature plots at the end of the roll forming operation, for the existing wrench forging process

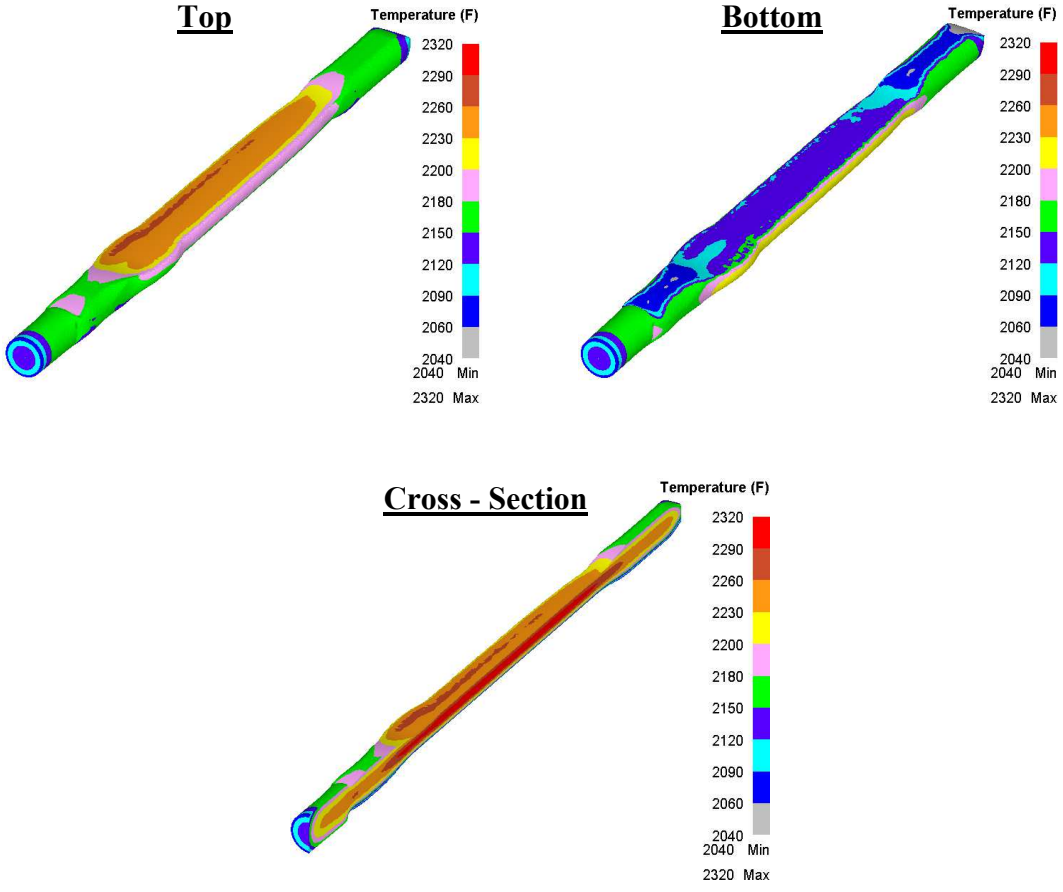

Figure B.4 Workpiece temperature plots at the end of the edger operation, for the existing wrench forging process

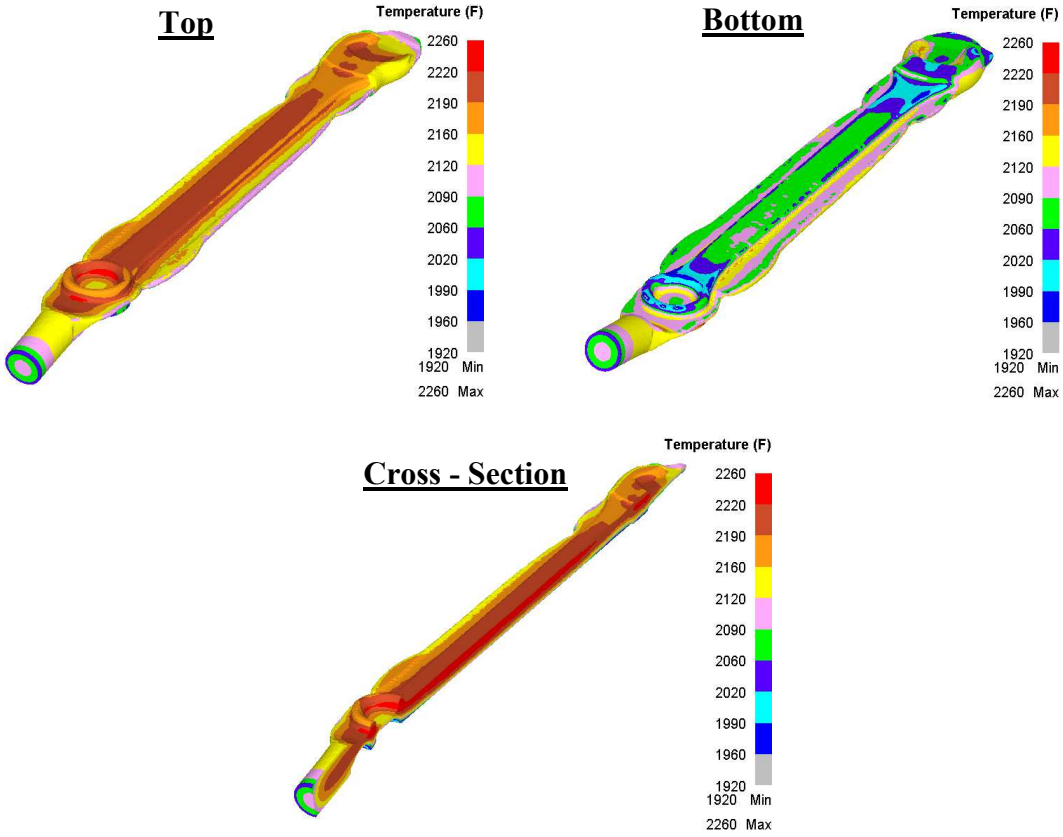

Figure B.5 Workpiece temperature plots at the end of the blocker operation, for the existing wrench forging process

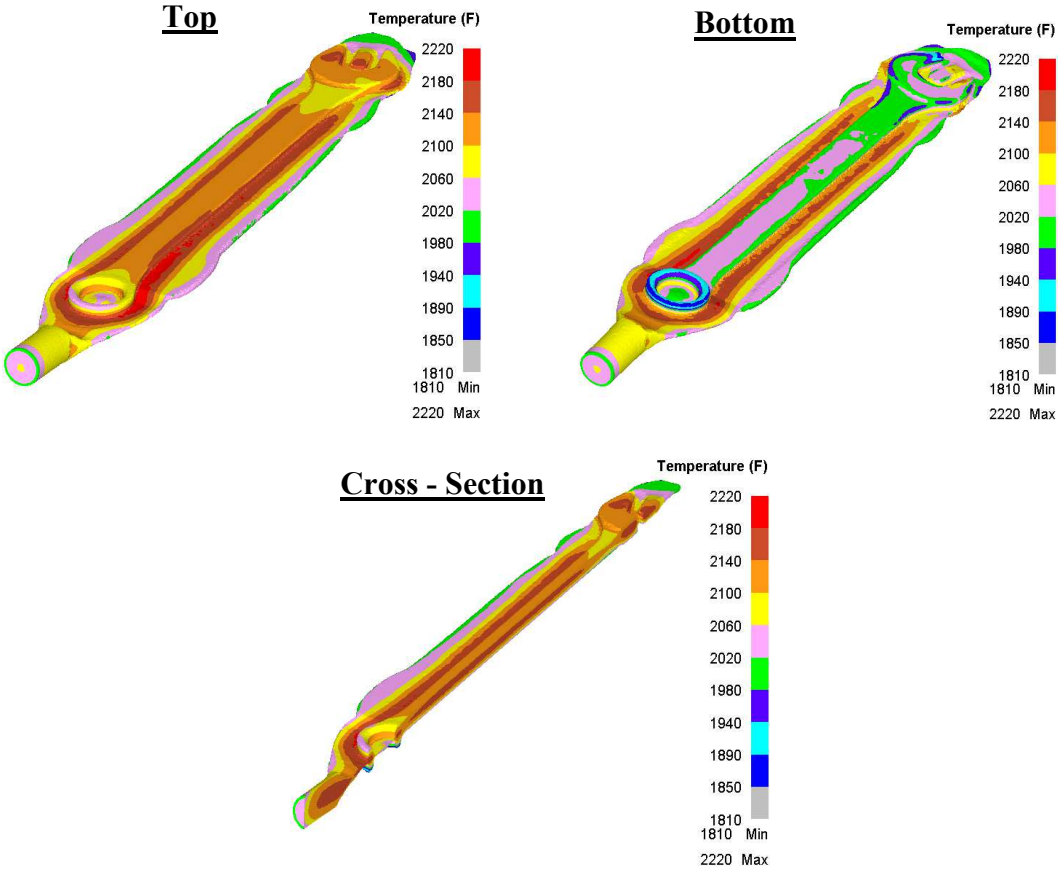

Figure B.6 Workpiece temperature plots at the end of the finisher operation, for the existing wrench forging process

APPENDIX C

SIMULATION MODEL RESULTS OF THE EXISTING WRENCH FORGING PROCESS

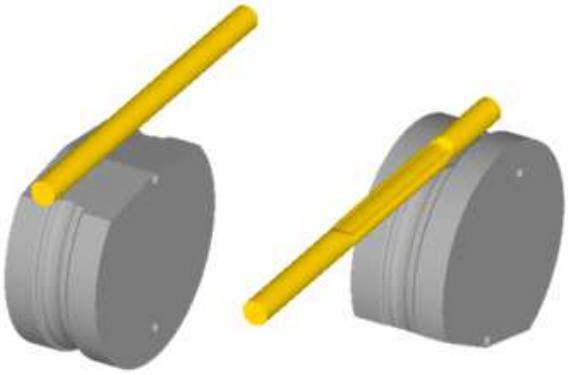

Figure C.1 Simulation workpiece model results of one pass in the roll forming operation, for the existing wrench forging process. (a) Before and (b) After deformation

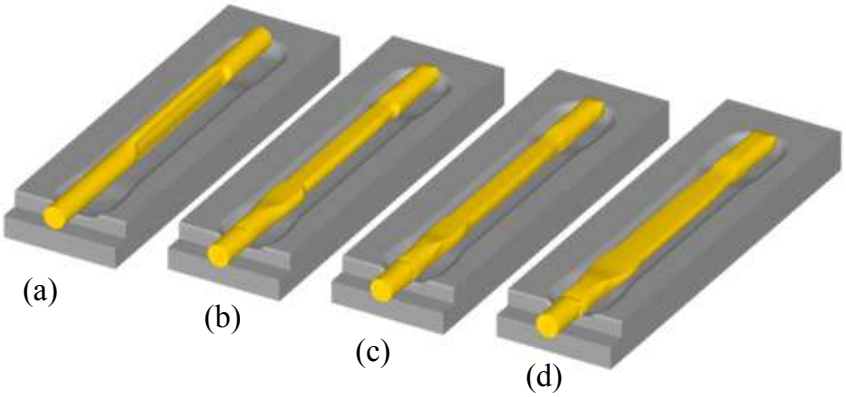

Figure C.2 Simulation workpiece model results of the edger operation, for the existing wrench forging process. (a) Before and after (b) 1st, (c) 2nd, (d) 3rd blow

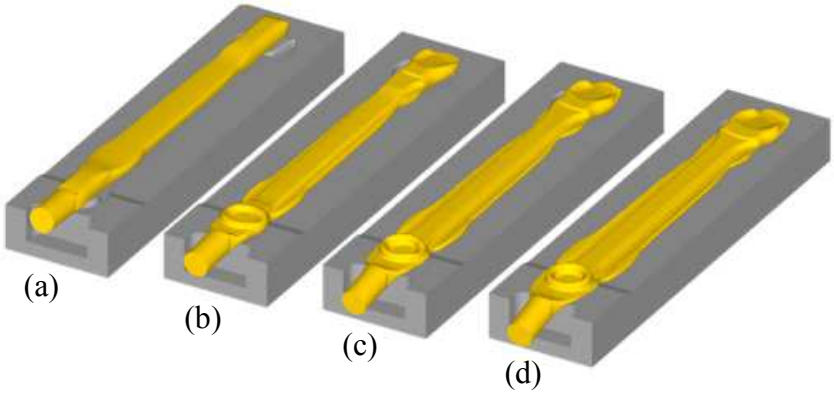

Figure C.3 Simulation workpiece model results of the blocker operation, for the existing wrench forging process. (a) Before and after (b) 1st, (c) 2nd, (d) 3rd blow

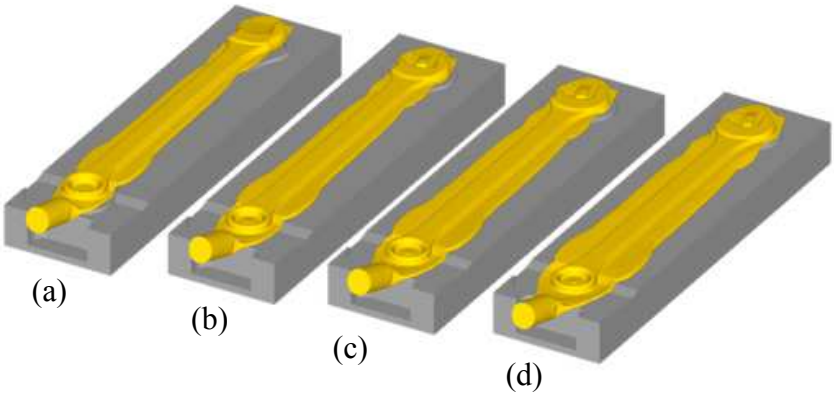

Figure C.4 Simulation workpiece model results of the finisher operation, for the existing wrench forging process. (a) Before and after (b) 1st, (c) 2nd, (d) 3rd blow

APPENDIX D

SIMULATION MODEL RESULTS OF THE INITIAL PROPOSED WRENCH FORGIN PROCESS

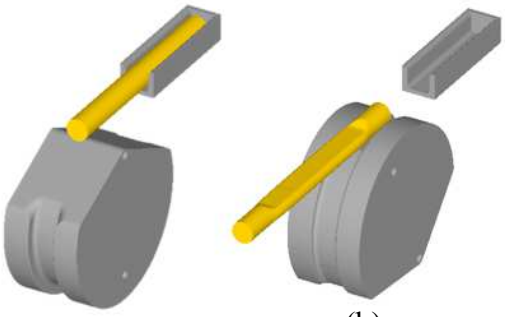

(a) (b)

Figure D.1 Simulation workpiece model results of the 1st pass in the roll forming operation, for the initial proposed wrench forging process. (a) Before and (b) After deformation

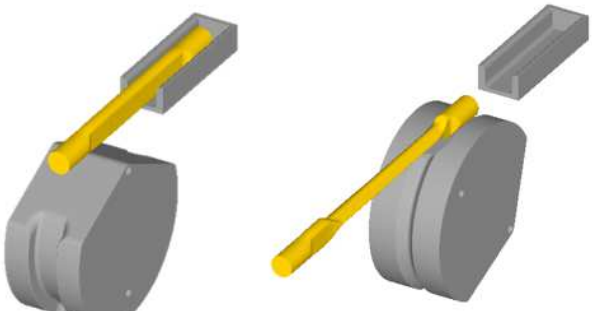

(a) (b)

Figure D.2 Simulation workpiece model results of the 2nd pass in the roll forming operation, for the initial proposed wrench forging process. (a) Before and (b) After deformation

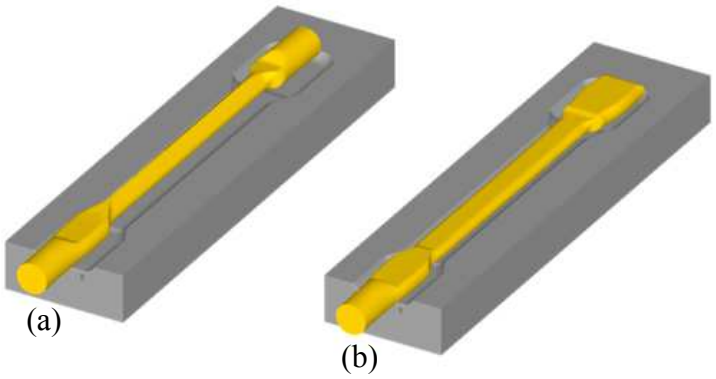

Figure D.3 Simulation workpiece model results of the edger operation, for the initial proposed wrench forging process. (a) Before and (b) After 1st blow

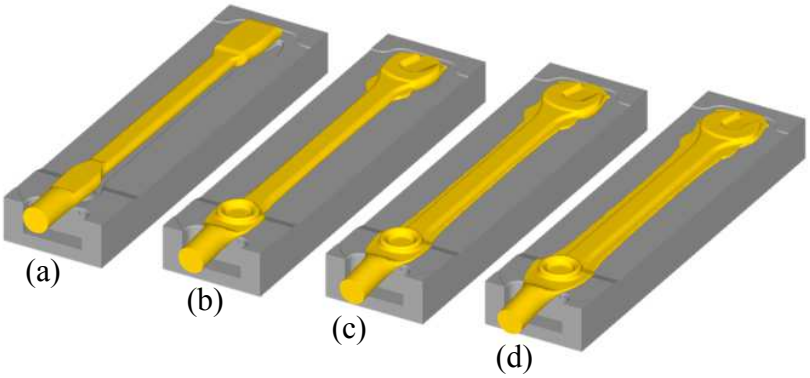

Figure D.4 Simulation workpiece model results of the blocker operation, for the initial proposed wrench forging process. (a) Before and after (b) 1st, (c) 2nd, (d) 3rd blow

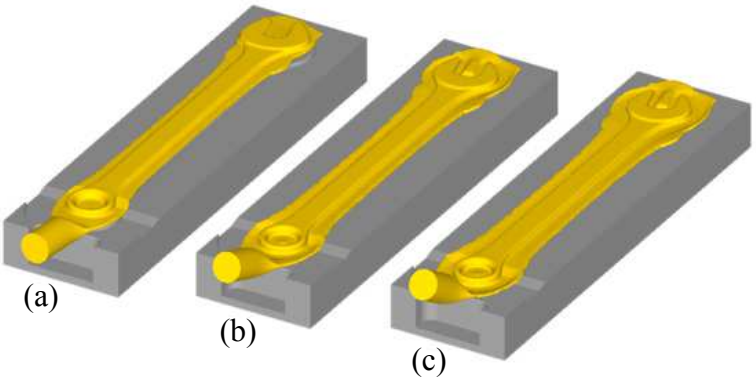

Figure D.5 Simulation workpiece model results of the finisher operation, for the initial proposed wrench forging process. (a) Before and after (b) 1st, (c) 2nd blow

APPENDIX E

SIMULATION MODEL RESULTS OF THE FINAL PROPOSED WRENCH FORGING PROCESS

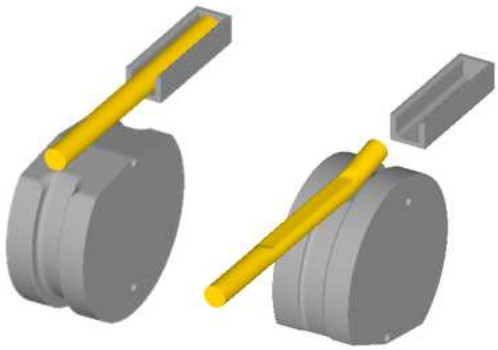

(a) (b)

Figure E.1 Simulation workpiece model results of the 1st pass in the roll forming operation, for the final proposed wrench forging process. (a) Before and (b) After deformation

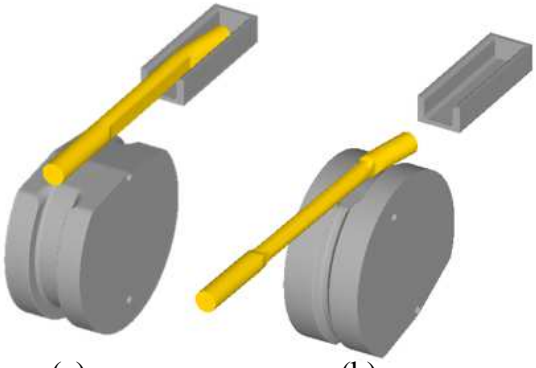

(a) (b)

Figure E.2 Simulation workpiece model results of the 2nd pass in the roll forming operation, for the final proposed wrench forging process. (a) Before and (b) After deformation

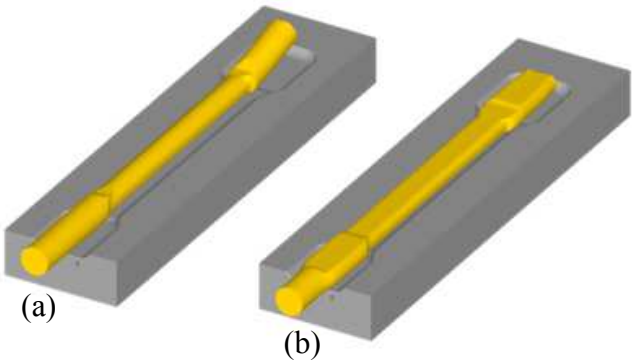

Figure E.3 Simulation workpiece model results of the edger operation, for the final proposed wrench forging process. (a) Before and (b) After 1st blow

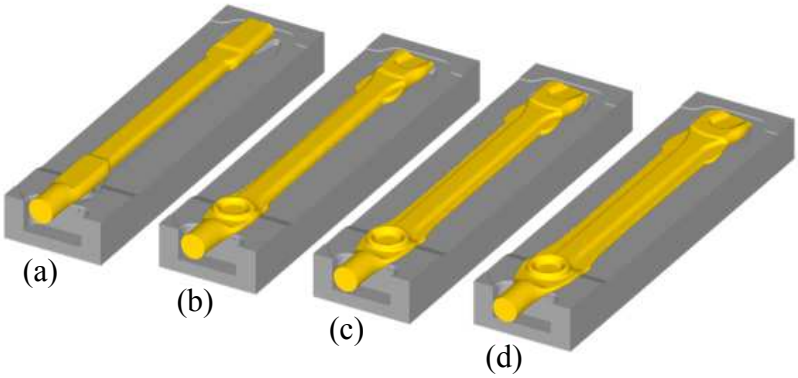

Figure E.4 Simulation workpiece model results of the blocker operation, for the final proposed wrench forging process. (a) Before and after (b) 1st, (c) 2nd, (d) 3rd blow

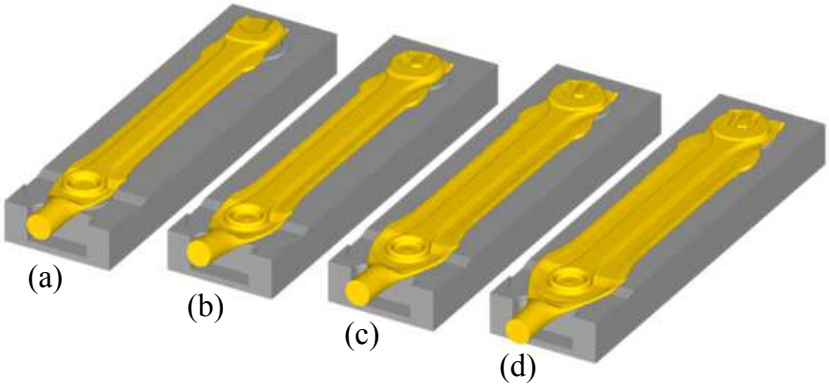

Figure E.5 Simulation workpiece model results of the finisher operation, for the final proposed wrench forging process. (a) Before and after (b) 1st, (c) 2nd, (d) 3rd blow

APPENDIX F

SIMULATION WORKPIECE MODEL AND GBDF FORGED PLATTER COMPARISON FOR THE EXISTING WRENCH FORGING PROCESS

Table F.1 Forged platter and DEFORM workpiece model comparison for the 1st pass in the roll forming operation, of the existing wrench forging process

	Measurement (in)	**Heat Expansion (in)**	**Measurement w/ Heat Expansion (in)**	**DEFORM (in)**
D	1.125	0.021	1.146	1.137
W1	1.460	0.027	1.487	1.390
L1	8.000	0.149	8.149	8.055
L2	18.750	0.350	19.100	19.339
H1	0.665	0.012	0.677	0.656

Table F.2 Forged platter and DEFORM workpiece model comparison for the 1st blow in the edger operation, of the existing wrench forging process

	Measurement (in)	**Heat Expansion (in)**	**Measurement w/ Heat Expansion (in)**	**DEFORM (in)**
W1	1.170	0.021	1.191	1.157
W2	1.713	0.031	1.744	1.550
W3	1.376	0.025	1.401	1.171
W4	1.425	0.026	1.451	1.225
L1	17.250	0.315	17.565	17.642
L2	19.125	0.349	19.474	19.607
H1	1.012	0.018	1.030	1.128
H2	0.610	0.011	0.621	0.719
H3	1.000	0.018	1.018	1.127

Table F.3 Forged platter and DEFORM workpiece model comparison for the 2nd blow in the edger operation, of the existing wrench forging process

	Measurement (in)	Heat Expansion (in)	Measurement w/ Heat Expansion (in)	DEFORM (in)
W1	1.086	0.020	1.106	1.196
W2	1.411	0.026	1.437	1.423
W3	1.245	0.023	1.268	1.125
W4	1.100	0.020	1.120	1.038
L1	17.375	0.318	17.693	17.674
L2	19.625	0.359	19.984	19.830
H1	1.037	0.019	1.056	1.105
H2	0.639	0.012	0.651	0.697
H3	1.031	0.019	1.050	1.109

Table F.4 Forged platter and DEFORM workpiece model comparison for the 3rd blow in the edger operation, of the existing wrench forging process

	Measurement (in)	Heat Expansion (in)	Measurement w/ Heat Expansion (in)	DEFORM (in)
W1	1.223	0.022	1.245	1.369
W2	1.855	0.034	1.889	1.842
W3	1.585	0.029	1.614	1.521
W4	1.320	0.024	1.344	1.254
L1	17.500	0.318	17.818	17.655
L2	19.750	0.358	20.108	19.837
H1	0.895	0.016	0.911	0.924
H2	0.501	0.009	0.510	0.527
H3	0.895	0.016	0.911	0.929

Table F.5 Forged platter and DEFORM workpiece model comparison for the 1st blow in the blocker operation, of the existing wrench forging process

	Measurement (in)	**Heat Expansion (in)**	**Measurement w/ Heat Expansion (in)**	**DEFORM (in)**
W1	1.974	0.035	2.009	2.059
W2	2.252	0.040	2.292	2.163
W3	1.926	0.034	1.960	1.726
W4	1.710	0.030	1.740	1.609
L1	18.250	0.325	18.575	18.284
L2	20.375	0.363	20.738	20.540
H1	0.737	0.013	0.750	0.686
H2	0.553	0.010	0.563	0.537
H3	0.795	0.014	0.809	0.857
Flash Thickness Average	0.233	0.004	0.237	0.295

Table F.6 Forged platter and DEFORM workpiece model comparison for the 2nd blow in the blocker operation, of the existing wrench forging process

	Measurement (in)	**Heat Expansion (in)**	**Measurement w/ Heat Expansion (in)**	**DEFORM (in)**
W1	2.150	0.038	2.188	2.269
W2	2.870	0.051	2.921	2.536
W3	2.396	0.043	2.439	2.010
W4	2.256	0.040	2.296	1.996
L1	18.500	0.329	18.829	18.583
L2	20.750	0.368	21.118	20.914
H1	0.822	0.015	0.837	0.843
H2	0.569	0.010	0.579	0.571
H3	0.709	0.013	0.722	0.738
Flash Thickness Average	0.148	0.003	0.151	0.180

Table F.7 Forged platter and DEFORM workpiece model comparison for the 3rd blow in the blocker operation, of the existing wrench forging process

	Measurement (in)	**Heat Expansion (in)**	**Measurement w/ Heat Expansion (in)**	**DEFORM (in)**
W1	2.404	0.042	2.446	2.516
W2	3.332	0.058	3.390	2.878
W3	2.834	0.049	2.883	2.216
W4	2.720	0.047	2.767	2.248
L1	18.750	0.327	19.077	18.806
L2	21.000	0.367	21.367	21.157
H1	0.851	0.015	0.866	0.887
H2	0.527	0.009	0.536	0.561
H3	0.669	0.012	0.681	0.692
Flash Thickness Average	0.106	0.002	0.108	0.133

Table F.8 Forged platter and DEFORM workpiece model comparison for the 1st blow in the finisher operation, of the existing wrench forging process

	Measurement (in)	**Heat Expansion (in)**	**Measurement w/ Heat Expansion (in)**	**DEFORM (in)**
W1	2.969	0.053	3.022	2.861
W2	3.873	0.069	3.942	3.272
W3	3.414	0.060	3.474	2.570
W4	3.195	0.057	3.252	2.523
L1	19.000	0.337	19.337	18.998
L2	21.250	0.376	21.626	21.248
H1	0.795	0.014	0.809	0.835
H2	0.469	0.008	0.477	0.509
H3	0.616	0.011	0.627	0.651
Flash Thickness Average	0.105	0.002	0.107	0.138

Table F.9 Forged platter and DEFORM workpiece model comparison for the 2nd blow in the finisher operation, of the existing wrench forging process

	Measurement (in)	**Heat Expansion (in)**	**Measurement w/ Heat Expansion (in)**	**DEFORM (in)**
W1	4.000	0.070	4.070	3.307
W2	4.875	0.086	4.961	3.706
W3	4.313	0.076	4.388	2.955
W4	4.000	0.070	4.070	2.867
L1	19.250	0.338	19.588	19.259
L2	21.750	0.382	22.132	21.468
H1	0.747	0.013	0.760	0.799
H2	0.424	0.007	0.431	0.472
H3	0.577	0.010	0.587	0.616
Flash Thickness Average	0.067	0.001	0.068	0.103

Table F.10 Forged platter and DEFORM workpiece model comparison for the 3rd blow in the finisher operation, of the existing wrench forging process

	Measurement (in)	**Heat Expansion (in)**	**Measurement w/ Heat Expansion (in)**	**DEFORM (in)**
W1	4.125	0.071	4.196	3.628
W2	5.125	0.089	5.214	4.158
W3	4.563	0.079	4.641	3.311
W4	4.375	0.076	4.451	3.181
L1	19.500	0.337	19.837	19.333
L2	21.750	0.376	22.126	21.623
H1	0.742	0.013	0.755	0.776
H2	0.420	0.007	0.427	0.453
H3	0.570	0.010	0.580	0.597
Flash Thickness Average	0.056	0.001	0.057	0.077

APPENDIX G

SIMULATION WORKPIECE MODEL AND GBDF FORGED PLATTER COMPARISON FOR THE FINAL PROPOSED WRENCH FORGING PROCESS

Table G.1 Forged platter and DEFORM workpiece model comparison for the 1st pass in the roll forming operation, of the final proposed wrench forging process

	Measurement (in)	**Heat Expansion (in)**	**Measurement w/ Heat Expansion (in)**	**DEFORM (in)**
D	1.188	0.022	1.210	1.203
W1	1.300	0.024	1.324	1.346
L1	8.500	0.158	8.658	8.730
L2	15.875	0.296	16.171	16.265
H1	0.800	0.015	0.815	0.810

Table G.2 Forged platter and DEFORM workpiece model comparison for the 2nd pass in the roll forming operation, of the final proposed wrench forging process

	Measurement (in)	**Heat Expansion (in)**	**Measurement w/ Heat Expansion (in)**	**DEFORM (in)**
D	1.188	0.022	1.210	1.203
W1	0.955	0.018	0.973	0.944
L1	11.000	0.205	11.205	11.276
L2	19.500	0.363	19.863	19.360
H1	0.959	0.018	0.977	0.980

Table G.3 Forged platter and DEFORM workpiece model comparison for the 1st blow in the edger operation, of the final proposed wrench forging process

	Measurement (in)	**Heat Expansion (in)**	**Measurement w/ Heat Expansion (in)**	**DEFORM (in)**
W1	1.515	0.027	1.542	1.590
W2	1.093	0.020	1.113	1.325
W3	1.300	0.023	1.323	1.252
W4	1.892	0.034	1.926	1.623
L1	17.000	0.306	17.306	17.500
L2	19.875	0.358	20.233	19.372
H1	0.695	0.013	0.708	0.760
H2	0.551	0.010	0.561	0.611
H3	0.705	0.013	0.718	0.760

Table G.4 Forged platter and DEFORM workpiece model comparison for the 1st blow in the blocker operation, of the final proposed wrench forging process

	Measurement (in)	**Heat Expansion (in)**	**Measurement w/ Heat Expansion (in)**	**DEFORM (in)**
W1	2.250	0.040	2.290	2.192
W2	1.757	0.031	1.788	2.017
W3	1.721	0.031	1.752	1.369
W4	2.325	0.041	2.366	2.105
L1	18.000	0.320	18.320	18.003
L2	22.625	0.403	23.028	19.504
H1ave	0.756	0.013	0.769	0.740
H2	0.554	0.010	0.564	0.606
H3	0.686	0.012	0.698	0.745
Flash Thickness Average	0.253	0.005	0.258	0.297

Table G.5 Forged platter and DEFORM workpiece model comparison for the 2nd blow in the blocker operation, of the final proposed wrench forging process

	Measurement (in)	**Heat Expansion (in)**	**Measurement w/ Heat Expansion (in)**	**DEFORM (in)**
W1	2.600	0.046	2.646	2.341
W2	2.290	0.041	2.331	2.354
W3	2.242	0.040	2.282	1.738
W4	3.188	0.057	3.245	2.438
L1	18.563	0.330	18.893	18.235
L2	20.625	0.367	20.992	20.065
H1	0.772	0.014	0.786	0.850
H2	0.457	0.008	0.465	0.544
H3	0.596	0.011	0.607	0.678
Flash Thickness Average	0.150	0.003	0.152	0.233

Table G.6 Forged platter and DEFORM workpiece model comparison for the 3rd blow in the blocker operation, of the final proposed wrench forging process

	Measurement (in)	**Heat Expansion (in)**	**Measurement w/ Heat Expansion (in)**	**DEFORM (in)**
W1	2.926	0.051	2.977	2.664
W2	3.543	0.062	3.605	2.699
W3	2.637	0.046	2.683	2.071
W4	2.629	0.046	2.675	2.715
L1	18.563	0.324	18.887	18.326
L2	23.125	0.404	23.529	20.320
H1	0.782	0.014	0.796	0.828
H2	0.465	0.008	0.473	0.506
H3	0.599	0.010	0.609	0.647
Flash Thickness Average	0.157	0.003	0.159	0.197

Table G.7 Forged platter and DEFORM workpiece model comparison for the 1st blow in the finisher operation, of the final proposed wrench forging process

	Measurement (in)	**Heat Expansion (in)**	**Measurement w/ Heat Expansion (in)**	**DEFORM (in)**
W1	2.812	0.053	2.865	3.020
W2	2.602	0.049	2.651	3.069
W3	2.792	0.053	2.845	2.335
W4	4.080	0.077	4.157	2.997
L1	19.000	0.359	19.359	18.867
L2	21.500	0.406	21.906	20.810
H1	0.786	0.015	0.801	0.815
H2	0.467	0.009	0.476	0.497
H3	0.619	0.012	0.631	0.642
Flash Thickness Average	0.107	0.002	0.109	0.122

Table G.8 Forged platter and DEFORM workpiece model comparison for the 2nd blow in the finisher operation, of the final proposed wrench forging process

	Measurement (in)	**Heat Expansion (in)**	**Measurement w/ Heat Expansion (in)**	**DEFORM (in)**
W1	3.375	0.059	3.434	3.358
W2	3.250	0.057	3.307	3.595
W3	3.313	0.058	3.370	2.742
W4	4.438	0.078	4.515	3.349
L1	19.250	0.337	19.587	19.122
L2	21.938	0.384	22.321	21.045
H1	0.759	0.013	0.772	0.787
H2	0.427	0.007	0.434	0.467
H3	0.591	0.010	0.601	0.612
Flash Thickness Average	0.064	0.001	0.065	0.091

Table G.9 Forged platter and DEFORM workpiece model comparison for the 3rd blow in the finisher operation, of the final proposed wrench forging process

	Measurement (in)	**Heat Expansion (in)**	**Measurement w/ Heat Expansion (in)**	**DEFORM (in)**
W1	3.625	0.062	3.687	3.739
W2	3.375	0.058	3.433	4.100
W3	3.563	0.061	3.624	3.137
W4	4.625	0.079	4.704	3.737
L1	19.313	0.331	19.644	19.243
L2	21.750	0.373	22.123	21.107
H1	0.746	0.013	0.759	0.768
H2	0.424	0.007	0.431	0.445
H3	0.569	0.010	0.579	0.591
Flash Thickness Average	0.064	0.001	0.065	0.068

APPENDIX H

GBDF FORGED PLATTER COMPARISON OF THE EXISTING AND FINAL PROPOSED WRENCH FORGING PROCESS

Figure H.1 GBDF forged platter comparison after the roll forming operation. (a) Existing and (b)1st pass, (c) 2nd pass of the final proposed wrench forging process

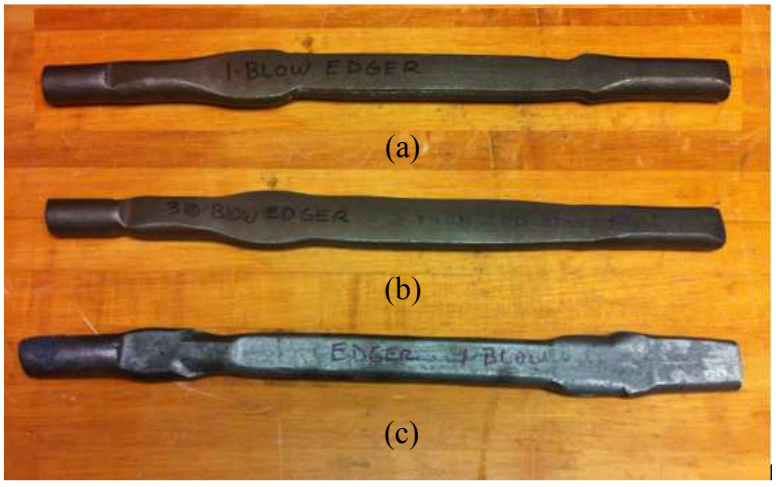

Figure H.2 GBDF forged platter comparison after the edger operation. (a) 1st, (b) 3rd blow of the existing and (c) 1st blow of the final proposed wrench forging process

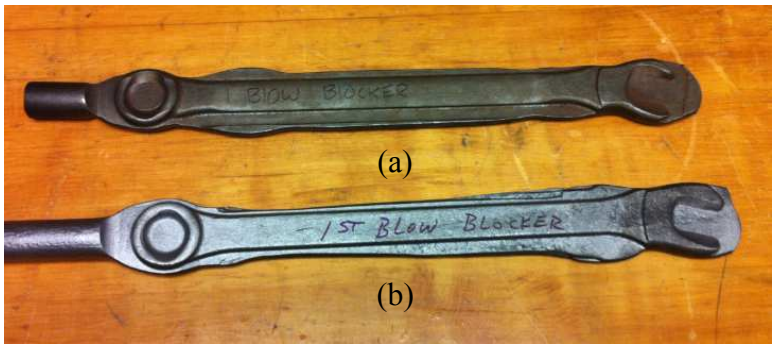

Figure H.3 GBDF forged platter comparison after the 1st blow in the blocker operation. (a) Existing and (b) Final proposed wrench forging process

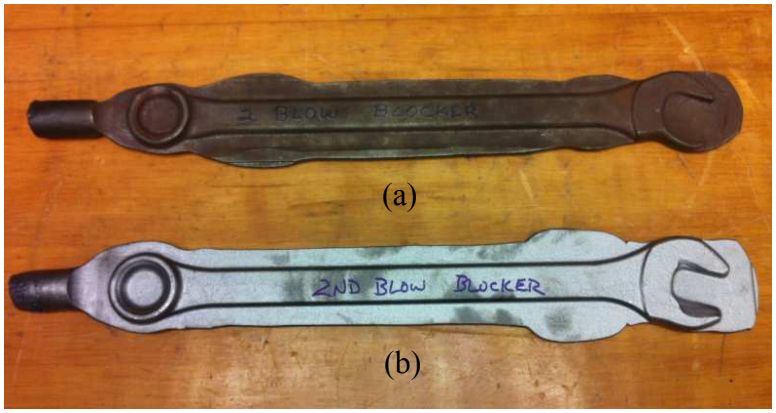

Figure H.4 GBDF forged platter comparison after the 2nd blow in the blocker operation. (a) Existing and (b) Final proposed wrench forging process

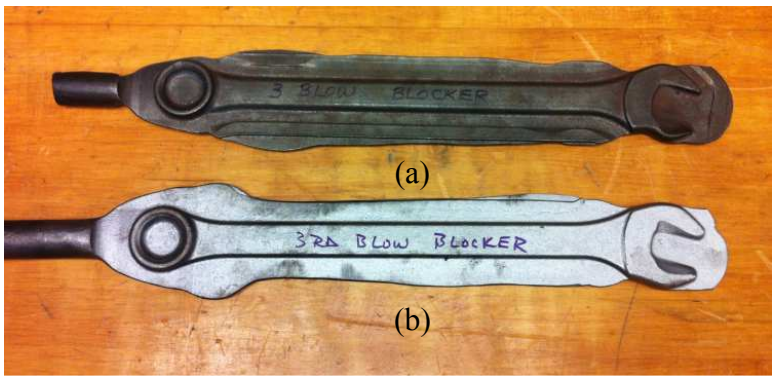

Figure H.5 GBDF forged platter comparison after the 3rd blow in the blocker operation. (a) Existing and (b) Final proposed wrench forging process

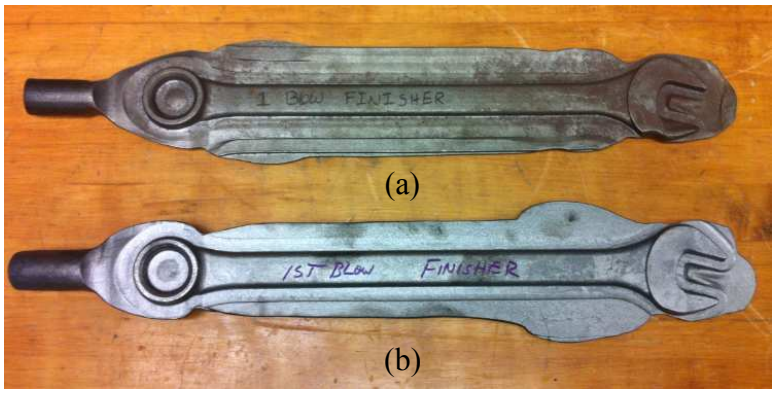

Figure H.6 GBDF forged platter comparison after the 1st blow in the finisher operation. (a) Existing and (b) Final proposed wrench forging process

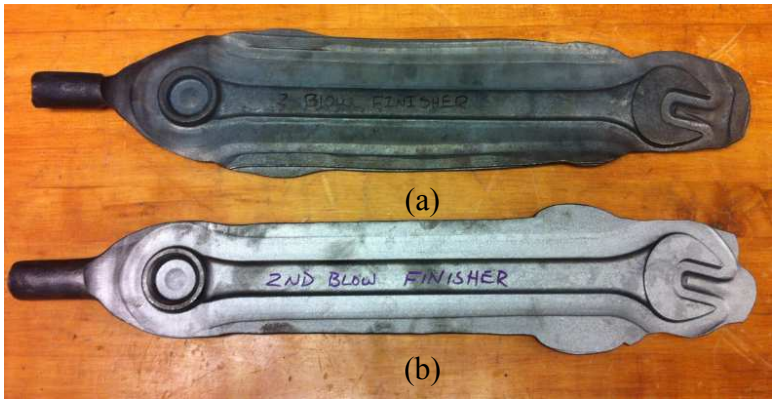

Figure H.7 GBDF forged platter comparison after the 2nd blow in the finisher operation. (a) Existing and (b) Final proposed wrench forging process

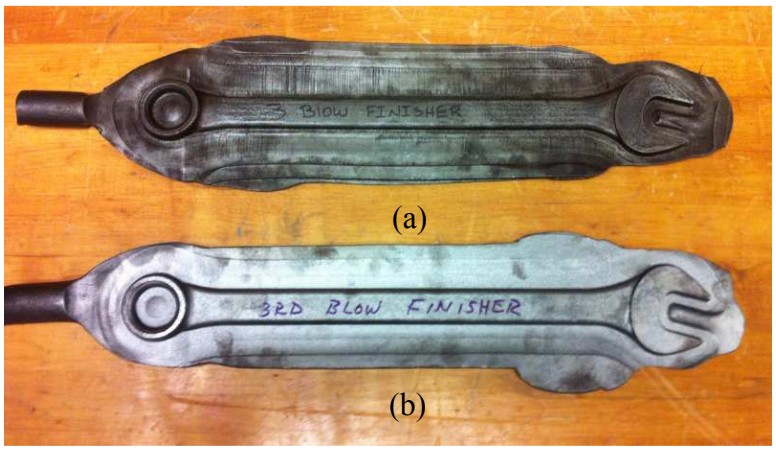

Figure H.8 GBDF forged platter comparison after the 3rd blow in the finisher operation. (a) Existing and (b) Final proposed wrench forging process